EviBAN

Evidence based assessment of NWRM for sustainable water management

Technical report about MAR solutions

Delivery number: D3.2

Stellenbosch University & BRGM

March 2021

Willem P. de Clercq, Géraldine Picot-Colbeaux, Marlene de Witt, Quentin Guillemoto, Loïc Thomas, Denis Neyens, Frédéric Mathurin, Nicolas Devau, Marie Pettenati, Jonathan Durand

Advertising

Study carried out as part of Research activities – Water JPI EviBAN project Evidence Based Assessment of NWRM for sustainable water management.

Call identifier: Water Joint Programming Initiative, Water challenges for a changing world 2018 Joint call

Topic: Closing the Water Cycle Gap

Start Date: April 2019

Duration: 36 months

Document info

Deliverable number: D3.2

Work Package: 3, Demonstration

Lead Beneficiary: Stellenbosch University

Dissemination level: This report is PU: public

Version: Draft, 19 March 2021

Version: Final 19 Sept 2021

Synopsis

Managed Aquifer Recharge solutions are assessed in the European Water JPI EviBAN project through two case study sites in South Africa and in France. The hydrosystem of each site is described and several MAR tool are applied and detailed.

The South African case study is investigating whether MAR could be a potential option for water diversification in the Goukou catchment. The point of departure is to better understand the Goukou system and to use hydrological modelling techniques to investigate potential environmental impacts and benefits of MAR under different circumstances. The aim is to apply a combination of methods to understand potential impacts of aquifer recharge on the Goukou River system and estuary.

The French case study concerns a Soil Aquifer Treatment scheme implemented on the coastal area of Agon-Coutainville since more than 20years that infiltrate in the sand dune aquifer the secondary treated wastewater coming through the main WasteWater Treatment Plant. The objective is to quantify the variations in residence time and dilution of infiltrated water (STWW) as a function of natural (natural recharge and runoff) and anthropogenic (controlled recharge) hydrodynamic forcing, and then to deduce their effects on Trace Organic Compounds concentrations in the aquifer at the spatial scale of the aquifer (kilometer scale) and at the multi-year temporal scale.

Contents

1. MAR in South Africa

1.1. INTRODUCTION

The South African case study is investigating whether managed aquifer recharge (MAR) could be a potential option for water diversification in the Goukou catchment. The point of departure is to better understand the Goukou system and to use hydrological modelling techniques to investigate potential environmental impacts and benefits of MAR under different circumstances.

The aim is to apply a combination of methods to understand potential impacts of aquifer recharge on the Goukou River system and estuary. This will be achieved through the following sub-aims:

- Determine the water balance of the catchment in terms of availability and demand.
- Better understand the surface-groundwater interaction of the system – how important is groundwater for maintenance of the river and estuary vs the importance of surface water.
- Determine the potential environmental impact on the estuary under different aquifer recharge options.
- Explore the best potential site for recharge.

1.2. CATCHMENT DESCRIPTION

The Goukou catchment is situated in the Southern Cape of South Africa. The river flows from the Langeberg Mountains in the north, southwards to Stilbaai at the coast. The river is only approximately 64km long. The catchment comprises of five quaternary catchments. Figure 1 shows the catchment delineation. The last 19km of the river is an estuary of high ecological importance (CSIR, 2011).

Figures 1 and 2 depicts the Goukou basin and it is clear from the catchment delineation the coastal zones East and West of Stilbaai, is not part of the catchment and in no way contribute to the water in the Goukou river. In fact, the Goukou river reaches see level about 18 km inland, where it meets the estuary.

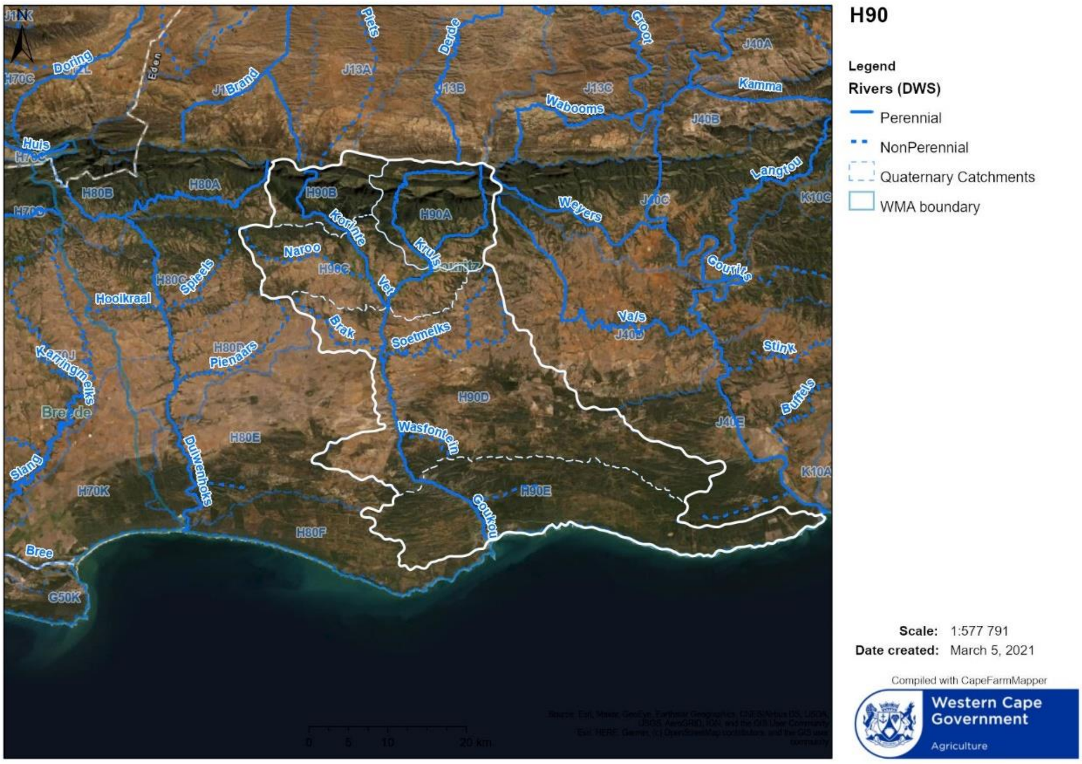

Figure 1. *The Goukou catchment, outlined with the solid white line. The catchment (H90) is divided into five quaternary catchments, outlined by the broken white lines. The Goukou River originates in catchment H90A. The Korinte River originates in catchment H90B*

Hydrological Response Unit (HRU) mapping with the Soil and Water Assessment Tool (SWAT) divided the catchment into three (Figure 2). The process, as can be seen in Figure 2, based the sub-catchment delineation on second order streams. This segmented the catchment in three catchment areas. The upper Goukou, including the mountain region is therefore represented in sub-catchment 1, while most of the coastal system is represented in sub-catchments 2 and 3. It is important the see the from this result the fact that the Goukou catchment makes a point contribution to the estuary while HRU 3 has a multitude of small streams connecting to the estuary.

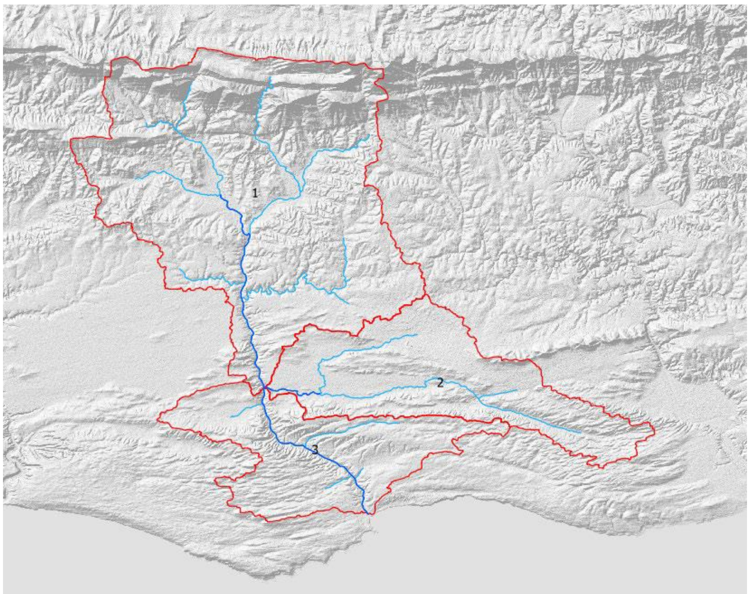

Figure 2. *Hydrological response units as mapped with the Soil and Water Assessment Tool (SWAT) in QGIS.*

1.3. CATCHMENT CHARACTERISTICS

1.3.1. Geology and aquifers

Figures 3 and 4 below shows the detailed geology of the catchment. Quaternary catchment H90E, situated at the coast, is the estuarine part of the river and where the coastal aquifers are located. Figure 3 shows aquifer types of the catchment. The coastal aquifers to the West of the Goukou River are situated on an aquiclude, above sea level and there are numerous springs that flow from the aquifers where the river cuts through the water-bearing rock (Ravenscroft, 2019). It is estimated that these aquifers are only approximately 5m thick and while they have a high yield, they will empty quickly if overused (Ravenscroft, 2019). The aquifers recharge through rain that percolates through the top sandy layer.

To the north of Riversdale, around the Korentepoort dam (Langeberg Mountains), groundwater potential is high due to the presence of large, deep aquifers that form part of the Table Mountain Group of aquifers (DWS, 2014). It has been recommended that this aquifer be developed and water pumped into the dam for distribution to Riversdale (DWS, 2014).

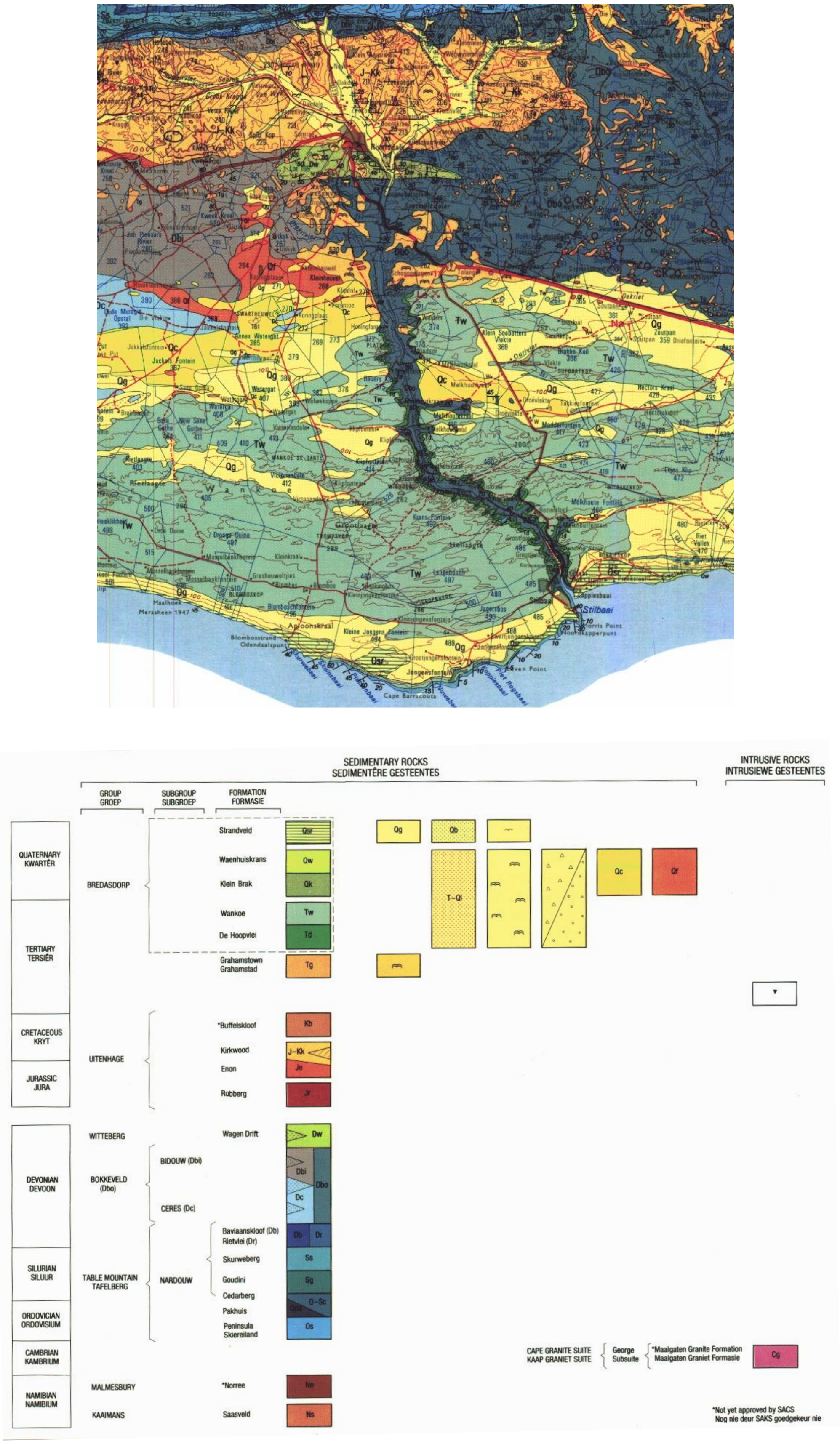

Figure 3. *The geology of the Hessequa Municipal district (Geosciences database)*

The Bredasdorp Group is elevated and underlain by the Enon Formation (of the Uitenhage Group) and forms the perched aquifer underlain by the Bokkeveld Group as an aquiclude. This perched aquifer as a water source provides fresh water to the estuary as this layer dips toward the south and is therefore also a direct contributor of water to the coastal sand aquifer system.

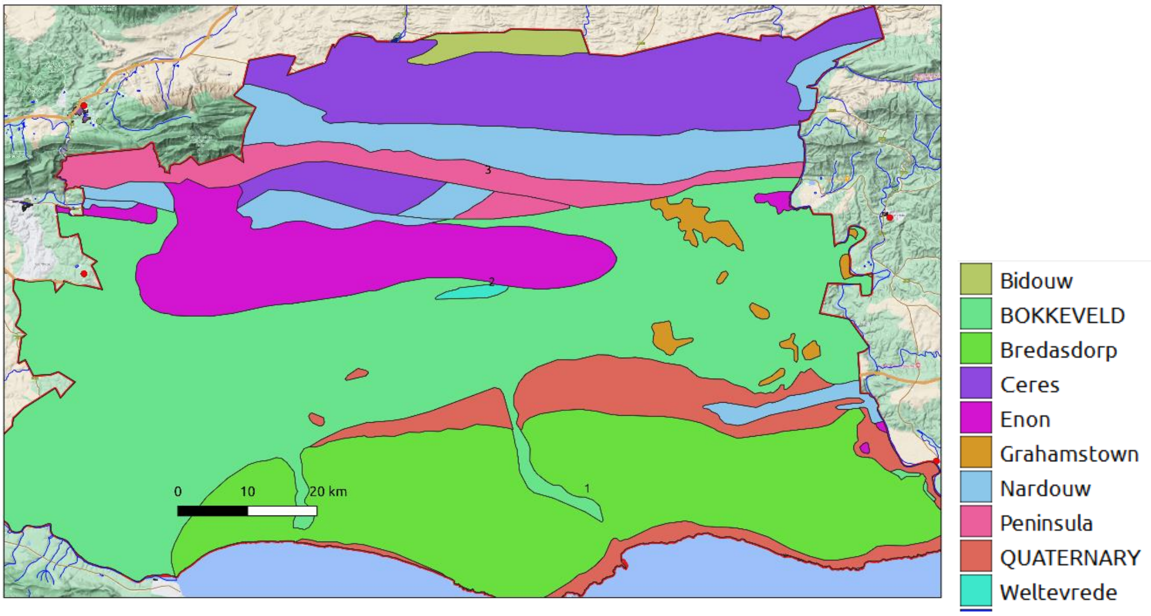

Figure 4. *The geology of the Hessequa Municipal district (SU database)*

Just below the mountain slopes, the geology is predominantly the Bokkeveld Group, with aquifers that are low yielding and have high salt contents. This is the predominant formation up to approximately 15km south of Riversdale. From here all the way to Stilbaai, there are outcrops of the Bredasdorp Group – De Hoopvlei formation overlain by Wankoe formation. The Wankoe formation is highly permeable calcarenite and calcareous sandstone, allowing a recharge of between 10% and 20% of MAP to the aquifer below in the De Hoopvlei formation. The De Hoopvlei formation is also mostly calcarenite and calcareous sandstone, with a bottom layer of pebbles that forms high-yielding, constant-flowing aquifers that discharge as springs where the river cuts through the outcrops. In this formation the aquifer with the highest groundwater potential in the catchment is around the village of Melkhoutfontein, which lies just north of Stilbaai in quaternary catchment H90E (see Figure 5). It has been recommended that the Melkhoutfontein be developed and utilised (Hough & Rudolph, 2017). The springs in this area provide all the farmers with water for household use and irrigation, as well as the towns of Stilbaai and Jongensfontein.

See Figure 4 for a geological map of the southern Hessequa municipal district. In summary, the aquifers in the north of the catchment are not connected to the coastal aquifers in the south. The aquifers with highest potential in terms of sustainable yield and quality are situated to the north of Riversdale around close to the mountains, and in the village of Melkhoutfontein just north-east of Stilbaai, and the higher region just north of Stilbaai West, indicated in Figure 12.

Figure 5 provides a regional summary of aquifer systems as was detected and mapped from the South African national borehole database. Similarly Figure 6 indicates the results of a more recent groundwater survey, taken from Hough & Rudolph, 2017.

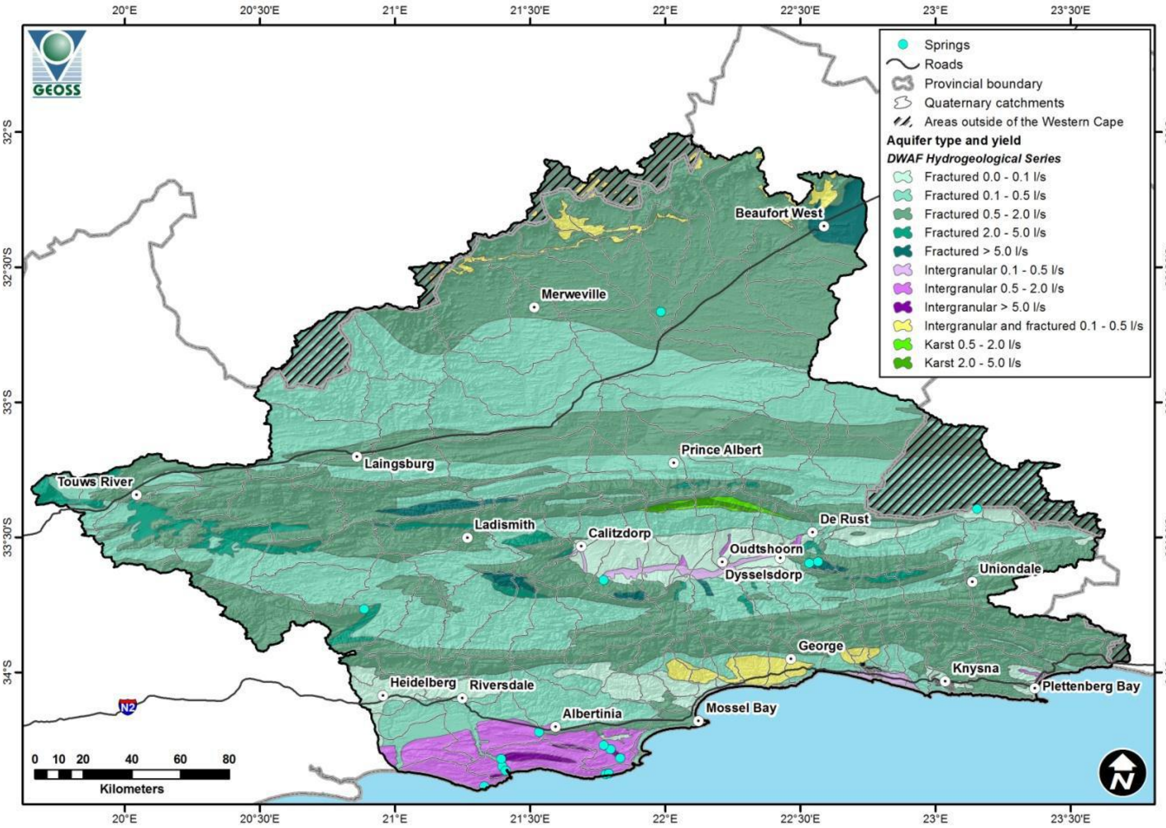

Figure 5. *Aquifer types of the Gouritz Water Management Area (taken from Western Cape Integrated Water Resources Plan, 2011). The high-yielding coastal aquifers are situated in quaternary catchments H90D and H90E. The map also shows how numerous springs originat*

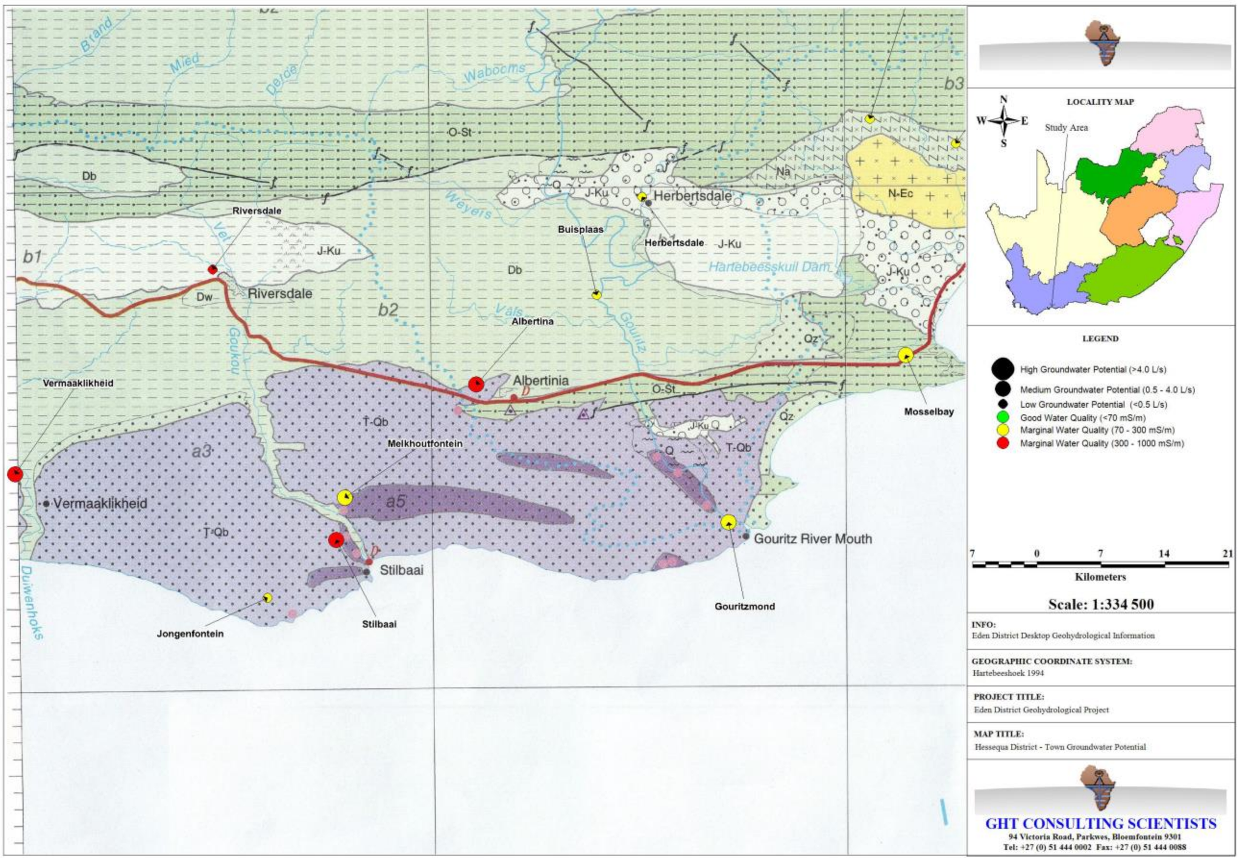

Figure 6. *Groundwater potential in the Goukou and surrounding catchments. The highest potential is around the settlement of Melkhoutfontein just north of Stilbaai, where the yield and water quality are good (taken from Hough & Rudolph, 2017).*

1.3.2. Topography and morphon mapping

Terrain and morphon mapping was done for the Goukou catchment by Stellenbosch University researchers as part of an earlier project in the region. These results are available for further modelling efforts. Figures 6 and 7 show the modelled topography and land types of the region. What is important to see is that the Goukou River System is carved into the landscape and that considerable landmasses occur above the river system. This makes coastal aquifer recharge along the coastal system from inland water sources quite difficult.

Figure 7 indicates the soils map developed for this project. The occurrence in soils also shows a marked difference between the soils towards the north (green) compared to the soils of the south (pink). The green soils are generally soils with lower infiltration capacity and therefore larger overland flow that generally causes floods to occur. The soils of the south (pink) on the other hand has higher infiltration capacity and more water is stored in the system. This GIS map (Figure 7) contains all the soil physical information needed for modelling.

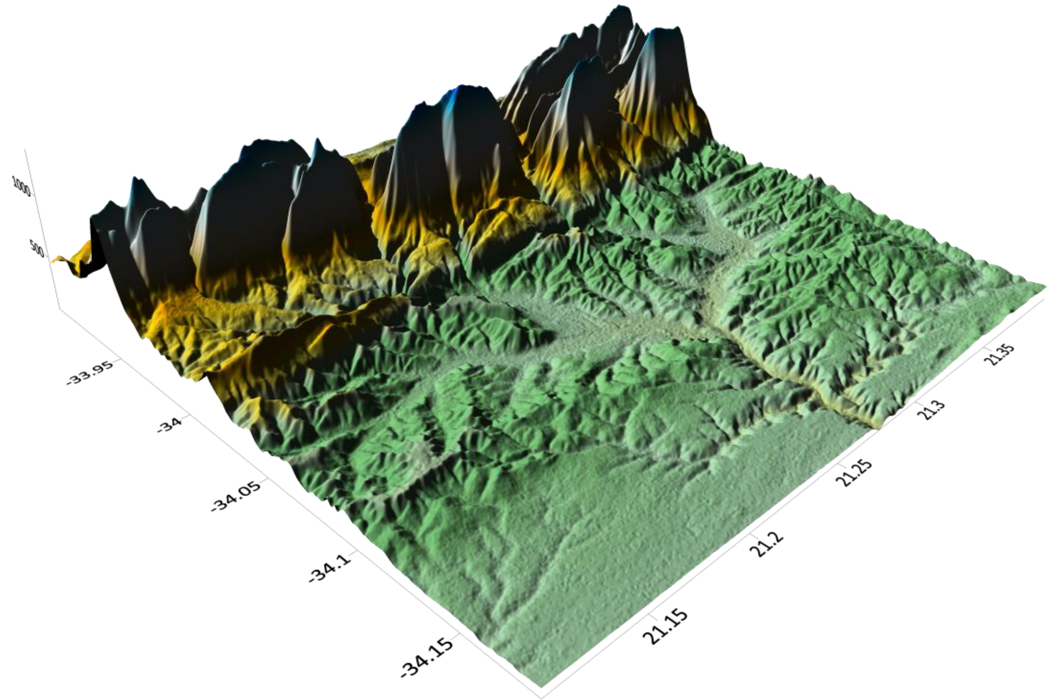

Figure 7. *The inflated topography of the Riversdale region*

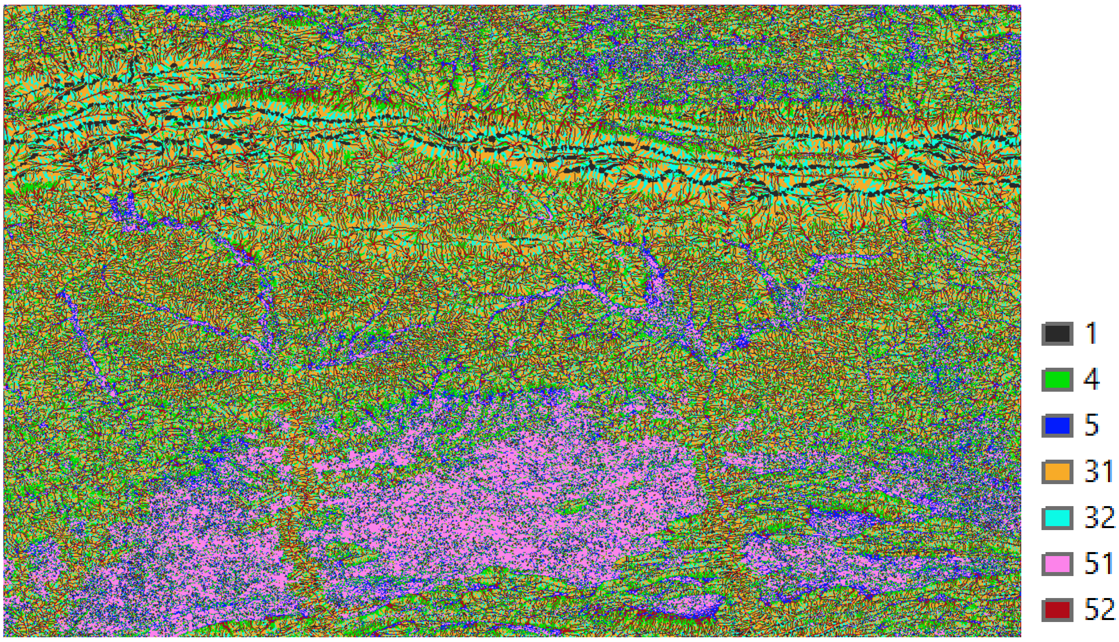

Figure 8. *Soils and Terrain map of the Hessequa region, with terrain classes as indicated, linked to the South African Land Type classification system. This is used as the basis for soils mapping and vegetation distribution. (developed in the project)*

1.3.3. Climate

Figure 8 indicates the average rainfall distribution in the catchment. For us to develop a model for the catchment, taking this distribution into consideration, we added 3 recording devices to the catchment as can be seen in Figure 12. The central weather station can be accessed online at: www.avitrack.co.za/aws/showmodels3 . The login is stellen and the password soil.

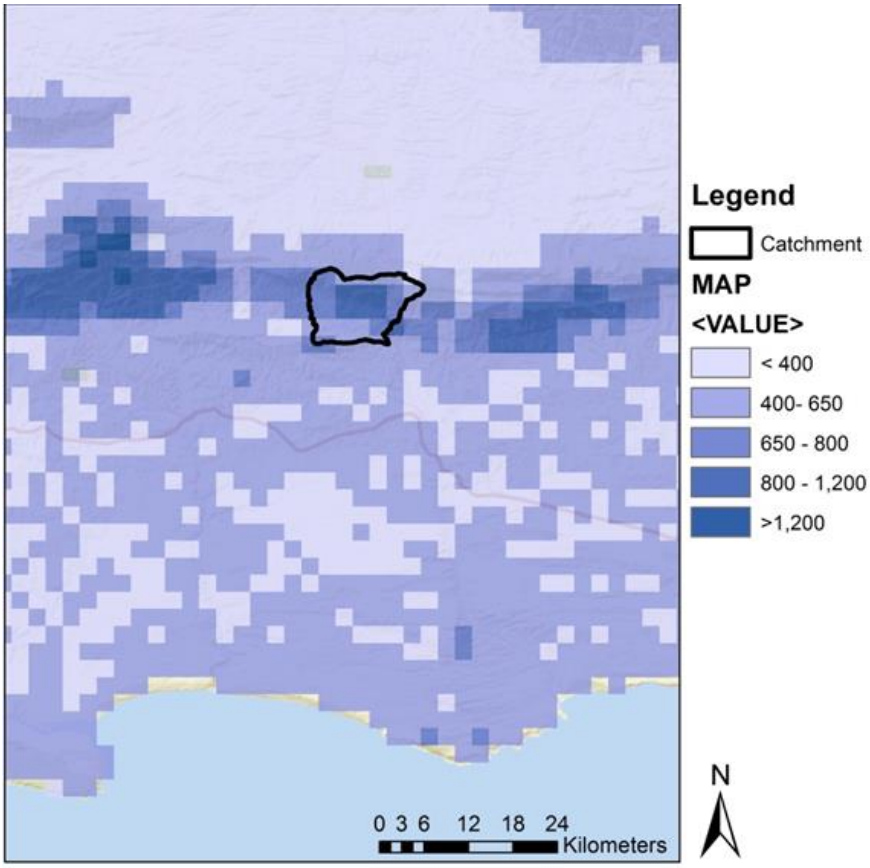

Figure 9. *The average yearly rainfall distribution of the Hessequa region.*

1.3.4. Interpretation of the results

Published information

From the published information, we did generate a full picture of the existing information base, but we lacked information that could help solve the logistical dilemma related to the different aquifers, the groundwater connections, undetected water flow paths, and therefore the feasibility of supporting the coastal aquifers with inland fresh water.

The geology of the region indicated a total dislocation of the geological strata going from the coast to the inland mountain range. A topographical analysis also indicated a separation between the Enon based aquifer (Figure 4) and the mountain aquifer. We are also still unsure about the deep groundwater, which is an ancient system. For this reason an isotope study is currently being conducted. The latter is however not being considered as a renewable water resource and is therefore not part of the study. We do however need to see where the water in the coastal aquifer originates from.

Topographical analysis.

A topographical analysis looked at the feasibility of using a high-flow water decanting system in support of the coastal aquifer system, utilizing gravitational flows. Since the central inland region is almost at sea level, the elevation of the Goukou River is a problem. We did however found the result presented in Figures 10 and 11 to provide a starting point towards a solution to the problem. The 90 m and 100 m contour lines south of Riversdale, indicate the spot in the green circle as a possible site for setting up a structure to aid managed coastal aquifer recharge. The site is indicated between the Riversdale golf course and the N2 highway. The analysis also highlighted the Ourivier as a prospect for supporting MCAR in the Stilbaai region. The Ourivier is joining to the Goukou from the East just south of the N2 highway. Figure 11 also indicates the position of Melkhoutsfontein. At this town, the runoff from the town is collected and treated and the current planning by the municipality is to use this as a source of water for MCAR.

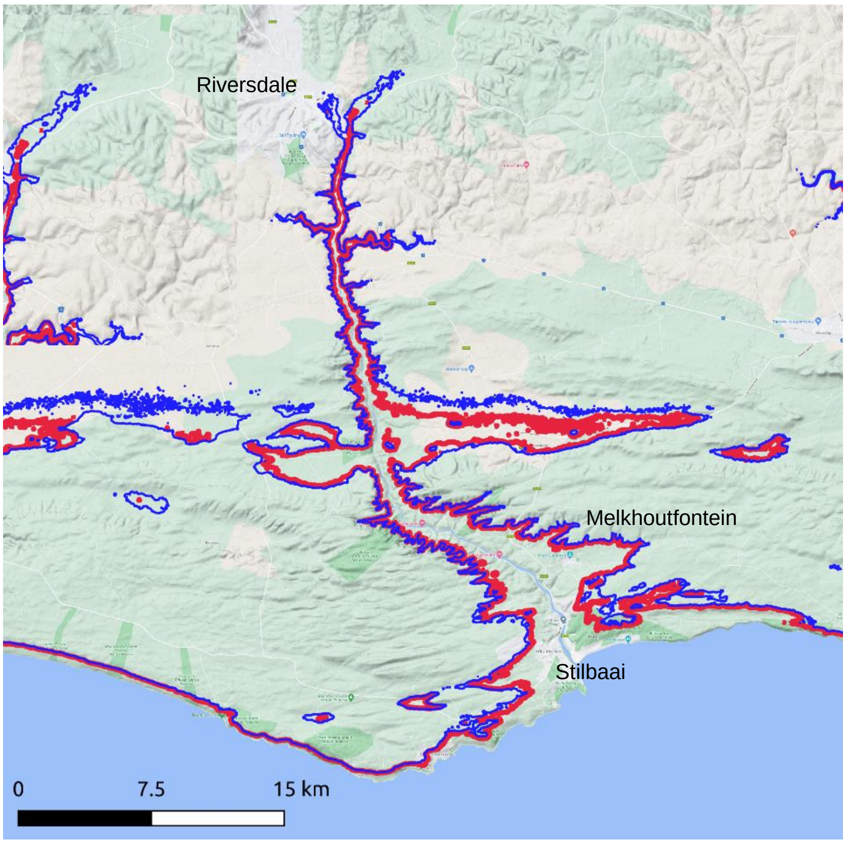

Figure 10. *Elevation contours 90 m (Red) and 100 m (Blue) indicating the differences in elevation between Riversdale and the Stilbaai coastal region*

Figure 11 indicates the zone where a structure to capture high flows could be built. This is close to the town Riversdale golf course.

Our preliminary field survey indicates that the perched aquifer meets the coastal aquifer system in the zone indicated in Figure 12, which is the source of water for Stilbaai West and Jongensfontein. This will be substantiated by the isotope study currently under way.

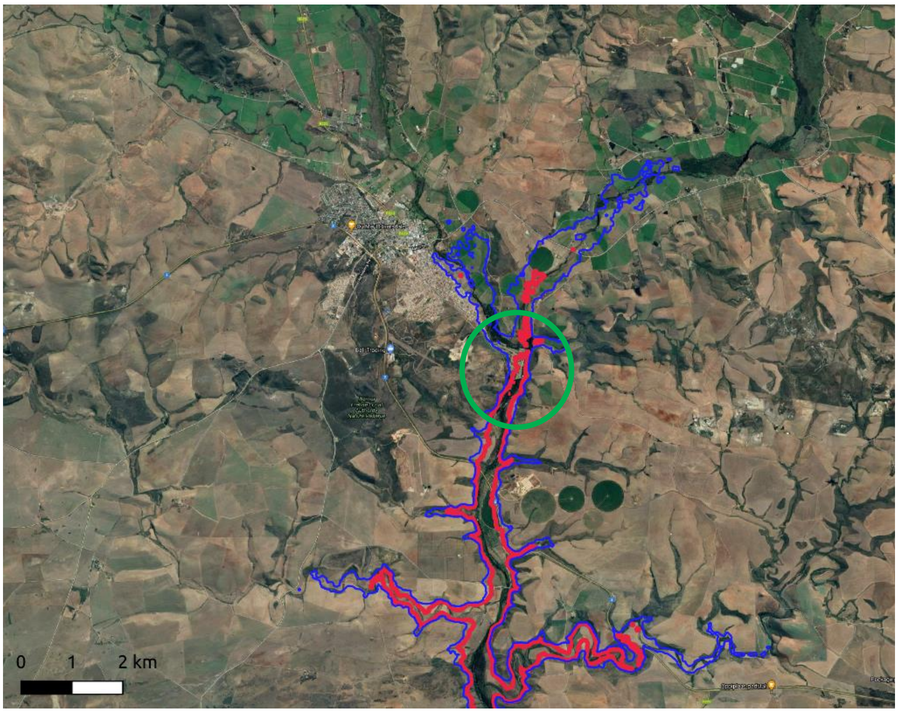

Figure 11. *The 90 m(red) and 100 m (blue) contour lines south of Riversdale, indicating the spot in the green circle as a possible site for setting up a structure to aid managed coastal acquifer recharge. The site indicated is between the riversdale golf caurse and the N2 highway.(also see the Ourivier joining to the Goukou from the East)*

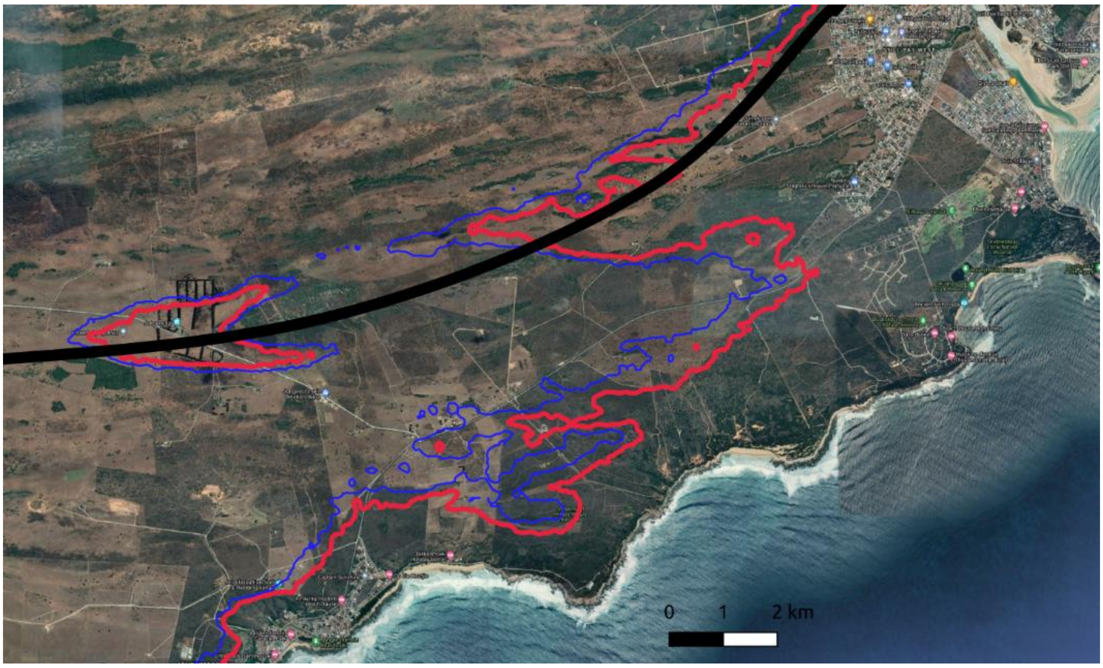

Figure 12. *The 90 m (red) and 100 m (blue) contour lines at Stillbaai, also indicating the contact zone (black line) between the perched aquifer with the coastal aquifer system. The aimed recharge zone is the region between the red line and the sea.*

1.4. HYDROLOGICAL MODELLING

1.4.1. WR2012 information and WRSM/Pitman model

A significant amount of information has been collected for hydrological modelling for the entire South Africa. All data are freely available on the WR2012 website (waterresourceswr2012.co.za). These data include geology, land-use, rainfall, streamflow, water quality, as well as high-quality maps.

Also available on this website is a locally produced hydrological model, the WRSM/Pitman model, which has been used by local water authorities since the 1970s. It was last updated in 2012 with the WR2012 information outline above, and is still widely used locally. The WRSM/Pitman model '*simulates the movement of water through an interlinked system of catchments, river reaches, reservoirs, irrigation areas and mines. It has five modules, namely runoff, reservoir, irrigation, channel and mining, linked by means of routes. The routes represent lines along which water flows between the different modules*' (Bailey & Pitman, 2012). The model and data were used to determine capacity and environmental flow levels for streams in South Africa.

The following data are available on WR2012 (https://waterresourceswr2012.co.za/):

- GIS Maps
- WRSM/Pitman and Data Sets
- Reports
- Quaternary data spreadsheets
- Patched Observed Streamflow Data
- Catchment Rainfall Groups
- Catchment based rainfall datafiles
- Rainfall stations
- Naturalised flow datafiles
- Water Quality
- Monitoring
- Land/ Water Use
- Present Day Flows
- Reservoir records/ Dam balances

A GIS database is also available with high-quality maps for the following:

- rainfall
- evaporation
- runoff
- land-use
- the Pitman model parameters
- geology
- soils
- sediment
- vegetation
- EWR
- water quality (TDS)
- population
- present day streamflow
- combined map of all the above (except land-use)

Maps from other sources that are also available on WR2012 are the following

- Groundwater Regions
- Average Groundwater Resource Potential
- Exploitation Factor
- Average Groundwater Exploitation Potential
- Potable Groundwater Exploitation Potential
- Sectoral WMA Groundwater Use
- Mean Water Level Depth
- Average Saturated Thickness of Weathered Aquifer Zone
- Average Thickness of Fractured Aquifer Zone
- Groundwater Volume in Weathered Zone
- Groundwater Volume in Fractured Zone
- Groundwater Volume in Aquifers
- Utilisable Groundwater Exploitation Potential
- Recharge Depth Grid
- Relative Variation in Transmissivity
- Average Transmissivity
- Transmissivity and NGDB T Data
- Electrical Conductivity
- Boreholes with Nitrate > 10mg/l
- Boreholes with Fluoride > 1.5 mg/l
- Boreholes with Iron > 0.2 mg/l
- Catchments Over-Exploited
- Geology Detailed

Apart from the above, we also have access to both monthly and daily time step climate data.

1.4.2. WRSM/Pitman model: Goukou

A locally produced hydrological model, the WRSM/Pitman model, has been used by local water authorities since the 1970s. It was last updated in 2012 with the WR2012 information outline above, and is still widely used locally. The WRSM/Pitman model '*simulates the movement of water through an interlinked system of catchments, river reaches, reservoirs, irrigation areas and mines. It has five modules, namely runoff, reservoir, irrigation, channel and mining, linked by means of routes. The routes represent lines along which water flows between the different modules*' (Bailey & Pitman, 2012). The model and data were used to determine capacity and environmental flow levels for streams in South Africa.

The South African project team has run the model for the Goukou catchment and is in the process of refining it with data collected through interviews with local farmers and stakeholders. The model provides the mean annual runoff at different sections of the catchment. It will be used to see the impact on the mean annual runoff when water is removed at different points for managed aquifer recharge.

The WRSM/Pitman model contains two network diagrams for the Goukou catchment. The first (Figure 13) is for catchment H90B – the Korente River. Figure 14 is the network diagram for the remainder of the catchment (H90 A, C ,D and E). Figure 14 has been edited to contain the names of the rivers associated with the channel reach modules.

Figure key:

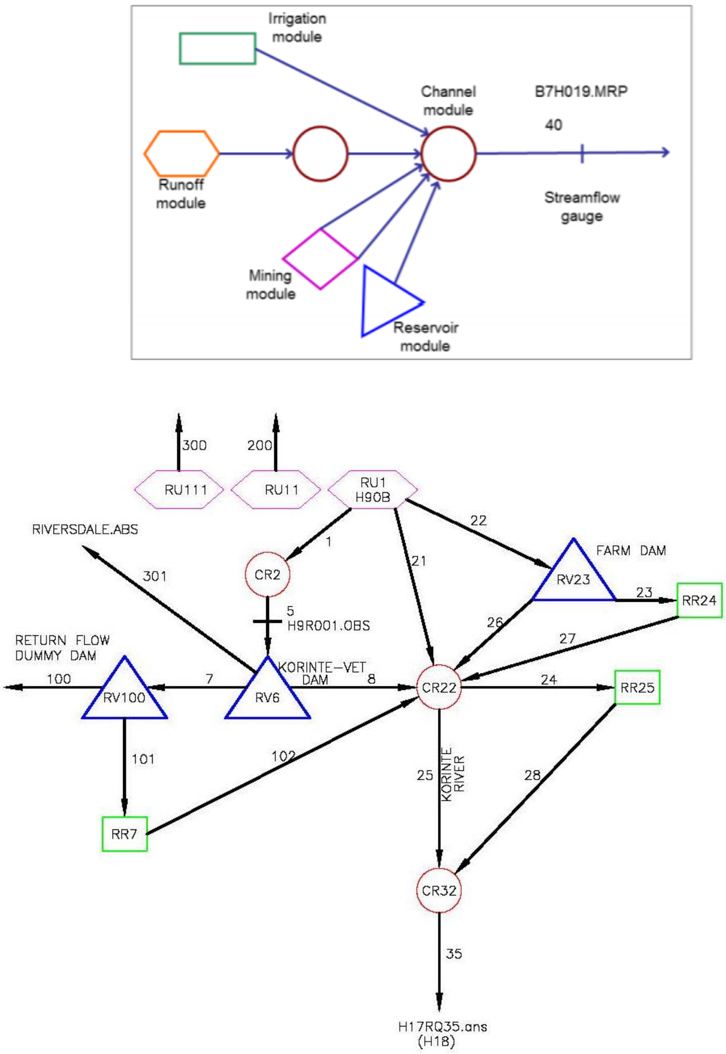

Figure 13. *The network diagram for quaternary catchment H90B of the Goukou catchment. Triangle RV6 is the Korentepoort Dam. RU11 represents alien invasives and RU111 represents forestry. (https://waterresourceswr2012.co.za/)*

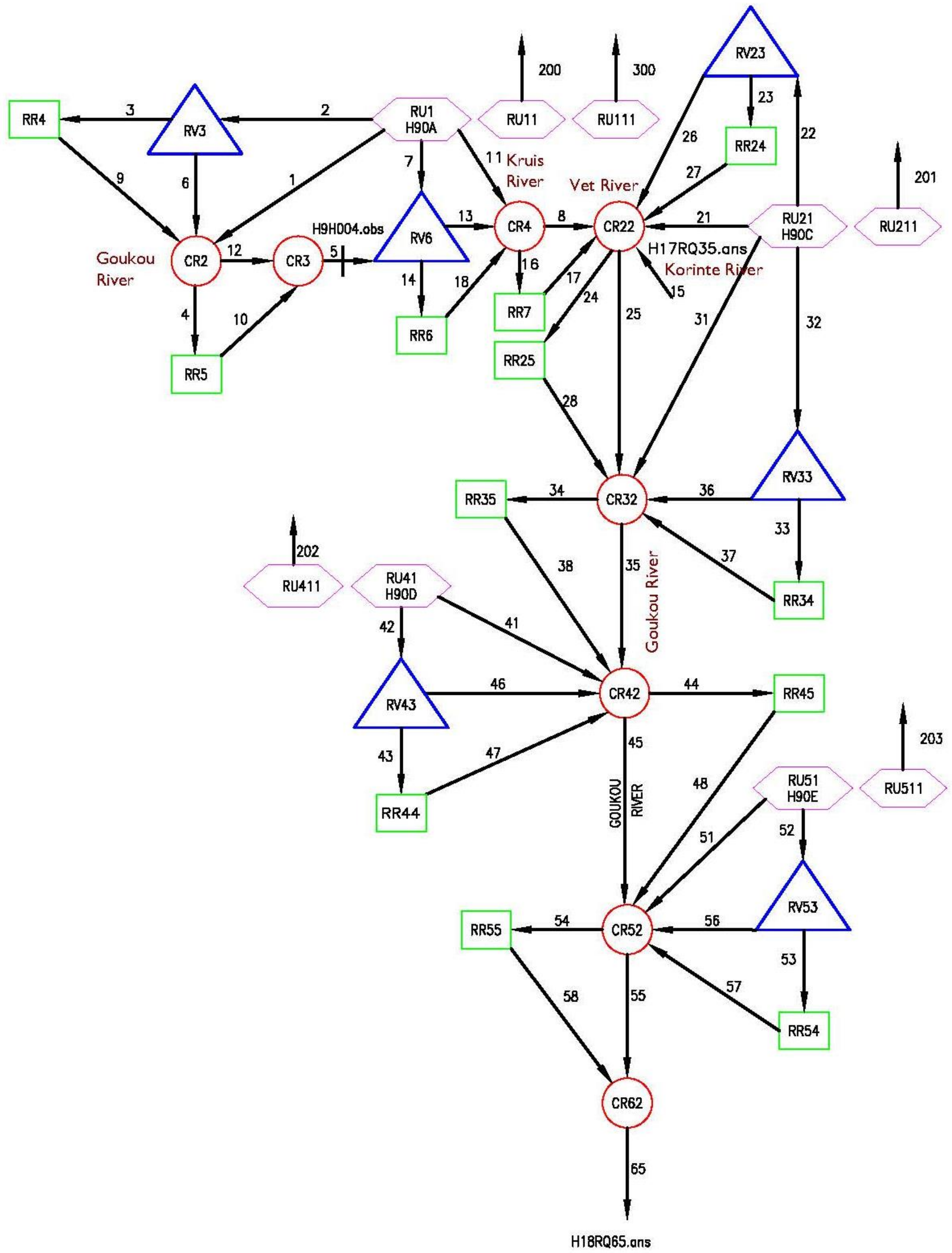

Figure 14. *Network diagram for the remainder of the Goukou catchment. The river names have been added to the figure. All triangles are farm dams. RU111 is forestry. RU11, RU211,RU411 and RU511 are invasives. (https://waterresourceswr2012.co.za/)*

Two gauging stations in catchments H90A and H90B have been used for calibration in the WRSM/Pitman model (Figure 15). H9H004 is situated in the Kruis River, in the mountains north-east of Riversdale and H9R001 is at the Korentepoort Dam. Data is also available on the DWS Hydrology website for an additional gauging station, namely H9H005, situated in the Goukou River just east of Riversdale (added to Figure 15 in red). This data can be used for further calibration of the model once additional information has been added to the model, as will be described in section 3.2 below.

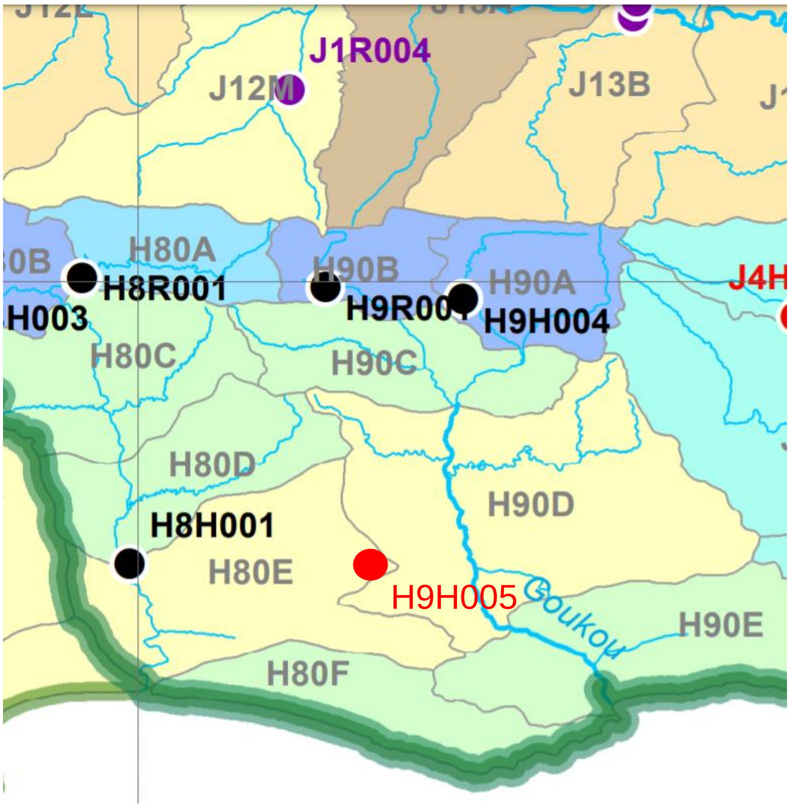

Figure 15. *1Gauging stations used in the WRSM/Pitman model are H9R001 at the Korentepoort Dam in catchment H90B, and H9H004 in the Kruis River in catchment H90A. Data for gauging station H9H005 just outside of Riversdale is available on the DWS website (https://waterresourceswr2012.co.za/) .*

1.4.3. Further information gathering

Further information to be gathered to refine the model include:

- More detailed land-use information and information on farm dams in the system will be obtained through the interview process and Google Earth will be used to cross-check this (especially the farm dams). The interview process will also provide more detail on crops planted in the area and the Cape Farm Mapper website of the Western Cape Government will be used to cross-check and validate this. All this information will be used to update the network diagram and various modules in the model.
- The Gouritz Cluster Biosphere Reserve will be asked for more detail on invasive species in the catchment, as they have a more recent grasp on the spread of invasives, and this will be used to update the invasives module in the model.
- Efforts will be made to obtain more detail on the plantation by the Korentepoort dam to update the afforestation module.
- The irrigation information of the network diagram will be checked with the manager of the Korente-Vette irrigation scheme and revised where necessary.
- SANBI has indicated that they will share their modelling work on the wetland, which will allow us to check and refine the wetlands information in the Pitman model.
- The weir information has been downloaded from the DWS website and will be used to calibrate the model once the above-mentioned refinements have been made.

- Climate data will be collected from existing climate and weather stations. The project team installed three new stations for data gathering – one in the mountains, one by the town of Riversdale, and one close to the coast (see Figure 16).

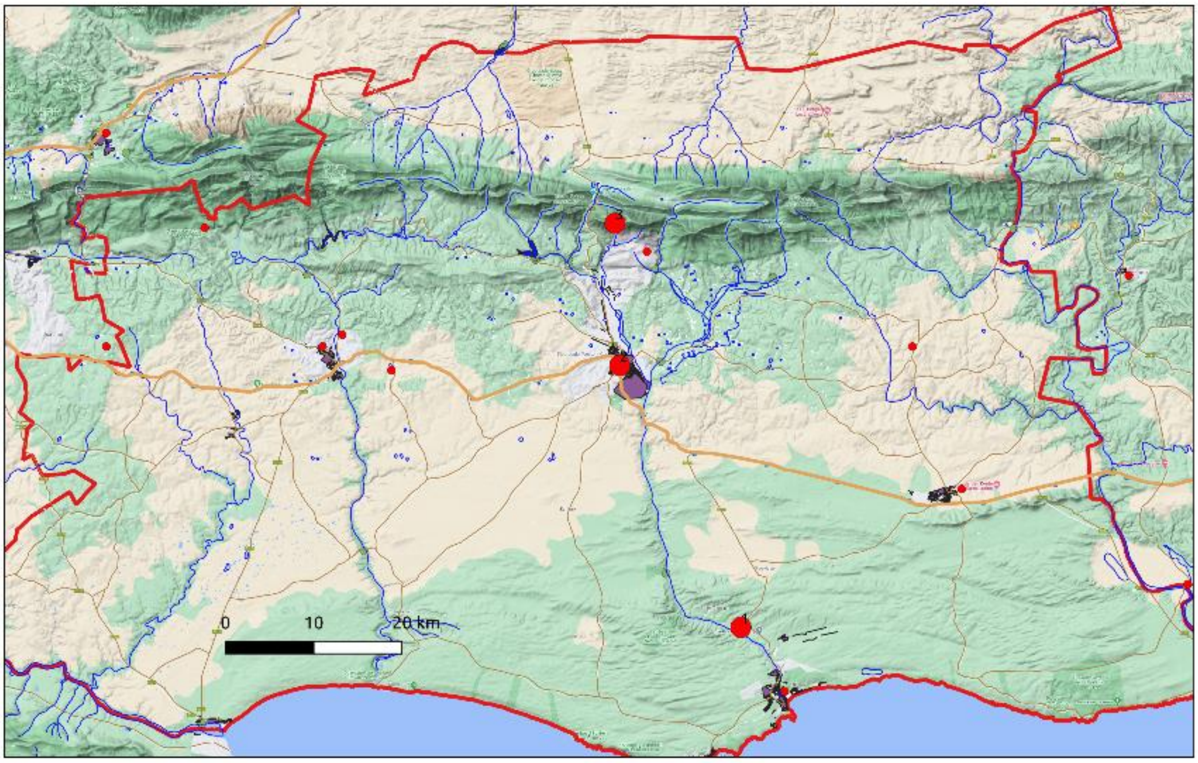

Figure 16. *The red dots show the position of climate stations in the municipal district. The three larger dots are stations that were installed by the project team (developed by team).*

1.5. FURTHER HYDROLOGICAL MODELLING

1.5.1. PITMAN

It is important for this study to present an analysis of the Pitman modelled data that was used as a directive for water planning of this region. This information forms the backdrop for this study, as the planning information is still used for this region to allocate water for the different sectors. Even if we find with further modelling that the volumes of water in the system was slightly miscalculated or modelled, the water used practices for the Hessequa region was designed with the Pitman modelled information.

In our quest for this research, it is therefore necessary to specifically look at sporadic high flows and some longer periods of high flows. It is also necessary to look at the seasons in which these higher flows occurred.

Sporadic high flows

The Pitman simulated flow results of the Goukou that reaches the estuary, is indicated in Table 1. The yearly total flows are indicated and it is easy to see the peaks within years. These peaks occur generally between 0 and 3 times per year, as can also be observed in Figure 17.

Table 1. Pitman simulated flow results of the Goukou that reaches the estuary

	J	F	M	A	M	J	J	A	S	O	N	D	TOT
1920	5.17	2.29	7.02	1.68	4.9	6.61	8.39	3.81	6	4.16	4.58	3.34	57.94
1921	1.38	0.12	3.19	17.19	5.78	17.15	7.17	3.11	3.32	6.18	4.66	2.54	71.78
1922	5.62	11.18	3.09	1.74	0.96	0.09	12.46	14.55	11.01	6.54	5.67	3.98	76.89
1923	6.8	6.69	0.68	0.98	2.83	1.64	1.31	2.66	5.2	4.85	16.96	7.97	58.57
1924	4.05	4.18	2.83	0.37	0.1	12.81	4.54	1.27	5.39	4.22	3.52	6.22	49.48
1925	8.69	6.91	1.88	2.69	1.95	3.59	6.13	2.46	1.89	7.79	6.8	6.23	57
1926	22.35	13.59	1.82	0.13	3.64	4.98	3.56	6.31	3.79	2.01	7.98	3.55	73.7
1927	1.84	7.67	2.71	0.95	0.1	20.1	6.07	1.94	3.14	2.26	4.51	9.83	61.11
1928	4.23	81.21	37.11	3.42	3.26	5.04	3.61	8.71	6.4	19.09	17.29	9.27	198.64
1929	6.54	1.77	5.34	3.13	42.66	20.66	4.38	11.91	5.83	3.44	6.81	5.82	118.3
1930	15.59	4.95	0.19	2.59	0.55	26.23	30.07	9.58	2.99	8.21	6.66	6.44	114.05
1931	22.83	7.37	23.39	6.26	4.79	4.5	1.22	1.31	2.62	3.28	2.57	81.8	161.96
1932	29.67	3.87	1.03	0.18	2.63	3.66	1.5	7.2	4.68	3.37	17.5	6.65	81.94
1933	1.03	23.24	5.55	9.16	7.57	14.02	4.08	0.86	0.65	11.75	13.74	7.1	98.76
1934	52.21	29.09	3.97	0.2	0.17	4.67	4.32	19.35	17.09	7.46	4.08	8.63	151.23
1935	7.09	12.27	5.26	0.24	2.54	1.11	0.33	6.82	2.96	5.51	4.01	11.37	59.5
1936	9.9	54.21	22.64	3.45	0.17	16.02	5	0.71	1.7	4.2	2.48	6.17	126.65
1937	2.4	3.9	11.42	6.13	0.17	7.44	9.52	4.15	3.22	4.79	3.93	5.61	62.69
1938	8.07	25.32	11.54	2.79	7.48	24.15	8.36	2.08	1.13	7.48	30.62	14.38	143.38
1939	5	3.57	0.22	3.66	30.61	12.85	8.36	4.01	3.09	2.73	1.41	6.28	81.79
1940	3	16.23	3.33	1.56	0.34	0.21	19.92	9.4	8.86	6.81	7.45	8.62	85.73
1941	13.12	6	2.34	7.12	1.41	2.73	3.79	7.43	4.74	3.07	3.12	4.83	59.7
1942	5.08	1.75	8.35	29.7	10.59	4.31	3.36	1.5	0.89	0.94	4.16	19.96	90.59
1943	9.12	28.84	7.99	0.24	0.13	10.75	4.38	13.28	7.98	7.09	9.6	17.52	116.92
1944	12.72	2.67	0.23	0.11	0.1	0.1	1.26	17.86	13.95	7.97	12.18	7.59	76.73
1945	15.86	4.55	0.31	0.15	0.13	28.35	8.81	1.05	1.54	3.75	4.54	3.07	72.09
1946	3.21	1.75	0.14	0.09	2.22	34.71	14.65	8.67	5.68	11.65	5.43	10.01	98.2
1947	6.13	7.17	0.75	6.87	1.01	9.96	13.87	4.62	2.7	3.35	1.79	5.38	63.59
1948	31.6	10.47	0.36	2.75	0.16	0.13	4.22	8.06	3.55	2.63	2.17	1.84	67.94
1949	1.05	32.37	7.75	0.2	0.13	0.1	4.17	4.58	1.66	5.12	6.65	4.49	68.28
1950	13.67	21.02	4.56	28.01	7.09	5.8	2.83	4.47	6.82	17.16	9.26	18.43	139.11
1951	7.31	0.66	0.22	3.55	1.47	0.18	2.38	1.7	1.64	2.08	5.77	24.01	50.98
1952	9.97	14.12	4.73	1.01	1.45	0.15	4.35	1.62	3.43	20.43	10.46	12.03	83.75
1953	14.62	10.06	0.97	0.18	0.15	2.46	15.44	25.72	10.96	7.57	27.31	11.14	126.57
1954	3.18	6.74	0.74	5.98	26.19	6.1	1.26	1.63	3.1	6.4	8.19	8.51	78.03
1955	7.02	3.51	0.28	0.17	0.15	9	5.46	20.64	8.96	6.23	8.14	5.77	75.34
1956	18.08	4.16	9.91	1.27	7.99	5.71	2.85	10.61	22.09	12.45	13.9	18.72	127.73
1957	10.48	1.47	0.25	0.16	0.15	11.79	7.8	46.64	18.78	4.25	16.96	8.12	126.83
1958	4.57	1.92	0.32	8.07	13.26	16.82	28.28	20.34	7.4	26.7	23.04	9.91	160.61
1959	25.58	6.99	0.43	2.03	0.35	7.93	6.93	7.88	10.06	7.27	4.63	7.18	87.26
1960	3.14	13.62	13.35	9	1.76	3.42	3.74	8.82	4.96	7.1	10.54	8.2	87.65
1961	12.78	4.3	0.24	1.21	6.8	13.12	10.88	4.71	4.06	3.53	76.14	24.23	162.01
1962	12.29	20.28	3.35	3.03	0.21	18.46	8.54	11.31	4.93	7.56	4.64	1.4	96.01
1963	6.92	4.12	5.84	10.67	3.11	12.06	4.29	2.09	15.39	6.64	11.77	18.43	101.32
1964	10.12	7.55	0.46	0.16	4.12	7.65	7.31	13	5.81	5.04	5.97	2.57	69.76
1965	32.09	27.07	9.39	5.82	0.19	2.97	4.3	13.83	6.64	3.57	22.98	18.5	147.33
1966	4.35	0.49	0.18	0.14	1.42	10.3	70.61	35.54	15	12.92	11.71	16.36	179.03
1967	5.58	8.41	0.73	0.2	0.17	2.24	6.28	11.17	15.16	5.64	14.82	8.73	79.13
1968	3.78	12.48	1.28	0.17	0.15	1.06	4.42	2.38	11.21	6.38	7.02	4.04	54.37
1969	2.15	0.3	0.15	2.44	6.98	0.58	0.13	0.53	2.03	3.11	12.77	4.29	35.47
1970	6.09	1.32	2.67	0.22	11.89	10.65	17.4	17.38	9.25	25.55	27.93	10.65	141
1971	4.62	12.92	2.4	0.24	6.98	7.19	9.97	9.53	5.46	5.62	15.16	15.93	96.02
1972	4.17	4.12	0.6	0.2	0.16	0.15	4.32	3.72	6.55	6.74	8.22	6.11	45.06
1973	2.74	2.97	3.04	10.33	16.18	16.39	3.86	21.99	9.24	2.4	16.64	11.27	117.05
1974	4.65	2.59	0.26	2.26	0.14	0.78	1.89	7.71	9.19	9.76	18.68	21.01	78.92
1975	7.25	8.94	3.52	0.9	8.5	11.83	8.16	9.08	18.85	14.58	8.22	6.93	106.76
1976	30.76	18.12	7.11	0.49	17.64	7.55	8.51	32.52	15.07	7.12	7.14	7.48	159.52
1977	6.22	10.92	4.42	0.25	0.19	0.82	7.96	3.91	3.27	5.72	10.25	6.23	60.16
1978	4.62	2.05	4.47	1.5	8.51	1.77	0.2	7.83	4.5	19.25	17.54	13.97	86.2
1979	10.73	2.38	4.33	4.36	0.89	0.18	2.46	1.41	5.91	3.06	5.04	7.09	47.84
1980	8.08	28.69	7.93	44.81	30.05	28.16	49.84	26.33	9.59	10.6	33.31	14.45	291.82
1981	4.11	1.32	9.04	1.11	1.86	6.02	74.49	23.04	9.27	12.03	11.29	23.5	177.08
1982	10.98	2.08	0.41	0.3	1.62	0.31	2.78	10.68	13.46	15.34	7.68	17.88	83.51
1983	8.84	10.95	1.64	0.31	0.5	7.8	3.61	2.08	1.9	5.93	3.08	0.95	47.59
1984	6.12	0.8	0.31	21.08	14.3	2.05	11.83	4.72	6.41	21.1	8.88	2.08	99.68
1985	31.72	18.65	9.84	0.4	0.28	1.45	2.72	1.22	1.19	2.26	96.27	32.48	198.48

1986	16.13	5.44	0.47	0.23	0.19	0.18	30.93	10.84	5.92	4.61	10.88	13.29	99.12
1987	3.25	0.5	1.63	0.2	0.16	3.03	17.15	6.65	7.05	6.14	8.83	5.73	60.33
1988	4.84	0.54	4.73	2.22	0.23	5.45	23.53	7.3	4.1	4.16	6.15	2.95	66.2
1989	35.87	21.16	0.64	0.22	1.43	0.61	30.67	14.74	15.36	6.93	4.53	2.94	135.12
1990	3.23	0.83	1.82	4.24	6.33	0.44	0.28	1.91	2.33	3.12	1.53	0.52	26.58
1991	48.19	11.8	1.88	0.29	2.43	3.94	2.99	3.61	10.03	12	7.68	5.62	110.46
1992	32.34	22.34	2.04	0.28	0.25	0.24	41.17	19.19	6.4	5.83	6.61	11.97	148.67
1993	3.5	0.6	14.61	2.53	4.17	6.04	7.8	4.69	4.31	5.47	17.93	9.03	80.66
1994	8.73	0.73	22.15	5.23	5.9	10.53	14.2	15	6.22	3.96	4.54	5.95	103.14
1995	3.08	31.28	35.5	7.67	0.24	5.28	2.1	0.75	0.75	5.85	2.65	4.1	99.25
1996	21.5	52.6	13.48	0.31	1.04	8.28	6.84	11.87	8.11	14.02	13.42	5.48	156.96
1997	2.11	2.34	0.2	2.08	1.78	19.08	17.33	9.96	4.45	5.45	4.64	2.75	72.18
1998	1.09	8.26	9.12	6.2	10.76	9.24	7.2	4.15	2.41	4.25	3.38	5.5	71.56
1999	10.23	1.97	0.15	12.81	3.8	35.52	10.36	9.62	4.04	2.17	2.29	1.96	94.92
2000	3.76	9.3	5.26	0.56	0.11	3.52	16.02	5.62	1.46	1.56	12.07	6.53	65.77
2001	3.01	7.11	0.93	2.99	2.55	0.13	3.73	6.64	4.67	5.51	10.96	10.92	59.15
2002	2.57	1.39	2.82	2.6	1.1	61.64	21.09	21.54	9.47	4.64	8.04	3.82	140.75
2003	12.11	2.46	0.24	0.18	4.14	2.69	15.75	6.62	4.18	5.53	3.59	4.08	61.57
2004	38.77	10.19	71.72	26.41	1.61	6.23	18.75	12.13	10.15	4.52	4.81	2.95	208.24
2005	0.54	0.31	0.15	3.06	2.33	1.23	14.99	13.42	7.36	26.73	54.42	20.11	144.64
2006	17.58	5.79	1.13	0.27	0.24	2.01	12.17	13.85	7.67	9.82	6.35	2.54	79.42
2007	3.1	131.12	48.94	5.08	4.19	1.87	1.88	0.97	5.65	2.71	4.02	3.29	212.83
2008	5.7	61.29	15.42	0.29	1.16	0.17	2.35	1.2	8.19	5.23	2.08	1.77	104.86
2009	11.66	4.24	0.25	0.1	0.09	0.18	1.84	1.68	6.6	5.24	3.43	1.59	36.91
AVERAGE	10.82	12.3	6.19	4.15	4.42	8.08	10.42	9.12	6.65	7.4	11.43	9.56	100.55

Table 2. Validation results for the Pitman modelled Goukou flow.

INDEX	UNITS	OBSERVED	SIMULATED
MEAN ANNUAL RUNOFF (M A R)	$m^3 \times 10^6$	14.5	14.65
STANDARD DEVIATION OF ANNUAL FLOWS (S)	$m^3 \times 10^6$	6.28	6.28
COEFFICIENT OF VARIABILITY (S/MAR)	PERCENT	43.27	42.88
COEFF. OF SKEWNESS	-	1.3072	1.3106
RANGE	PERCENT MAR	131	143.34
AUTOCORRELATION COEFF OF ANNUAL FLOWS	-	-0.1945	-0.1517
MEAN OF LOGS OF ANNUAL FLOWS	($m^3 \times 10^6$)	1.1252	1.1303
STD. DEV. OF LOGS OF ANNUAL FLOWS	-	0.1795	0.1773
INDEX OF SEASONAL VARIABILITY	PERCENT	7.55	6.05

In Figure 17 the average values indicates the average flow volume ($m^3 \times 10^6$) that reaches the estuary each year. 1X indicates the total volume of water that reached the estuary above the average flow, and 2X indicates the total amount of water above 2 times the average flow that reaches the estuary. These events therefore indicates a huge amount of water that runs off to the sea and therefore does provide merit for utilizing the water for MCAR.

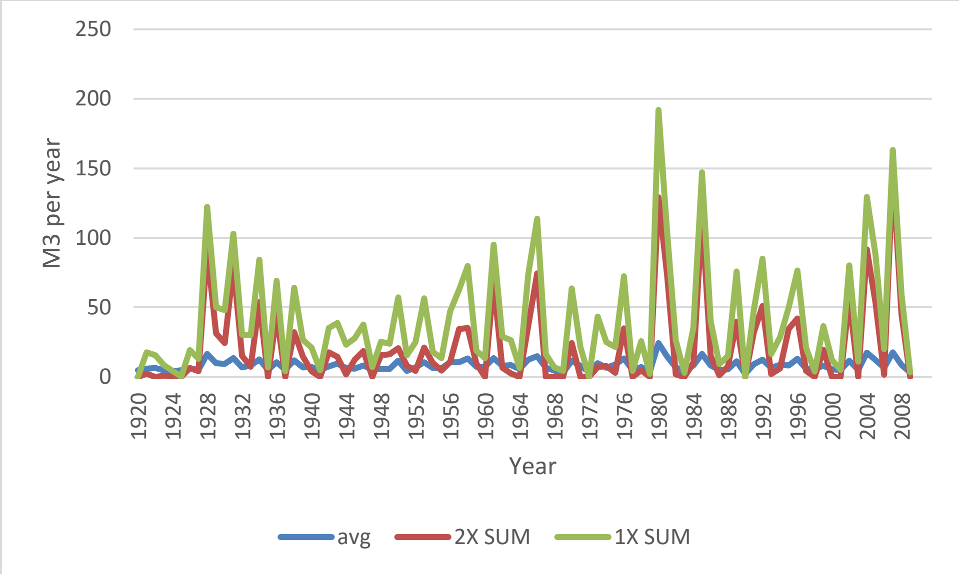

Figure 17. *Avg indicates the average flow volume (m3 x 106) that reaches the Estuary each year. 1X indicates the total volume of water that reached the estuary above the average flow, and 2X indicates the total amount of water above 2 times the average flow that reaches the estuary.*

1.5.2. SPATSIM

Once the WRSM/Pitman model has been refined, it will be used as input for the SPATSIM (Spatial And Time Series Information Modelling framework) model. SPATSIM was developed from the earlier HYMAS system (Hughes & Palmer, 2005 ; Rhodes University, 2020). It is based on the Pitman model, but is more extensive and will be used in this project to model baseflow and the ecological reserve. The ecological reserve is important for MAR projections, as it is the minimum flow that has to be maintained to ensure the health of the river.

https://www.ru.ac.za/iwr/research/software/

1.5.3. JAMS

The Jena Adaptable Modelling System (JAMS) J2000 was set up for the catchment and we are in the process of calibrating the model. At first glance, we do not get better results than the Pitman results and we think that the deep aquifers are not linked. We hope to solve this through isotope analysis.

More information about the JAMS model can be found here: http://jams.uni-jena.de/

2. SAT scheme at Agon-Coutainville, France

The MAR/SAT system in Agon (Normandie, France) is based on a treatment of secondary WWTP effluent by an activated sludge process and by a combined reed bed and sand dune filtration. Since 2016 (implementation in the H2020 Aquanes project), the imaGeau Subsurface Monitoring System (SMD) has provided real time monitoring of saline intrusion. Water quality and quantity have been monitored and analysed by SAUR and BRGM or sending information and data towards an ICT tool (BRGM/Géo-Hyd) dedicated to assess efficiency of SAT in context of saline intrusion (implementation in the H2020 Aquanes project). The monitoring systems and modelling efforts are enhanced with the EviBAN Project.

MAR in France

In France, the main objectives of using current artificial recharge are to improve the quantitative or qualitative state of the water resource for the final use of groundwater intended for the production of water for human consumption (irrigation, AEP). On a database of 75 artificial recharge sites (Casanova et al., 2013), 20% of the sites allow the improvement of the qualitative state, 30% of the quantitative being, 20% the mixture of the two. The rest were not identified.

Managed aquifer recharge (MAR), as currently implemented in France, aims to improve the quantity and/or quality of water resources, the recharged water being mostly taken from surface water courses and conveyed directly to infiltration basins. This method allows the water to undergo a second filtration before it reaches the groundwater table. Direct injections into the water table are rarely used.
Recharge water is either taken directly after bank filtration, taking advantage of the self-purifying capacity of the soil, or treated directly by UV treatment, microfiltration and decantation techniques according to the necessary quality objectives. The use of surface water is explained by its availability, its chemical and microbiological quality. The use of reuse of treated water remains limited in France, as the regulatory context does not easily allow it but under development.
Most of the sites in France allow for: generate piezometric domes making it possible to protect catchment fields from AEP withdrawals, to prevent against saline intrusion, to preserve groundwater, to support an over-exploited groundwater table. There are also MAR scheme to regulate the flow of rivers in order to prevent floods or low water levels (Oise basin, project on the Garonne River).

Apart from increasing water security, MAR is also being used internationally as a nature-based solution to reduce environmental pollution, through soil aquifer treatment (SAT). MAR combined with SAT is one of the most efficient and affordable strategies to recycle treated wastewater to enhance the quantity and quality of groundwater and secure groundwater systems under stress (Dillon et al., 2019). SAT consists of a controlled passage of treated wastewater through porous media mainly for purification purposes. Some organic pollutants are not fully transformed during wastewater treatment process e.g oxidation, ozonation, or bioreactor. Many organic compounds and contaminants of environmental concerns can be found in the treated wastewater. SAT can serve as an additional treatment of these contaminants and natural improvements of water quality have been demonstrated using SAT systems for reducing contaminants of environmental concerns contained in treated wastewater (Dillon et al., 2019).

Secondary Treated Wastewater (STWW) from wastewater treatment plants (WWTPs) is typically used for SAT systems because it is a continuous source of water released daily from human activities, less subject to climate change than surface water. Many sites, primarily coastal, favor infiltration of STWW into the aquifer (Kloppmann et al., 2012; Masciopinto and Carrieri, 2002; Shammas, 2008; Vandenbohede et al., 2008). Infiltrated water then allows for increased groundwater recharge to address local issues (i.e. freshwater quantity, salt wedge, restoring the resource, avoiding direct discharge to surface water), in addition to providing a complementary treatment step for water treated by the wastewater treatment plant.

Recent studies have revealed the ubiquitous presence of Trace Organic Compounds (TrOCs) in wastewater treatment plant effluents and receiving surface waters (refs). These TrOCs (i.e. pharmaceuticals, personal care products, pesticides), are not totally degraded during the passage in conventional wastewater treatment plants (Drewes et al., 2002; Ternes, 1998) where the treatment technique (activated sludge) is the most used in France and in the world for the treatment of domestic wastewater. TrOCs are then discharged in considerable quantities into receiving waters through treated wastewater effluents. In recent years, their concerns have been increasing about environmental and human health effects (Lapworth et al., 2012) examples. Although the mode of release of STWWs into SATs provides an additional treatment step prior to their release into the environment (Bekele et al., 2011), many uncertainties reside in the fate of TrOCs in SAT systems. Understanding the fate and transport of TrOCs after their release into the SAT are challenges that must be addressed.

In France and Europe, there are no specific national regulations, standards or guidelines on the practice of MAR. French regulations allow managed aquifer recharge on a case-by-case basis after prefectural authorization provided that its use does not compromise the achievement of environmental objectives for the recharged groundwater body, an environmental impact assessment is carried out for the implementation of such systems. The Water Framework Directive (WFD, 2000/60/EC) also establishes a framework for water policy and requires that a water monitoring programme be established in each river basin district and sets objectives for achieving good quality and quantity status in the aquatic environment.

SAT challenges regarding Trace Organic Compounds (TrOCs)

The fate of TrOCs in the context of SAT, depends on both hydrogeological conditions and reactive processes via microbial transformations (biodegradations) and/or sorption (Maeng et al., 2011 and references therein). The reactivity of TrOCs, depends on many site-specific factors that provide a very wide range of degradation (Greskowiak et al., 2017) or sorption (Scheytt et al., 2005, 2006) depending on study sites and experimental conditions. Redox conditions strongly alter the reactivity of TrOCs (Burke et al., 2017; Regnery et al., 2015). Degradation is often quantified by first-order laws, where the decrease in concentration C in time t (the degradation rate of a contaminant r) is expressed as μ, the first-order degradation rate (1/d, with d the half-life of the molecule) (Greskowiak et al., 2017):

$$r = \frac{dC}{dt} = -\mu C$$

Knowledge of the residence time of water infiltrated through the SAT and the dilution of groundwater with other waters transiting the aquifer (e.g. groundwater, infiltrating rainwater, water exchanged with rivers or the sea) is necessary for the interpretation of the reactivity of TrOCs and the quantification of the degradation rates of the molecules studied (Massmann et al., 2008). For this purpose, low/non-reactive elements (tracers) are often used to trace the infiltrated waters in the SAT and infer their dilutions and residence times (i.e. Amy and Drewes, 2007; Bekele et al., 2014; Guillemoto et al., 2022; Massmann et al., 2008; Moeck et al., 2017). These experiments conducted under specific conditions characterise the dynamics of the SAT in question at a particular spatial and temporal scale, the results of which are difficult to transfer to another scale. At an annual temporal scale, the groundwater flow regime is modified by local meteorological conditions, anthropogenic uses of groundwater (pumping, irrigation...), surface water dynamics, and possible water exchanges between rivers and the aquifer and the sea.

To take into account all the modifications of the groundwater flow regimes, the dynamics and the exchanges with surface waters (sea, rivers) at these temporal and spatial scales, groundwater flow and solute transport models are often used (Kloppmann et al., 2012). Flow and solute transport models allow, among other things, to quantify the volumes of water exchanged and their speed of movement in the hydrosystem in order to deduce the residence time of water infiltrated via the SAT and its dilution (i.e. Henzler et al., 2014; Vandenbohede et al., 2008). Simple models (analytical models) provide estimates of groundwater residence times, dilution but are not suitable for highly variable boundary conditions. More often, numerical models are used. Numerical models can simulate flow and solute transport, suitable for simulating variable flow conditions and water exchange with the external domain.

Coastal SAT site: Agon-Coutainville, Normandy, France

The commune of Agon-Coutainville (Normandy), with an estimated population of 2,800 residents (INSEE, 2015), is one of the oldest seaside resort of the Manche department and the location of the largest production of shellfish in France. The preservation of the coastal ecosystem, and the associated sanitary stakes are essential for local economy and has to be fully integrated to the ongoing development of residential areas, tourism and shellfish aquaculture. Subject to a large tidal range, the groundwater resources are prone to salinization in this coastal area, resulting in a superficial hydraulic area with low capacity for water supply. Sustainable water management has to take the seasonal variation of the population and the irrigation needs of the backshore golf courses into consideration. In addition there is a need to adhere to environmental regulations (eg.French Coastal acts) and an ambitious water quality target, in spite of financial constraints (requiring a minimal cost system). To face this demanding challenge and to preserve the estuary ecosystem in Agon-Coutainville, a SAT system has been considered as locally more efficient and sustainable than the conventional direct discharge system of secondary effluent to surface water (river or sea). For this reason, a SAT system was integrated at this site as part of the full-scale operational wastewater treatment plant and sustainably integrated within the municipal wastewater treatment line during more than 15 years (French sanitation database).

The Agon-Coutainville site (Picot-Colbeaux et al., 2021) is a SAT system where STWW is alternately discharged into a dune aquifer via different infiltration basins. At the Agon-Coutainville site, recent studies have highlighted the reactivity of the SAT on several TrOCs (Carbamazepine, tolyltriazole, benzotriazole, oxazepam, caffeine) under specific conditions, on a monthly temporal scale and in the vicinity of one of the infiltration basins (Guillemoto et al., 2022). Monitoring of 32 TrOCs, including pharmaceuticals, antibiotics, anticorrosive compounds, and industrial, in STWW and groundwater at the site scale also shows a decrease in their concentration with no clear distinction between the reactive portion of the SAT and the dilution portion with other waters transiting the aquifer (Pettenati et al., 2019; Picot-Colbeaux et al., 2021).

The particularity of the Agon-Coutainville site is that it is part of a coastal system where strong piezometric variations are observed, mainly caused by tides, natural recharge and STWW volumes. Consideration of variations in groundwater quality and residence times is necessary to distinguish the portion of reactive and hydrodynamic processes that affect TrOCs concentrations in groundwater.

EVIBAN Aim study

The objective is to quantify the variations in residence time and dilution of infiltrated water (STWW) in the Agon-Coutainville SAT as a function of natural (natural recharge and runoff) and anthropogenic (controlled recharge) hydrodynamic forcing, and then to deduce their effects on TrOCs concentrations in the aquifer at the spatial scale of the aquifer (kilometer scale) and at the multi-year temporal scale.

Applied to the SAT site of Agon-Coutainville, a groundwater flow and transport numerical model is developed to simulate the variations of groundwater flow velocities and the mixing of water infiltrated via the SAT (STWW) at the scale of the hydrosystem by taking into account the dynamic forcing of groundwater (meteorology, tides, SAT infiltrations).

The method used is 1) to conceptualize the major groundwater flow and transport processes taking place in the system and the associated modeling assumptions: conceptual model; 2) to adapt the conceptual model into a mathematical model: numerical model; 3) to analyze the results of the simulations and particularly the velocities and dilutions of the water infiltrated into the SAT; 4) to identify the major groundwater flow lines and the impacts of the forcing factors on the efficiency of the SAT with respect to the TrOCs.

This work is part of the understanding of the fate of TrOCs in a dynamic coastal SAT system. From the modeling results, the quantification of residence and dilution times are relevant tools to predict the fate of TrOCs at the scale of a site and/or to distinguish between reactive processes and others related to flows on the removal of TrOCs observed on the site.

2.1. SAT MODELLING (BRGM)

Draft paper Quentin et al. in WATER – ISMAR11 special issue, deadline January 2023

Interaction of a SAT system with the hydrosystem at multi-annual scale and consequences on TrOCs attenuation

Q. Guillemoto, G. Picot-Colbeaux, D. Valdès, N.Devau, C. Thierion, D. Idier, F. Mathurin, M.Pettenati, W.Kloppmann, J-M. Mouchel.

2.1.1. Introduction

Managed Aquifer, Recharge (MAR) is a palette of active aquifer management methods that can provide a local response to water scarcity, water security, water quality degradation, depleted aquifer, and endangered ecosystems (Dillon et al., 2020). In coastal environments, Soil Aquifer Treatment (SAT) is one possible MAR technique that not only recharges the aquifer, but also provides natural purification of the incoming water as it passes through the soil and the unsaturated and saturated zone of the aquifer.

Wastewater Treatment Plant (WWTP) is one of the water sources that can be used for SAT systems. Domestic or municipal treated wastewater is a source of water released daily by continuous human activities and therefore not subject to climate change. Many SAT sites, primarily in the coastal zone, favor infiltration of this type of water into the aquifer (Kloppmann et al., 2012; Masciopinto and Carrieri, 2002; Shammas, 2008; Vandenbohede et al, 2008), often via infiltration basins where recharge occurs intermittently to maintain infiltration rates (avoid clogging) and good soil oxygenation to renew the biological and chemical treatment capacity allowed by the soil and subsoil (Sharma and Kennedy, 2017). Infiltrated water recharges the groundwater and provides a complementary treatment step for the water treated by the wastewater treatment plant, in response to local water stress or environmental issues (e.g., freshwater quantity, saltwater intrusion, resource restoration, avoidance of direct discharge to surface water or the sea).

Many trace organic compounds (TrOCs), such as pharmaceuticals, personal care products, and pesticides, are present in wastewater and are not fully degraded during passage through WWTPs (Drewes et al., 2002; Ternes, 1998). TrOCs are then discharged in considerable quantities into receiving waters via WWTP effluent and can reach various environmental compartments such as groundwater (Bunting, 2021) and rivers (Aemig et al., 2021). Some TrOCs and/or their metabolites persist in their active forms and can be ecotoxicologically hazardous to the environment as well as to human health (Pereira et al., 2015). SAT can provide additional treatment of TrOCs present in treated wastewater (Amy and Drewes, 2007; Drewes et al., 2002). Nevertheless, many uncertainties reside in the fate of TrOCs in SAT systems.

The behavior of TrOCs in the context of SAT depends on both hydrogeological conditions and reactive processes (Maeng et al., 2011). The reactivity of TrOCs, depends on many factors which results in a very wide range of values for the commonly used degradation coefficient (Greskowiak et al., 2017) or sorption coefficient (Scheytt et al., 2005, 2006) depending on hydrodynamic conditions, soil properties (e.g. redox conditions, temperature, biomass, organic matter inputs...) and physicochemical properties of the molecules (e.g. pKa, charge, hydrophobicity; Maeng et al., 2011; Regnery et al., 2017). On an annual time scale, large changes in reactivity conditions (e.g., redox conditions, organic matter, temperature) and system flow (e.g., groundwater dilution, flow velocities) can alter system performance.

To estimate and optimize the performance of MAR systems, numerical modeling tools are often preferred (Kloppmann et al. (2012). At the scale of an operational SAT system, few studies evaluate TrOC removal using flow and reactive transport modeling (e.g., Henzler et al., 2014; Sanz-Prat et al., 2020). Reactive transport modeling is often simplified by using first-order degradation rate constants and linear adsorption coefficients. Nevertheless, interpolation of these parameters can be tricky if reactivity and/or flow conditions are variable.

The Agon-Coutainville site (Picot-Colbeaux et al., 2020) is a SAT system where Secondary Treated Wastewater (STWW) is alternately discharged into a dune aquifer via different infiltration basins. This SAT system was implemented in order to avoid direct discharge of STWW into coastal surface waters and thus protect coastal economic activities (tourism, shellfish farming, natural protected area). A follow-up of 32 TrOCs, including pharmaceuticals, antibiotics, anticorrosive and industrial compounds, in STWW and groundwater at the site scale also shows a decrease in their concentration without a clear distinction between the reactive part of the SAT and the dilution part by other waters transiting the aquifer (Pettenati et al., 2019; Picot-Colbeaux et al., 2020). To quantify the reactive part of SAT, an experiment at a monthly temporal scale and in the vicinity of one of the infiltration basins (Guillemoto et al., 2022) highlighted the reactivity of SAT with several TrOCs (carbamazepine, tolyltriazole, benzotriazole, oxazepam, caffeine).

The particularity of the Agon-Coutainville SAT site is that it is part of a coastal system where strong piezometric variations are observed, mainly caused by tides, natural recharge and infiltrated STWW volumes. Due to the uncertainties regarding the reactivity of TrOCs in a SAT and the possible variations in hydrodynamic conditions, the understanding of the fate of TrOCs in a SAT context on an annual scale is very complex. The identification of the reactive processes and their variations over time in such systems requires first of all a precise characterisation of the hydrodynamic variations that modify the residence times and the dilution of STWW infiltrated into the hydrosystem.

The objective of the present study is to quantify the variations in residence time and dilution of infiltrated water (STWW) in the Agon-Coutainville SAT site as a function of natural hydrodynamic forcing (natural recharge and runoff, tide) and anthropogenic forcing (controlled recharge via the SAT), and then to anticipate their effects on TrOC concentrations in the aquifer on the spatial scale of the aquifer (kilometre scale) and on the multi-year temporal scale.

Applied to the Agon-Coutainville SAT site, a numerical flow and transport model is developed to simulate variations in the flow and mixing velocities of infiltrated water (STWW) in the SAT at the hydrosystem scale. The method used is 1) to conceptualise the major flow and transport processes taking place in the system on the basis of piezometric measurements and concentrations of an intrinsic tracer (here the Chloride non-reactive element, Cl^-) 2) to transform this conceptual model into a numerical model; 3) to calibrate the numerical model, the hydrodynamic and transport parameters on the piezometric measurements and Cl^- concentrations; 4) to analyse the results of the simulations and particularly the velocities and dilution of the water infiltrated into the SAT; 4) to identify the major flow lines and the impacts of the forcing on the effectiveness of the SAT with regard to the TrOCs.

This work is part of the understanding of the fate of TrOCs in a dynamic coastal SAT system. From the modelling results, the quantification of residence and dilution times are necessary tools to predict the fate of TrOCs at the scale of a site, while making a distinction between the reactive processes and the processes linked to flows on the abatement of TrOCs observed on the site.

2.1.2. Study area, METHODS AND MATERIALS

a) Study area : Agon-Coutainville, Normandy, France

The Agon-Coutainville commune is located in France in Normandy, along the West coastline of the English Channel, between the Hague pointe, and the bay of Mont Saint Michel and is 10 km from Coutances (Figure 2). The commune is one of the oldest seaside resorts in the Manche department and is home to the largest shellfish farming area in France. The SAT system has been implemented for more than 20 years as a complement to the treatment of wastewater from the wastewater treatment plant (WWTP) instead of a direct discharge of secondary-treated wastewater (STWW) into the sea. The WWTP is designed for 35,300 population equivalents and uses activated sludge biological treatment. The STWW is transferred by gravity to the SAT and infiltrates via infiltration basins with a total surface area of 29,000 m² to reach a sand dune aquifer. The infiltration basins are separated in 3: basin 1, basin 2 and basin 3 (Figure 2). Each basin infiltrates STWW during 4 months in an alternating way then not solicited the rest of the year according to a theoretical calendar followed by the operator.

The geology of the site is mainly composed of Precambrian metamorphic rocks (schists) surrounding the Coutances quartz diorite (granites) (Figure 2) on which Quaternary aeolian sands and recent dune sands lie (Dupret et al., 1987). These sands constitute the dune aquifer in which the SAT is developed. It lies on the shale metamorphic rocks which, to the east, delimit it when they outcrop. The sand dune aquifer extends into the marine area to the west.

Located on the coast at about 600m from the sea (Figure 2), the SAT system is subject to tidal cycles. On this site, the main cycles are (1) semi-diurnal cycles (with a period of 12.25 h), (2) bi-monthly cycles (with a period of 14.8 days) between a period of high tide and a period of low tide, (3) annual cycles, linked to the solstice and equinox cycles. Tidal variations are very significant, with a tidal range of up to 13m. The position of the salt water zone and the freshwater/salt water interface are poorly identified in the study area in the absence of vertically discretised observations.

The climate is temperate and oceanic with an average annual rainfall of 850mm. Seasonal variations in sunshine and rainfall are observed between the winter period from October to March (the wettest months) and the summer period from April to September (the driest months). Two rivers cross the study area (Figure 2), the Ganne to the north and the Goulot to the south, which have their source on the heights of the metamorphic and granitic hills to the east and flow into Blainville Harbour.

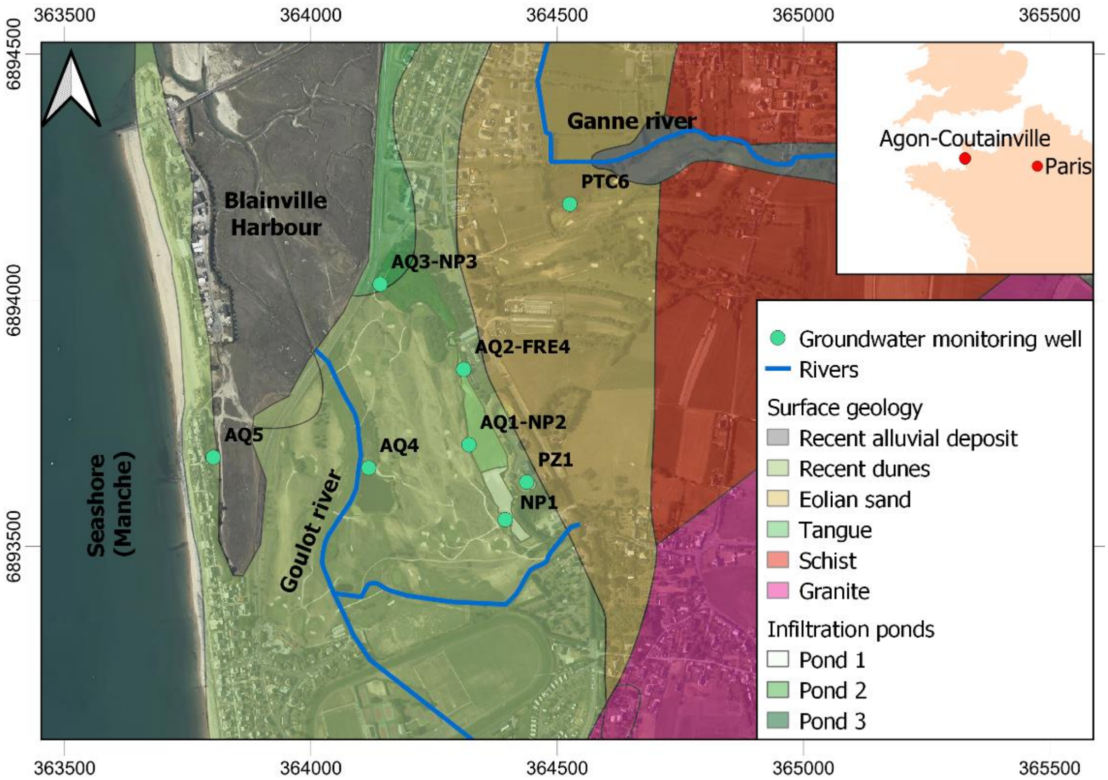

Figure 2 Location map of the SAT site in Agon-Coutainville (3 infiltration basins=ponds), position of the wastewater treatment plant (WWTP), monitoring observation wells (NP1, AQ1-NP2, AQ3-NP3, AQ2-FRE4, AQ4, AQ5, and Pz1), hydrographic network (blue lines), coastline and harbour, and surface geological formations

b) Available and acquired data

The data available on the study site are summarised in the Table 1. Surface geological information, detailed by Dupret et al., 1987, and spatialized information translated into a geographic information system by BRGM (Vernhet, 2003) are used. Vertical geological information is provided during the creation of the piezometers present on the site (Figure 2). Spatial topography information is provided by a 1 m and 25 m resolution digital elevation model (DEM) and by point measurements of differential GPS (Global Positioning System) to measure the altitude of the boreholes and to delimit the spatial geometry of the site (delimitation of the infiltration basins). The spatial position of the watercourses is delimited with the BDTOPO® database (IGN). Precipitation and PET data for the period 2006 to 2021 are available on a daily basis from the Gouville-sur-Mer weather station (Météo-France) located 10 km south of the study site.

For the period 2010 to 2021, the daily flows of STWW are acquired by means of radar monitoring of the levels in a Venturi channel. Between 2010 and 2021, the biological oxygen demand (BOD5) was measured at a frequency of 24 measurements per year. Between 2016 and 2021, Chloride, Cl^-, was analysed 9 times in the STWW.

Eight piezometers screened across the thickness of the dune aquifer (Figure 2) provide access to groundwater measurements. Groundwater quality, STWW and STWW flows have been monitored for over 20 years within a regulatory framework (Picot-Colbeaux et al., 2020). From 2016 to 2021, the site was the subject of 9 measurement campaigns on groundwater quality and STWW as part of the AQUANES (Pettenati et al., 2019) and EVIBAN (Water JPI, 2022) research projects. The data used in this study were obtained in the framework of regulatory monitoring and the various research projects. In groundwater, Cl^- concentrations were measured in piezometers NP1, AQ1-NP2, AQ2-FRE4, AQ3-NP3 and PZ1 between 2010 and 2021 at a monthly frequency from September to June and every two weeks from July to August. From 2017 to 2021, water level measurements (based on pressure measurement corrected by atmospheric pressure) are acquired continuously at piezometers AQ1-NP2, AQ2-FRE4, AQ3-NP3, AQ4 and AQ5 (Garceran, 2017). In addition, continuous electrical conductivity measurements are acquired at piezometer AQ5. The initial measurement frequencies are 15 minutes, but due to difficulties in obtaining complete data (remote transmission, equipment maintenance), gaps and frequency changes are present in the acquired time series. From 2017 to 2021, nine manual measurements of piezometric levels were carried out on piezometers NP1, AQ1-NP2, AQ2-FRE4, AQ3-NP3. Three manual measurements of piezometric levels were carried out on point PTC6. From 2020 to 2021, pressure and conductivity measurements were carried out for piezometers NP1 and PZ1 by CTD-Diver probes (Van Essen®) at a time step of 15 minutes (barometric probe located at NP1).

Table 1 Available and acquired data on Agon-Coutainville SAT site

Type of data	Location	Measurements & Frequencies	Sources
Groundwater level	AQ1-NP2, AQ2-FRE4, AQ3-NP3, AQ4, AQ5,	Probes 15 min, 2017-2022*	Projects AQUANES (04/2017 to 04/2019) + EVIBAN (04/2019 to 12/2022)
	NP1, AQ1-NP2, AQ2-FRE4, AQ3-NP3, AQ4, AQ5, PZ1**, PTC6**	9 Manual measurements from 2017 to 2021	Projects AQUANES (6 from 04/2017 to 04/2019) + EVIBAN (3 from 04/2019 to 12/2022)
	NP1,PZ1	Probes 15 min, 2020-2022	EVIBAN project
GW analysis of Cl^-	NP1, AQ1-NP2, AQ2-FRE4, AQ3-NP3, PZ1	12-14 per year	SAUR operator
	NP1, AQ1-NP2, AQ2-FRE4, AQ3-NP3, PZ1	9 field campaigns from 2016 to 2021	Projects AQUANES (6 from 04/2017 to 04/2019) + EVIBAN (3 from 04/2019 to 12/2022)
STWW analysis of DBO5	WWTP outlet	24 per year	SAUR operator (2006 to 2022)
STWW Flow	WWTP outlet	Radar Ventury channel, hourly	SAUR operator (2010-2022)
Meteorology	Gouville	Precipitation and PET, daily	METEO-FRANCE
Geology	Normandie	Maps – cross section	(Dupret et al., 1987) (Vernhet, 2003)
	NP1, AQ1-NP2, AQ2-FRE4, AQ3-NP3, AQ4, AQ5, PZ1, (PTC6)	logs	SAUR Operator
Topography	Normandie Agon-Coutainville	normalized to elevation (ASL) 25m normalized to elevation (ASL) 1m	Region Region
Rivers	France	Map - Streams - network	BDTOPO® (IGN)

**Numerous missing data on continuous measurements ** only 3 piezometric measurement campaigns for PTC6 and 2 for PZ1*

c) Methodological approach

To quantify the residence time of STWW through the SAT and further into the dune aquifer as well as their dilution with other waters transiting the aquifer (groundwater, natural recharge, exchange with rivers and/or the sea), the proposed approach relies on numerical modeling tools for simulating flow and solute transport within hydrosystems under various external forcings.

The main steps proposed to quantify the flow velocities and STWW proportions at the SAT study site on a multi-year and dune aquifer scales (Figure 3) are i) the elaboration of a conceptual flow and transport model of the hydrosystem ii) the implementation of the conceptual model in a numerical model according to the selected code and the imposed boundary conditions adopted to take into account the major forcings, iii) the calibration of the numerical model, iv) the simulations of the flow and the groundwater mixing, v) the sensitivity analysis of the model and vi) adequacy of the simulation results to the question on the fate of TrOCs in the SAT.

The model describes the key hydrogeological processes in the study area, thus making simplifications and proposing boundary conditions that are assumed to be acceptable to achieve the modelling objective (Refsgaard and Henriksen, 2004). The conceptual model is developed from the field features of the study area and the available site data (piezometry, water quality, STWW flows, etc.) and includes both the description of flow processes, geological features, river network elements, etc.

Boundary conditions and geometry are implemented in a manner consistent with the conceptual model to allow for multi-year transient flow and solute transport calculations to represent the dynamics of external forcing and the operational dynamics of the SAT. The modelled domain allows the extension of the SAT, the natural groundwater outlet of the aquifer, and the identified aquifer boundaries to be framed.

The hydrodynamic model is then calibrated from 2017 to 2021 using time series of piezometric levels observed at the site. Due to its conservative nature and the contrasting concentrations between the different waters (STWW, sea, natural recharge, river), chloride (Cl^-) was chosen to calibrate the hydrodispersive parameters of the solute transport model. To distinguish the progression of STWW from other waters transiting through the aquifer, the calibrated model is also used by simulating for the same period from 2017 to 2021 a concentration of a theoretical non-reactive element present at 100% only in the STWW infiltrated in the SAT. The calculated concentrations in the hydrosystem (initially at 0% in this theoretical element) indicate the proportions of STWW present and thus their dilution to other waters in the hydrosystem (saline intrusion, natural recharge, river) considered at 0% presence of theoretical non-reactive element.

The modelling results allow the calculation of hydrodynamic balances, identification of flow directions, calculation of water flow velocities in the pores, transit times along the main flow lines, and STWW proportions.

The average and the coefficient of variation (CV) of the velocities and proportions of STWW is proposed from the simulation results to represent in each cell of the model the variations over a hydrogeological year (from October 1st to September 30th) accodring to:

$$CV = \frac{\sigma}{\mu} \tag{1}$$

With σ the standard deviation and μ the mean. The larger the CV coefficient the greater the dispersion around the mean. The calculation is mapped for two distinct hydrogeological years, 2017-2018 (low winter recharge) and 2020-2021 (high winter recharge). Temporal variations in flow velocity and dilution ratio are quantified from 2017 to 2021 on 4 main flow lines from the SAT STWW infiltration basins to the natural groundwater discharge.

The calculated flow velocities and STWW proportions are related to natural and anthropogenic forcings to identify their impacts on the SAT. To identify the similarities between the time series of the forcings and the calculated time series of flow velocities and STWW proportions, the cross-correlation function (CCF) is used. Between two time series x and y, it is defined by:

$$\rho^{xy}(k) = \frac{\sum(y_t - \bar{y})(x_{t-k} - \bar{x})}{\sqrt{\sum(y_t - \bar{y})^2}\sqrt{\sum(x_t - \bar{x})^2}} \tag{2}$$

Where x and y are the velocity and forcing time series, $\bar{x}$, $\bar{y}$ are the means of the series, k is the lag (Shumway and Stoffer, 2017), and ρ is the correlation coefficient, which varies between -1 and 1. The closer the value of ρ is to 1 or -1, the more correlated the two series are, or inversely correlated (at lag k), the closer ρ is to 0, the less correlated the series are (at lag k).

A sensitivity analysis is then carried out to assess the sensitivity of the flow velocity and STWW proportion results to modelling choices (boundary conditions) or model calibration parameters. The analysis then allows the identification of key parameters or model choices to be characterised more precisely in order to reduce the uncertainties of the results.

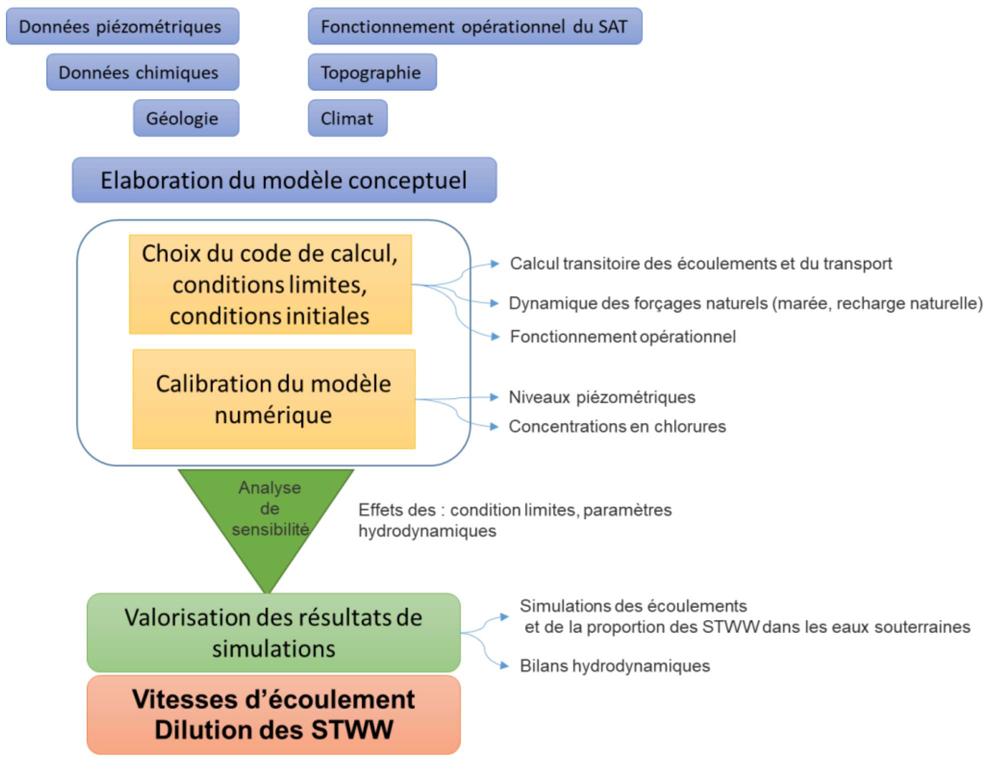

Figure 3 Modeling approach for the quantification of flow velocities and STWW proportions of the SAT in its hydrosystem.

2.1.3. MODELING

d) Conceptual model: the local SAT system in its hydrodynamic aquifer context.

Coastal sand dune aquifer

The topography of the study area is closely linked to the geological nature of the subsoil. The ground elevation ranges from 50 mASL at the level of the prominent reliefs formed by the outcropping metamorphic rocks in the east, to 0 mASL at sea level towards the west at the reliefs planed by the presence of sands that form the coastal dune aquifer (Figure 4). In the sand deposition zone (Figure 2), the topography delimiting the top of the aquifer is a subhorizontal zone of 5-6mASL of low slope marked locally by natural topographic depressions where the zone of interest (SAT) is located. This zone is separated from the harbour of lower altitude by a dam-road of 8-9mASL altitude. The topography defines several hydrological watersheds, including the Ganne and the Goulot, which cross the sandy deposits on their lower part and both flow into Blainville Harbour (Figure 4). The surface of the Ganne and Goulot watersheds on the lower part represents 2.2km^2 of the area of interest while the surface of the watersheds on the upstream part where metamorphic rocks outcrop is 3.7km^2 (Figure 4). On the upstream part of the watersheds a transfer of water to the sandy areas is more than likely via runoff and infiltration at the foothills or via the streams.

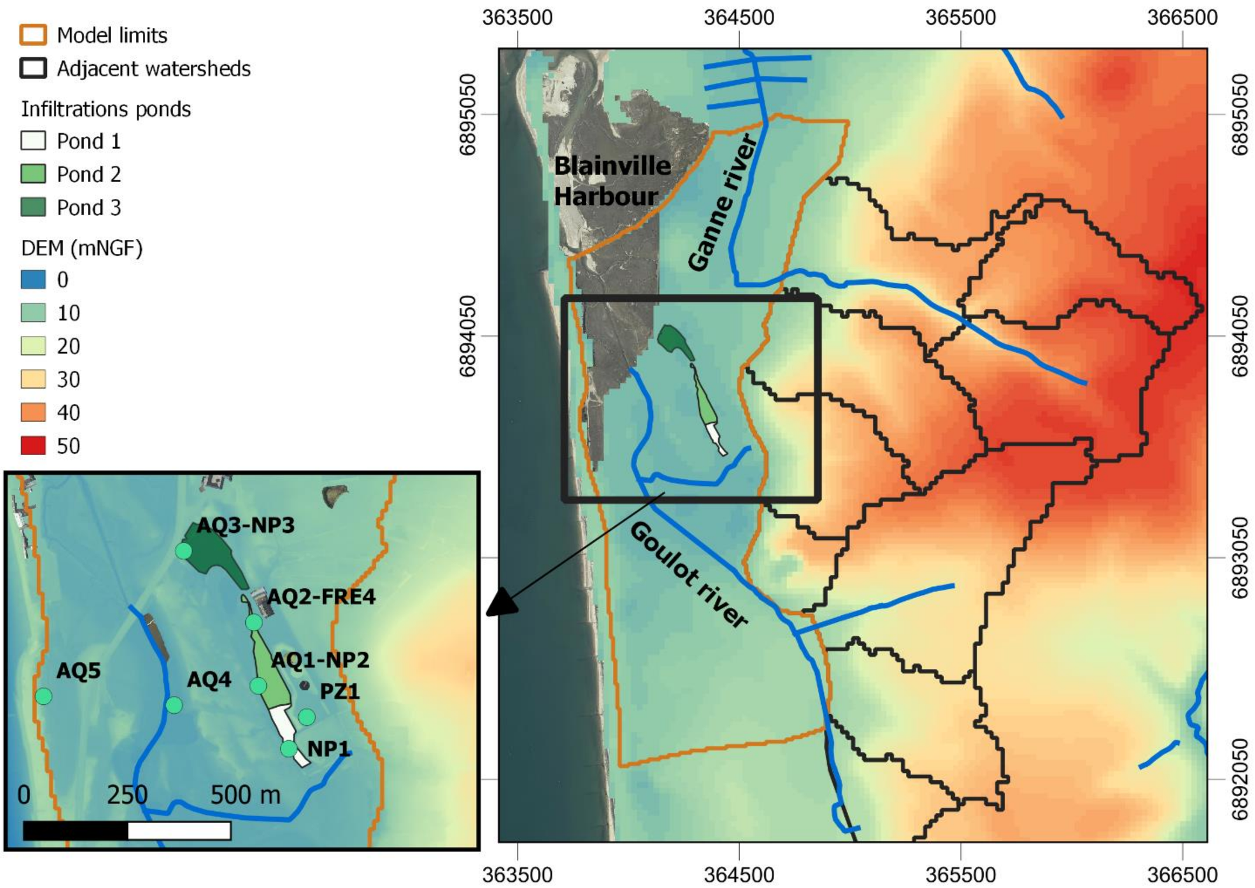

Figure 4 Topography (25m DTM and 5m DTM) and boundaries of the adjacent upstream watersheds and of the hydrologeological model extent including the SAT system (infiltration ponds).

The dune aquifer is covered by a very thin layer of vegetal soil. The aquifer bottom is delimited by the assumed impermeable metamorphic bedrock. Although groundwater can circulate in the fractured networks of the bedrock schists, giving rise to low-flow emergences (Dupret et al., 1987), no observation or exploitation has been confirmed at the study site (no measurements attesting to possible water exchange between the dune aquifer and the metamorphic rocks have been made). The thickness of the dune aquifer is thicker to the west (9m at piezometer AQ5, close to the sea) and the layer bevels towards the east reaching thicknesses of about 5m close to the infiltration basins (Garceran, 2017; Lithologic; 2014) and disappearing at the metamorphic foothills. The boreholes show a vertical overlay of coarse and shell sands, and at depth the presence of green clays is an indication of erosion of the shale bedrock. "Tangue" deposits (fine clayey to peaty material with low permeability) may be present as discontinuous layers within the sands (Dupret et al., 1987) but was not observed in the various boreholes available at the site. The hydraulic conductivity (K) of coarse non-clay sands is estimated to be between 10-2 and 10-5 m/s, and between 10^{-5} and 10^{-9} $m.s^{-1}$ for fine clay sands (de. Marsily, 1983). The effective porosity of coarse sands can range from 15 to 35% (Appelo and Postma, 2005). For eolian sands, with a smaller grain size, the effective porosity can decrease significantly (de. Marsily, 1983).

The dune aquifer contains a free sub-surface groudwater which piezometric measurements show higher average levels in the east (5.1 ± 0.50 mASL at PZ1; 45.1 ± 0.46 mASL at NP1) than in the west (4.5 ± 0.17 mASL at AQ4 and 3.1 ± 0.32 mASL at AQ5) (Figure 12). A main flow gradient is then observed from east to west on the order of 10^{-3}. On an annual scale, the groundwater table changes by about 0.5m to 1.0m due to the variation of the STWW infiltration rates in the SAT and the natural recharge of the aquifer. Vertical flows through unsaturated zone can be assumed to be negligible compared to horizontal flows due to the small thickness of the unsaturated zone ranging from 0 to 1.5m. The storage capacity in the unsaturated zone of the dune aquifer, for a porosity of 15% to 35%, is approximately 0.49 to 0.99 Mm^3.Depending on the year, the piezometric levels exceed the ground surface especially in the topographic depressions and in the infiltration basins (5.4 mA on average in the basins). The groundwater then overflows and remains on the surface before infiltrating back into the aquifer, which can be observed in the field by localized flooding during the winter period. The Cl^- concentrations measured in the aquifer vary from one piezometer to another (i.e. on average 36 ± 46 mg/L at PZ1; 151 ± 90 mg/L at NP1 and 500 ± 1000mg/L at NP3) but also temporally in the same point (Figure 13). The observed variations in piezometric levels and groundwater concentrations indicate different sources of water input to the aquifer. The main contribution of external forcing may come from natural recharge and runoff (freshwater input), from the tide (brackish water input), from STWW discharges infiltrated into the SAT (variable salinity water input) or from aquifer-river exchanges (freshwater input).

Natural recharge and runoff

Over the period 2006 to 2021, the month with the highest average precipitation is November (109 mm/month on average) and the months with the lowest precipitation is April (40 mm/month on average). The natural recharge of the water table takes place mainly during the winter period from October to March, when the PET values are low and the precipitations are higher (Figure 5). The hydrogeological years defined between October 1st and September 31th integrate the recharge-discharge cycle of the water table: a period of natural recharge from October to March at the end of which the groundwater table is in a high-water situation and a period of natural discharge from April to September at the end of which the groundwater table is in a low-water situation. Specifically over the period synchronous with the piezometric measurements from 2017 to 2021 the average annual rainfall is 825mm. Precipitation is minimum in 2018-2019 with a total of 628 mm and maximum in 2020-2021 with a total of 952 mm.

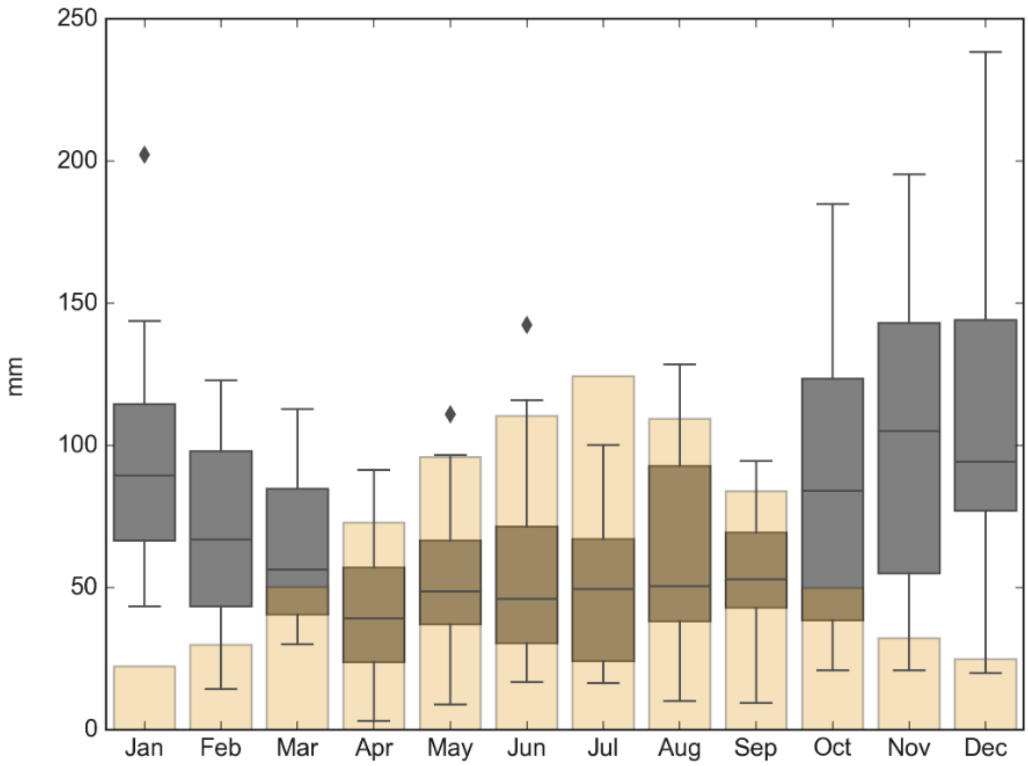

Figure 5 Monthly inter-annual variations calculated over the period from 2006 to 2021 for rainfall in mm/month (gray) and median PET (orange) in mm/month at the Gouville-Sur-Mer station. The bar in the centre of the boxplot represents the median of the monthly data, the "extreme" observations are represented by diamonds; these are observations that contrast greatly with the overall observations (x1.5/interquartile)

The quantity and distribution of natural recharge are estimated using a GARDENIA reservoir model (Thiéry, 2014) applied at the scale of the dune aquifer (surface 2.2km^2 see Figure 4) from daily rainfall and PET records. Due to the very low slopes of the dune aquifer and its sandy character, the natural recharge is considered close to the effective rainfall with a negligible part of runoff. The model reservoir parameters (soil and unsaturated characteristics) are therefore selected to minimize the amount of runoff and maximize the natural recharge (Supplementary Material 1). Calculated "direct" natural recharge flows that reach the modeled aquifer surface (Figure 4) average 0.84mm/d (1707m^3/d) over the period 2017 to 2021 (Figure 6). Minimum flows are calculated over the 2018-2019 water year averaging 0.45mm/d (1008m^3/d) and maximum flows over the 2019-2020 water year averaging 1.1mm/d (2452m^3/d). Cumulative annual recharge (280mm) represents 34% of cumulative precipitation, which corresponds to the order of magnitude of natural recharge in Metropolitan France (Seguin, 2015).

In addition, runoff from adjacent watersheds (Figure 4) probably constitutes an additional natural indirect recharge of the dune aquifer considering that part of the effective rainfall infiltrates at the foothills. Due to the presence of outcropping shales, considered non-aquiferous, with significant slopes on the upstream parts of the watersheds (4% slopes), runoff reaches the dune aquifer either via the network of streams or via the eastern edge of the aquifer. The Cl^- concentration measured at PZ1 (Figure 2) is very low (36mg/L on average); local infiltration of runoff from the upstream catchments on the eastern edge would prevent the progression of STWW infiltrated in the SAT towards PZ1 located between the eastern edge and the catchments. The amount and distribution of runoff is also estimated using the GARDENIA model. The model reservoir parameters are chosen this time to maximize runoff and limit recharge. The runoff rate, considered as additional natural recharge of the dune aquifer along its eastern edge, is estimated by taking into account the surface of the watersheds adjacent to the aquifer which corresponds to the upstream metamorphic part (3.7km^2). The calculated runoff flow (indirect recharge) average 156mm/y (1579 m^3/d) over 2017 and 2021 (Figure 6) which represents 84% of the direct recharge flows.

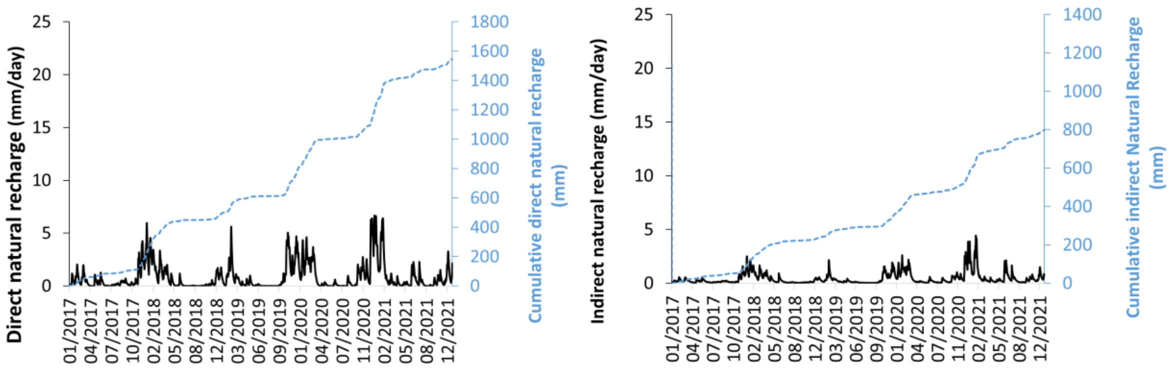

Figure 6 Estimation of "direct" natural recharge on the dune aquifer (left) and local natural recharge on the eastern edge of the aquifer by runoff (right).

Streams and rivers

The Ganne stream to the north is far from the SAT area of interest and crosses the dune aquifer for a very short distance, in contrast to the Goulot stream, which crosses it from south to north perpendicular to the major east-west groundwater flow directions, probably impacting the groundwater flows from the SAT. The Goulot lies directly on the dune aquifer with a bottom on which a deposit of organic matter and fine sediments can accumulate. The clogging permeability of a streambed can be highly variable, from 10^{-9} to 10^{-2} $m.s^{-1}$ (Nguyen et al., 2017), depending on the presence of fine sediments in the stream. The water level of the Goulot is around 4.7mASL and can vary seasonally. The depth of the streambed varies between 30cm and 60cm, its width between 4.0 and 5.5m. The river is locally artificialized to pass under a part of the city (in its southern part) before being blocked on a part of the Golf by the dam limiting its discharge into the harbour. Further upstream, intermittent and smaller streams supplied mainly by runoff from metamorphic rock areas flow into the Goulot. No monitoring stations record stream flows. However, field observations indicate a low flow of the Goulot (order of magnitude 500-5000 m^3/day) and the streams are often dry depending on weather conditions and groundwater levels.

See and harbour

The dynamics of the sea modify the piezometric levels and the salinity of the groundwater along the coast. The piezometric levels are marked by the tidal cycles, in particular by monthly variations ("high water" and "low water" cycles) on the piezometers AQ3-NP3, AQ4, AQ5 located closer to the sea and the harbour and by daily variations of low amplitude (approximately 0.1 m) on the piezometer AQ5 (Figure 7). Cl^- analyses and electrical conductivity measurements attest to the salinity of the groundwater and its spatial and temporal evolution. The main variations in salinity linked to the sea are observed at piezometers AQ3-NP3 and AQ5. During high tidal coefficients, which occur most of the time at equinoxes, the sea progressively fills the Blainville harbour, which borders basin #3 of the SAT, where the AQ3-NP3 piezometer is located, by a few metres and can cause significant increases in Cl^-, particularly during equinoxes (Figure 7).

Cl^- analyses indicate maximum point concentrations of 11 180 mg/L in AQ3-NP3, and electrical conductivities in AQ5 of 12 481± 3 678 µS/cm on average. Given a Cl^- concentration of 19 000 mg/L in the sea (Millero et al., 2008) and the characteristics of the groundwater at PZ1 with an average Cl^- concentration of 36 ± 46 mg/L and an average conductivity of 568 ± 47 µS/cm, the proportion of seawater in the groundwater can reach more than 50% at the edge of the sea and the harbour. Analyses and measurements are carried out on the entire water column due to the presence of the observation well screens that cover almost the entire thickness of the aquifer.

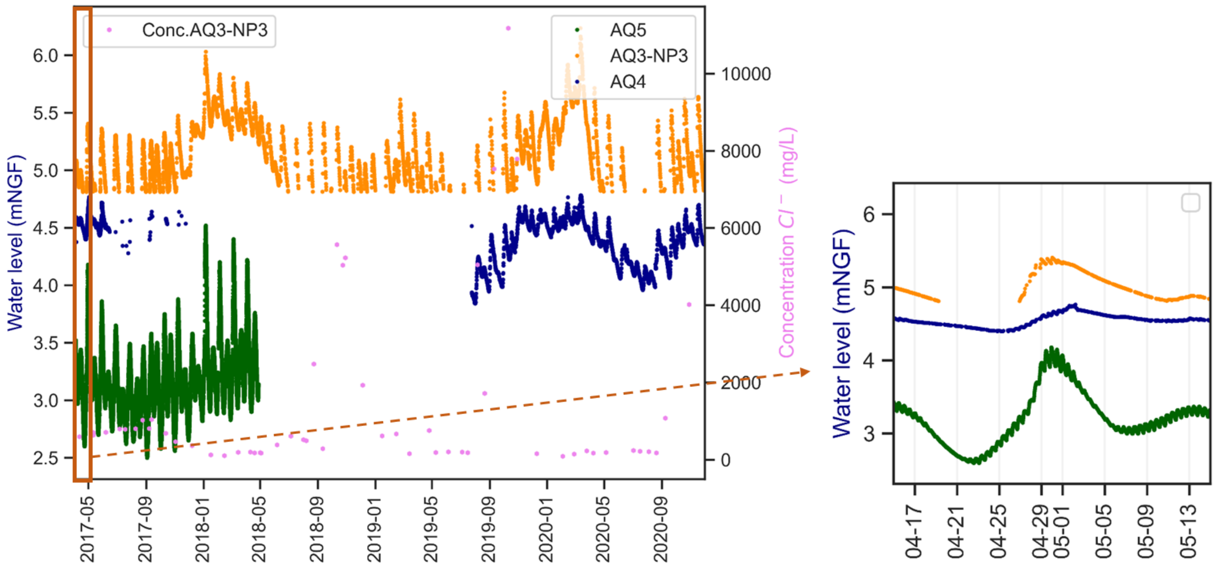

Figure 7 Piezometric data on AQ5, AQ4 and AQ3-NP3 observation wells and Cl^- concentrations on AQ3-NP3 over the period from 01/01/2017 to 01/05/2018 and zoom on the period from 15/04/2017 to 15/05/2017

STWW infiltrated in the SAT

The STWW is discharged alternately into the different infiltration basins of the SAT (basin #1, basin #2 and basin #3) according to a theoretical schedule conducted by the operator. The dates of switching of STWW infiltration from one basin to another are not rigorously archived. Precise knowledge of the evolution of the volumes infiltrated in each basin from 2010 to 2021 is impossible to know. Only the theoretical timetable and the information gathered from memory from the operator's technicians can be used to reconstruct a chronicle of the probable distribution of volumes by infiltration basin (Table 2). During the winter period, the infiltration basins are sometimes all loaded to avoid overloading the hydraulic network and flooding the WWTP, without exact knowledge of the distribution of volumes between the three infiltration basins. From January 2019, the rotation of STWW infiltration into the basins is stopped for technical reasons. Since this date, with all valves open, the volume of STWW is continuously infiltrated into the three basins without exact knowledge of the distribution of volumes per basin. From June 2021, the rotation is restored according to the theoretical planning initially defined. During the "winter" period from October to March, the average flow (inlet and outlet of the WWTP) is 1 728 ± 845 m^3/d with maxima of up to 5 500 m^3/d and minima of 379 m^3/d, whereas during the "summer" period from April to September, the average flow is lower, it is 1 235 ± 299 m^3/d with maxima of 3 600 m^3/d and minima of 174 m^3/d. These variations are mainly explained by the infiltration of parasitic clear water into the wastewater network, which is more significant during periods of heavy rainfall and in winter. In the summer period (March to October), part of the STWW is abstracted and stored for the irrigation of the nearby golf course (abstraction rate of approximately 500 m^3/d).

Table 2 STWW volume distribution schedule for the three infiltration basins.

Time period	***Basin #1***	***Basin #2***	***Basin #3***
from April to May	*100%*	*0*	*0*
from June to September	*0*	*0*	*100%*
from October to March	*0*	*100%**	*0*
**with the possibility of December to February*	*Opening the valves without knowledge of the distribution*	*Opening the valves without knowledge of the distribution*	*Opening the valves without knowledge of the distribution*
January 2019 to June 2021	*Opening the valves without knowledge of the distribution*	*Opening the valves without knowledge of the distribution*	*Opening the valves without knowledge of the distribution*

Cl^- is more concentrated in the STWW (417 ± 234 mg/L) than in the waters not/less affected by STWW (PZ1, Cl^- = 36 ± 46 mg/L). The variations in Cl^- observed in the piezometers near the NP1, AQ1-NP2 and AQ2-FRE4 infiltration basins follow a seasonal dynamic, possibly linked to dilution by parasitic clear water in the winter period. Cl^- is considered as a tracer of STWW in the areas not affected by the sea. Nevertheless, only a few point analyses of Cl^- are available for STWW, only since 2016, not allowing to capture the seasonal dynamics of Cl^- concentrations in STWW. The chloride concentrations are estimated from the BOD5 concentrations. The dilution variations of the STWW are, however, visible in the BOD5 concentration measurements acquired continuously since 2010. The BOD5 concentration reaches maximum average concentrations in summer (average in July 367 ± 77 mg/L) and minimum in winter (average in February 115 ± 70 mg/L). BOD5 represents the input of anthropogenic organic matter. Assuming that the variations in BOD5 concentration are mainly due to the dilution of STWW water by parasitic clear water, the variations in BOD5 are (like Cl^-) impacted by the dilution occurring during the winter period; this is verified by a linear relationship between the concentrations of Cl^- and BOD5 measured (coefficient of determination of 0.65 on 9 concentrations of Cl^- measured) The Cl^- time series can therefore be reconstructed from the BOD5 concentration chronicle (371 measurements between 2006 and 2021) by considering a factor of 0.61 between the BOD5 and Cl^- measurements available at the same dates ($Cl^- = \frac{DBO5}{0.61}$). The Cl^- concentration of STWW is estimated to average 408 ± 200 mg/L following the same seasonal variations as the measured BOD5 measurements. (Figure 10).

Synthesis of the conceptual model

All the flows and exchanges on the groundwater of the SAT site at Agon-Coutainville are summarised in Figure 8. The dune aquifer formed by homogeneous sands, 5m to 9m thick, contains a free groundwater table which flows mainly horizontally towards the west (gradient of the order of 10^{-3}), the thickness of the unsaturated zone is low with maxima of 1.5 m. The maximum storage capacity in the unsaturated zone is about 0.495 to 0.990 Mm^3 over the total surface area of the aquifer. Recharge and discharge of the groundwater vary according to the (1) seasonal inflow of natural recharge with an average of 1864 m^3/d of direct recharge and 1579 m^3/d of indirect recharge with a concentration considered negligible in Cl^-, (2) exchanges with the sea which cause significant variations in piezometric levels (e.g. AQ3-NP3, AQ4, AQ5) and saline intrusions (close to the Blainville harbour and the coastline) through inflows of salty water with high Cl^- concentrations (19 000 mg/L), (3) STWW inflows into the various infiltration basins with average flows of 1525 m^3/d and average Cl^- concentrations of 408 mg/L, These inputs vary seasonally in quality and quantity depending on the contribution of parasitic clear water (which increases in winter), (4) exchanges with the Goulot stream by draining the groundwater or adding water to the aquifer.

There is considerable uncertainty about the capacity of the stream to exchange with the groundwater body; the variations in altitude of the water level in the stream, the flow rates and the capacity for exchanges with the groundwater body are not known. Exchanges with the sea are not quantified, as they depend on the hydrodynamic conditions of the groundwater and the tidal conditions.

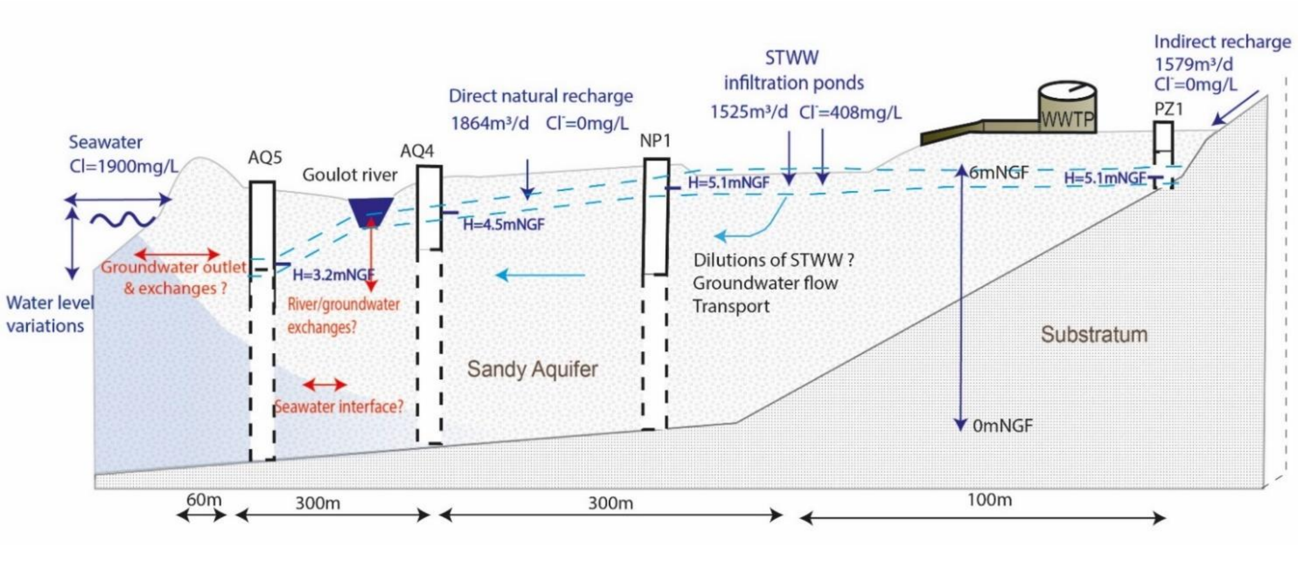

Figure 8 Conceptual model of the Agon-Coutainville SAT. Water blance and Cl^- concentrations in the hydrosystem.

e) Flow and solute transport equations

In this study, groundwater flow and solute transport are governed by the differential equations of flow and non-reactive solute transport (for Cl^-). These equations can be solved especially for multidimensional spaces by numerical methods (finite elements, finite differences, finite volumes).

The law of conservation of mass, associated with Darcy's law, leads to the free sheet equation:

$$\mathrm{div}\big(\mathrm{K.grad(H)}\big) + \mathrm{Q} = \frac{1}{\Delta z} S_L \frac{\partial H}{\partial t} \quad (3)$$

With K the hydraulic conductivity [L.T^{-1}], H the hydraulic head [L], Q the external flow rate per unit area [L.T^{-1}], Δz the vertical thickness of the layer [L], S_L the free-sheet storage coefficient, equivalent to porosity [-], and t the time [T]. The parameters K and S_L affect the rate at which groundwater moves through the aquifer, the volume of water stored, and the response of groundwater to stresses in the aquifer system.

The 3D solute mass conservation equation, in the absence of interaction between the solute and the solid phase and biochemical transformation is written:

$$\frac{\partial(\theta_m \cdot C)}{\partial t} = div\left(\overline{\overline{D}}\,\theta_m\,\overrightarrow{grad}(C) - \vec{q}C\right) + q_m \quad (4)$$

With C the concentration in mobile water [M.L^{-3}], θ_m the mobile water content [-], D the coefficient of dispersion [L^2.T^{-1}] with $\overline{\overline{D}}$ the dispersion tensor comprising $D_L = \alpha_L|v|\ et\ D_T = \alpha_T|v|$ with v the pore water velocity defined by $v = q/n_c$ where n_c is the effective porosity [L.T^{-1}], α_L the longitudinal dispersivity and α_T the transverse dispersivity [L], q_m= Injected mass flux per unit volume [M.L^{-3}.T^{-1}] and t the time [T], $\vec{q}$ the Darcy velocity [L.T^{-1}]. The diffusion is assumed to be negligible compared to convection and dispersion.

For solving the flow and transport equations, the MARTHE computational code (Table 3, Thiéry, 2021, 2020) was used. The differential equations of fluid flow and mass and energy transfer in three-dimensional porous media are solved numerically in transient regime. The hydrodynamic calculation is performed using a finite volume method (Finite Difference Integration). For the transient mass transport, the TVD (Total Variation Diminishing) method with flow limiter is used to solve the system of equations. Sub-time steps are automatically generated for the transport calculation by MARTHE to respect the low current conditions and thus reduce the numerical dispersion.

The convergence of iterative calculations is controlled by several criteria, mainly the average and maximum load and mass differences between two successive iterations (global on the whole model). In practice, the state of convergence of a model is mainly evaluated by indicators concerning the hydraulic and mass balance for the whole model. Hydroclimatic, hydrological and hydrogeological processes are coupled to model flow and solute transport. The calculation of the direct natural recharge on the dune aquifer aquifer is the result of the hydroclimatic calculation performed by the GARDENIA reservoir calculation scheme coupled with the MARTHE aquifer flow model.

A RIVER module included in the MARTHE code allows the calculation of water table-river exchanges.

Concerning the water table-river exchanges, for a river resting on a free water table but whose bottom is clogged by a low permeability mud layer, the exchanges between the river and the water table ($Q_{\acute{E}ch}$ [L^3.T^{-1}]) are calculated according to Darcy's law according to the water level in the river in relation to the water table level and according to the permeability of the river bed K_R [L.T^{-1}]:

$$Q_{\acute{E}ch} = SURF_{\acute{E}ch} \cdot K_R \cdot \frac{(H_R - H_N)}{\acute{E}pais} \quad (5)$$

With H_R river level [L] and H_N the water table level [L], $SURF_{\acute{E}ch}$ the river exchange area [L^2] and $\acute{E}pais$ the thickness of the riverbed clogging [L].

The table-river exchange is calculated according to equation (5). The volumes exchanged from the river to the aquifer are limited by the calculated in-stream flow (Q_{Amont}, Suppl. Mat.). The calculated runoff and overflow volumes (of the water table relative to the ground level) are taken over by the RIVER module and assigned to the river meshes.

Table 3 Features and parameters used in the MARTHE calculation code

Features	**Parameters**
Transient calculation	Time step, number of time steps, boundary conditions, initial conditions of water level H (t=0), concentration C(t=0)
Square mesh	Mesh sizes (x, y), number of active meshes, bedrock mesh heights, number of layers
Hydrodynamic calculation	Storage coefficient (SL), Hydraulic conductivity (K)
Transport	Longitudinal or transverse dispersivity (α_L and α_T), effective porosity n_c
River coupling (Groundwater and river exchanges calculation)	Hydraulic conductivity of the riverbed K_R, river level H_R, river exchange area $SURF_{Éch}$ and thickness of the riverbed clogging $Épais$
Hydroclimatic coupling (Recharge and Runoff calculation)	GARDENIA; parameters of soil and unsaturated zone (Supplementary material 1)

The systems of differential equations are solved from the constraints applied to the modeled domain. The definition of the initial conditions and the boundary conditions allow the numerical solution of equations (1) and (2). The boundary conditions represent the rules of exchange of water and mass flows between the modeled domain and the external environment. The initial conditions define the initial state of the system before the calculation of the system of equations.

f) Numerical modeling: the local SAT system in its hydrodynamic aquifer context

Geometry

The modeled domain of the dune aquifer follows the extension in Figure 4. The distance between the northern boundary (including Blainville Harbour) and the southern boundary of the model domain (including the Goulot stream) is considered sufficient to reproduce the main regional flows occurring in the SAT zone of influence. The aquifer top elevation corresponds to the topography derived from the Digital Terrain Model (DTM). In the modelled area, the altitude varies between 3.6 mASL and 14.2 mASL. The bedrock elevation of the aquifer is derived from interpolation of lithological sections from historical drilling on the site's piezometers. The thickness of the layer is between 14.4 m and 1.7 m with a decrease in thickness from west to east until the limit of the aquifer and the aquifer and the basement.

Discretisation in space and time

The domain is discretized into 22 192 square active meshes of 10 m by 10 m. Due to the small thickness of the thickness of unsaturated zone, and considering the predominantly horizontal flows, a 2D horizontal model has been horizontal model was selected, represented by a single layer.

A number of 310 river meshes allow for the modeling of the Goulot stream, the location of which is defined according to the hydrographic network of BDTOPO. The width of the river sections is 2 m. The bed elevation is set at 0.5 m below the local topographic elevation and the thickness of the clogged river bottom is 0.2 m.

In order to consider the temporal evolutions of the hydrogeological system, the model is built in transient regime integrating at the same time the variations of piezometry, concentration and flow related to (1) the tide, (2) the natural recharge, (3) the STWW infiltrated in the SAT. The daily time step is chosen to reproduce the variations related to these different forcings. At the scale of the modeled domain, the initial state of Cl- concentration being unknown and the solute transport process being inertial, a preliminary simulation is carried out from 2010 to 2017 to define a steady state of the groundwater concentrations from the different Cl^- inputs coming from the recharge, the sea and the infiltrated STWW. The period used for the calibration is from March 1, 2017 to December 31, 2021, discretized in 4 350 daily time steps.

Boundary conditions

The boundary conditions considered in the numerical model concern the overflows, the tidal boundary conditions (on the harbour and the western limit of the modelled domain, the boundary conditions considered in the numerical model concern the overflows of the water table, the tidal boundary conditions (on the harbour and at the western limit of the modelled area, *Figure 9*), direct natural recharge on the dune aquifer and indirect natural recharge at the eastern limit of the at the eastern boundary of the model domain from the basement catchments, the STWW discharged to the three infiltration basins and the Goulot and Ganne streams (*Figure 9*).

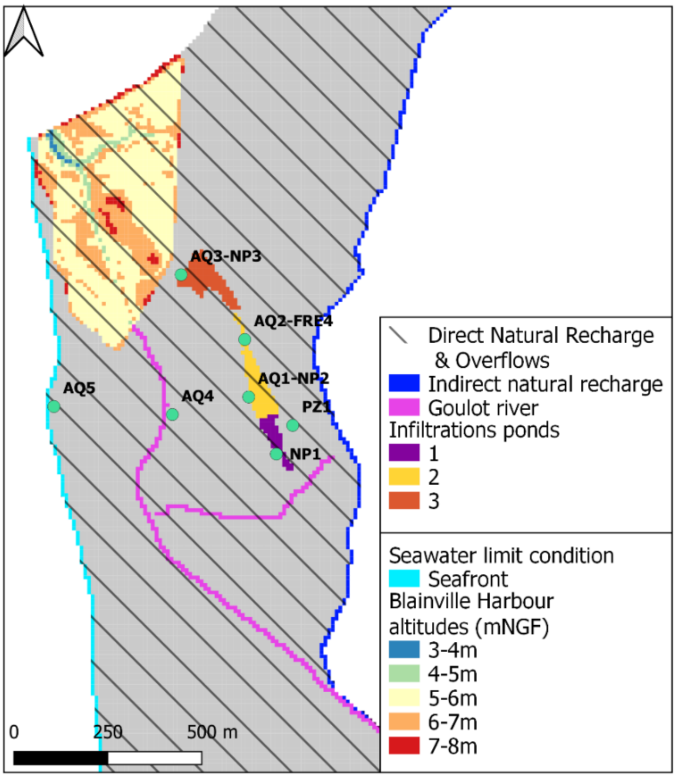

Figure 9 Boundary conditions applied to the numerical mesh hydrodynamic model MARTHE. The sea boundary conditions concern the boundary conditions of the sea front, the boundary conditions in Blainville Harbour, the direct natural recharge on the dune aquifer, the overflow on the modeled domain, the indirect recharge of the the indirect recharge of the bedrock catchments, the STWW flows infiltrated in alternation on the three infiltration basins, river boundary conditions.

In each of the meshes, the water table is considered to be free to overflow if the water table elevation exceeds the topographic altitude.

Direct natural recharge and runoff to the dune aquifer are calculated from the daily recorded rainfall and recorded daily rainfall and PTE time series from 2010 to 2021 via the GARDENIA calculation scheme. The calculation of direct natural recharge and associated low runoff is coupled to the coupled to the MARTHE model and is applied in each grid cell of the modelled area.

Indirect natural recharge flows to the dune aquifer from the basement watersheds are imposed on the aquifer meshes along the rim continuously and consistently at 1 500 m^3/d total based on estimates previously defined by the conceptual model. These fixed flows entering the edge meshes are homogeneously distributed corresponding to a flow of 6.0 m^3/d corresponding to a flow of 6.0 m^3 /d per mesh. The Cl^- concentrations of these waters brought by natural recharge and runoff are fixed at 0.0 mg/L.

The water table-river exchanges are calculated from the water level fixed in each river mesh (*Figure 9*), which is chosen to be constant and equal to the topographic altitude of the model meshes. River mesh (*Figure 9*), which is chosen to be constant and equal to the topographic altitude of the model meshes (or dune aquifer roof elevation).

The time-varying hydraulic head boundary condition is fixed on the meshes located at the western boundary of the model from north to south (*Figure 9*) which delineates the seafront.

These conditions are those representing the sea dynamics perceived in the water table and observed at AQ5 located near the sea. The measurements available at AQ5 over a one-year period between April 2017 and May 2018 and their piezometric dynamics are reconstructed over the modeling period from 2010 to 2021 based on the diffusivity equation via the computational code CATHERINE (Thiéry, 2012, Supplementary Material 2 : CATHERINE and tidal level simulation) that relies on the diffusivity equation and temporal sea level rise data reconstructed from the FES2014 harmonic component database (Lyard et al., 2021, Supplementary material 2: CATHERINE and tidal level simulation).

The progression of the sea in Blainville Harbour is represented by imposed hydraulic heads boundary conditions for some of the meshes comprising the harbour. The assignment of boundary conditions varies at the meshes in space as a function of sea level (*Figure 9*). At each computational time step, a hydraulic head corresponding to the maximum daily sea level is fixed on the aquifer meshes in the harbour with a topographic elevation below that level. At the highest tide levels (6 to 7 mASL) 96% of the harbour is considered as fixed hydraulic heads while a sea surface elevation below 3 mASL implies 0% fixed hydraulic heads in the harbour.

These boundary conditions imply lateral water exchange in the dune aquifer in both directions. Water entering the aquifer from these boundaries has a Cl^- concentration set to that of the sea of 19 000 mg/L (Millero et al., 2008).

The daily STWW flows imposed on the model vary over time based on data acquired by the operator (from 2010 to 2021) acquired by the operator (from 2010 to 2021) by subtracting summer withdrawals from the water needs of the golf course. The daily flows are imposed in a homogeneous way to the meshes of each basin. The daily flows are imposed in a homogeneous way on the meshes of each pond impounded according to the theoretical schedule of alternation of pond supply (*Figure 10*) as identified by the conceptual model. For the periods when the gates are open without precise knowledge of the position of the discharges (*Figure 10*) from December to February (before January 2019), the distribution of STWW flows set is 16%, 34%, and 49% for basin #1, 2, 3 respectively. Over the period after the alternation stops (January to June 2021), the flow distribution is set at 60%, 40%, 20% for basin no. 1, 2, 3 respectively. Outside of these periods, the meshes of the non fed basins are subjected to the flows and transport of solute transport without STWW injection constraints.

The Cl^- concentrations of STWW infiltrated in the basins are variable in time and the time series imposed in the model is reconstructed (*Figure 10*) from the chronicles of BOD5/0.61 concentration.

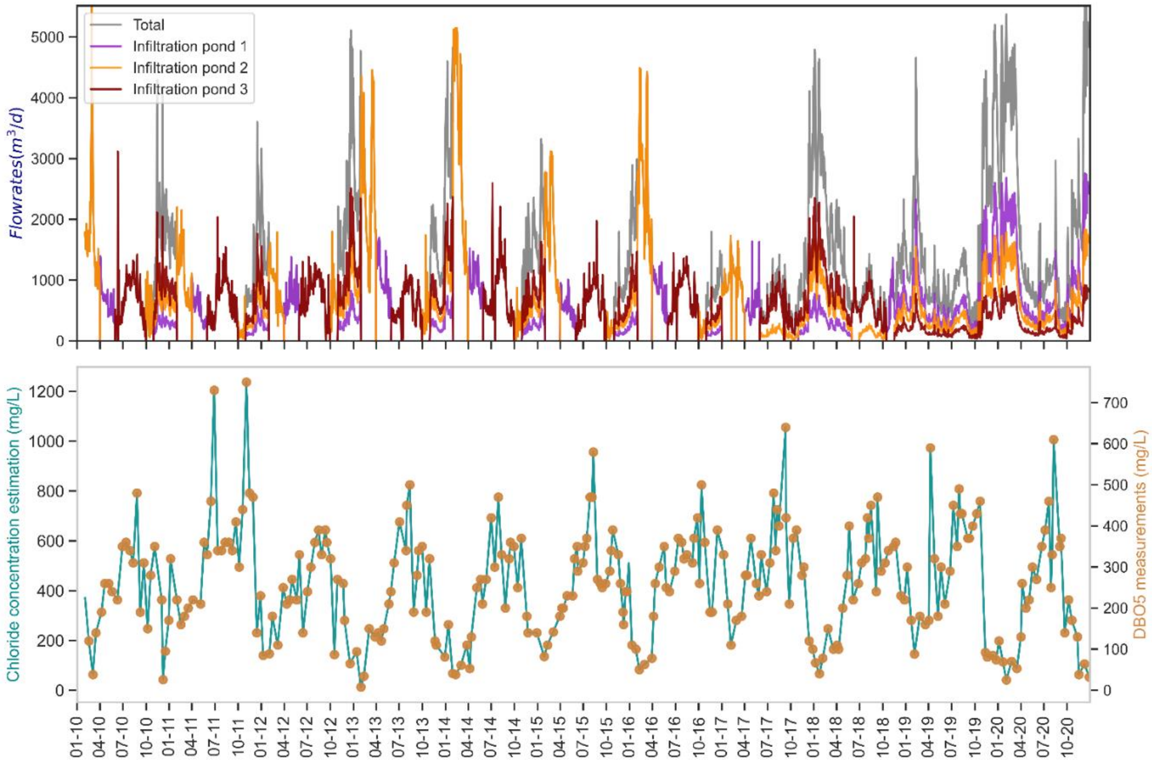

Figure 10 Time series of STWW infiltration flows in the different infiltration basins over the 2010 to 2021 and Cl^- concentration in the STWW reconstructed from the measured BOD5 concentrations.

Initial conditions

The initial conditions of hydraulic loads and Cl^- concentrations of the water table as of March 1, 2017 cannot be defined in all model grids, they are calculated with a seven-year of seven years, taking into account the conditions of tides, flows of STWW and natural recharge since 2010 by the natural recharge since 2010 by the model itself. It is ensured that the water table level and the Cl^- concentration simulated at the end of this period of equilibration of the model are of the same order of magnitude as those order of magnitude as those measured at the piezometers.

Modeling calibration

The model is calibrated for the period 01/03/2017-31/12/2021 by error testing on a range of parameter values that realistically represent the aquifer characteristics as identified by the conceptual model. The adjustment of the hydrodynamic and transport parameters is done in such a way as to reproduce the dynamics of the observed piezometric levels, and as much as possible, those of the Cl^- concentrations observed in the piezometers. The orders of magnitude of the stream flows are taken from the literature in the absence of measurements.

The root mean square error (RMSE) is used as a calibration criterion, especially for piezometric levels. RMSE is defined as:

$$RMSE = \sqrt{\sum_{i=1}^{n} \frac{(\hat{y}_i - y_i)^2}{n}} \quad (6)$$

With y_i the observed value and $\hat{y}_i$ the predicted value and n the number of observations. It therefore has the same dimension, and unit, as the variable of interest. The fitted hydrodynamic parameters are the hydraulic conductivity (K) and the free-sheet storage coefficient (S_L), assigned to two main zones that correspond to the outcrops of dune sands and eolian sands. Locally the permeability and clogging thickness of the river (K_R, $\acute{E}pais$) are adjusted.

The solute transport parameters in the aquifer, effective porosity, and dispersivity on (1) the actual velocities of water in the aquifer and (2) the dispersion of the solute. Since the effective porosity corresponds to the free storage coefficient S_L, these two values are equal. The longitudinal dispersivity value αL varies with the scale of investigation and reflects the influence of variability in aquifer heterogeneities. For sandy aquifers, αL values between 10 and 100 m are acceptable values at our scale of investigation (Gelhar et al., 1992; Schulze-Makuch, 2005). The vertical dispersivity αL weaker than αL (de Marsily, 1983), is set here at αL/10.

Modeling sensibilities and limits

The purpose of the model sensitivity analysis is to identify, on the basis of the calibrated model, the main parameters affecting the simulation results and the relevance of the assumptions. The values of the hydrodynamic and hydrodispersive parameters and certain boundary conditions (natural recharge, sea, northeast and southeast exchanges) are (natural recharge, sea, groundwater-river exchanges) individually modified within the ranges of values ranges of values identified by the conceptual model in order to evaluate their impact on flow velocities flow velocities and simulated water mixtures.

Different pairs of hydrodynamic and hydrodispersive parameters are tested. The sensitivity analyses sensitivity analyses concern (1) hydraulic conductivity values of the aquifer tested in the possible ranges of coarse sands from 2.0 10^{-3} $m.s^{-1}$ to 2.0 10^{-4} $m.s^{-1}$, (2) a homogeneous value of hydraulic conductivity value tested over the entire aquifer, (3) porosity values and the free storage (3) porosity values and free storage coefficient tested on the ranges of the bibliography for coarse sands 0.2 to 0.35, (4) a longitudinal dispersivity parameter tested here over a range of 10m to 100m.

For the direct natural recharge of the dune aquifer, the parameters of the GARDENIA model parameters are modified to simulate the effect of a lower recharge of about 10%. For the indirect natural recharge two simulations are tested: (1) the calculated chronic flows by the GARDENIA model are integrated into the numerical model. The flows calculated by GARDENIA (1579 m^3/d) are similar to the average flow initially set at 1500 m^3/d but vary with lower flows in summer and higher flows in periods of high precipitation, (2) an imposed load corresponding to the minimum values of the levels observed at PZ1 (4.5 m^3 /d) at PZ1 (4.5 mASL) is imposed at the limit of the dune aquifer.

In a simulation, only the tidal boundary conditions on the coastline west of the model are maintained (according to the model are retained (according to the piezometric levels reconstructed at AQ5 and the concentrations of 19000 mg/L) without considering a flooding of the harbour.

In view of the uncertainties on the characteristics of the Goulot stream (water level and geometry), the characteristics of the Goulot geometry), the characteristics of the Goulot are modified according to two conditions: (1) the water level is lowered by 0.4m with respect to the topographic altitude on the downstream part of the stream (located between the infiltration basins and the between the infiltration basins and the sea) and (2) the depth of the riverbed level is increased from 0.5 to 1.5 m in depth.

2.1.4. Results

g) Calibrated hydrodynamic and hydrodispersive parameters

The calibration of hydrodynamic and hydrodispersive parameters is performed over the period 03/01/2017-31/12/2021 for two geological zones, the recent dunes and the eolian sands (Figure 2). In these two zones, the values of the free storage coefficients are respectively 20% and 10%, and the respectively of 20% and 10%, and the values of hydraulic conductivity are respectively 2.0 10^{-3} m.s^{-1} and 5.0 10^{-6} m.s^{-1}. The dispersivity and groundwater-river exchange parameters are kept uniform over the modelled area in the absence of field observations indicating possible heterogeneities (Table 4).

Table 4 Calibrated hydrodynamic and hydrodispersive parameters for the coastal dune aquifer hydrosystem coastal dune aquifer (two zones corresponding to the outcropping geological layers of recent dunes and eolian sands)

Parameters	Recent dunes	Eolian sands
Storage coefficient S_L	20%	10%
Effective porosity n_c	20%	10%
Hydraulic conductivity K	$2 \cdot 10^{-3}$ m.s^{-1}	$5 \cdot 10^{-6}$ m.s^{-1}
Hydraulic conductivity of the riverbed K_r	$1 \cdot 10^{-6}$ m.s^{-1}	
thickness of the riverbed clogging $\acute{E}pais$	0.2 m	
Longitudinal dispersivity α_L and transverse dispersivity α_T	10 m, 1 m	

Comparisons of observed and simulated mean hydraulic loads align with the 1:1 line indicating a robust calibration of the hydrodynamic parameters, nevertheless with nuances highlighted by the root mean square results (*Figure 11*). For example, the lowest RMSEs are calculated for piezometers PTC6 and AQ4 with 0.10 m, 0.12 m respectively. Higher RMSE of 0.17 m, 0.18 m, 0.29 m and 0.24 m correspond to the respectively to the piezometers located near the infiltration basins AQ1-NP2, NP1 and AQ2- FRE4 and near the coast with AQ5. Finally, the maximum RMSE values are calculated at 0.31 m and 0.35 m at piezometers PZ1 and AQ3-NP3.

In addition, the modeled hydraulic heads reproduce the dynamics observed in the piezometric chronicles of the annual high water and low water cycles (*Figure 12*). The tidal cycles from high tides to low tides (14.8 days period) and their visible effects on the piezometric measurements are reproduced at piezometers AQ4, AQ3-NP3 and AQ5.

Differences are identifiable punctually on the piezometers close to the infiltration basins (e.g. August-October 2021 at NP1, PZ1) - related to the lack of information on the activated infiltration basins - or continuously as at AQ3-NP3 where the impact of the cycles of high and low tides is overestimated by the model.

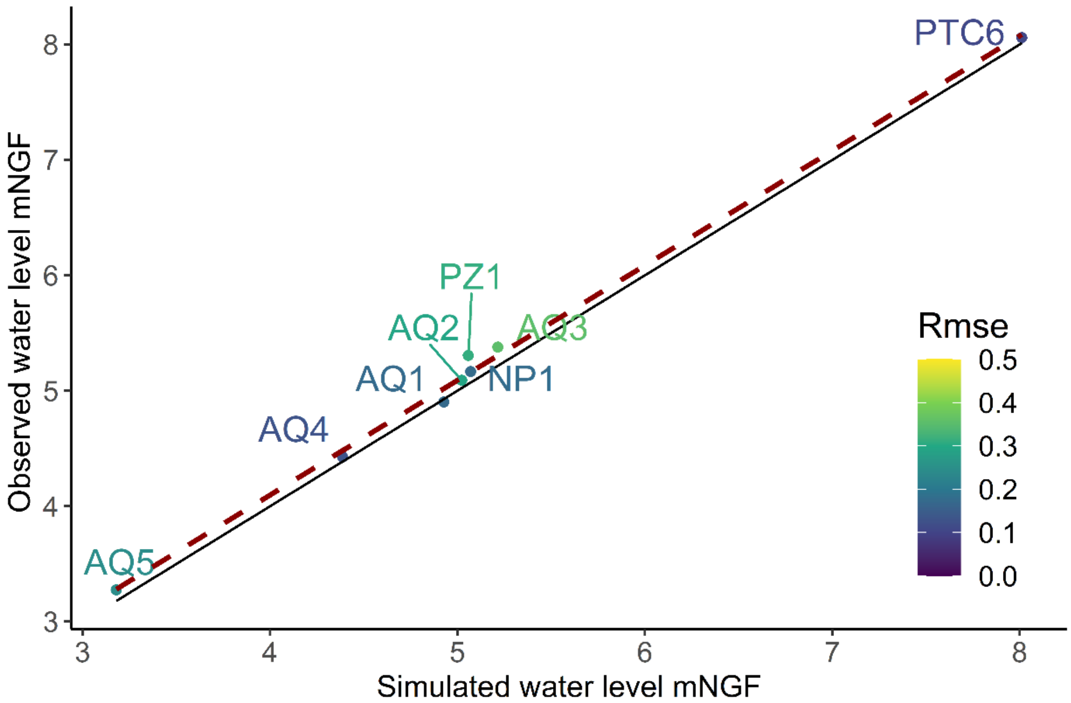

Figure 11 Plot of observed and simulated mean piezometric levels and associated calculated RMSE for the different piezometers.

The quality of the calibration can also be appreciated from the Cl^- concentrations. Over the calibration period, the simulated concentrations respect the orders of magnitude of the measurements (Figure 13). The concentration variations are globally well reproduced by the model with however a strong overestimation of the simulated concentrations near the Blainville harbour (AQ3-NP3, differences in average of 6700 mg/L), in connection with the condition at the sea limits in the harbour. Upstream, near the eastern edge (PZ1), a slight overestimation of Cl^- concentrations is observed (average differences of 66 mg/L), in connection with the indirect natural recharge boundary condition. At the piezometers close to the infiltration basins, the differences between the observed and simulated average concentrations vary between 12 mg/L (AQ1-NP2) and 146 mg/L (AQ2-FRE4) and punctually the differences can reach 500 mg/L (overestimation or underestimation). The calculated river flow varies from 8600 m^3/d to 25000 m^3/d at the outlet of the Goulot stream. The calculated flow is higher than the expected flow (500-5000 m^3/d).

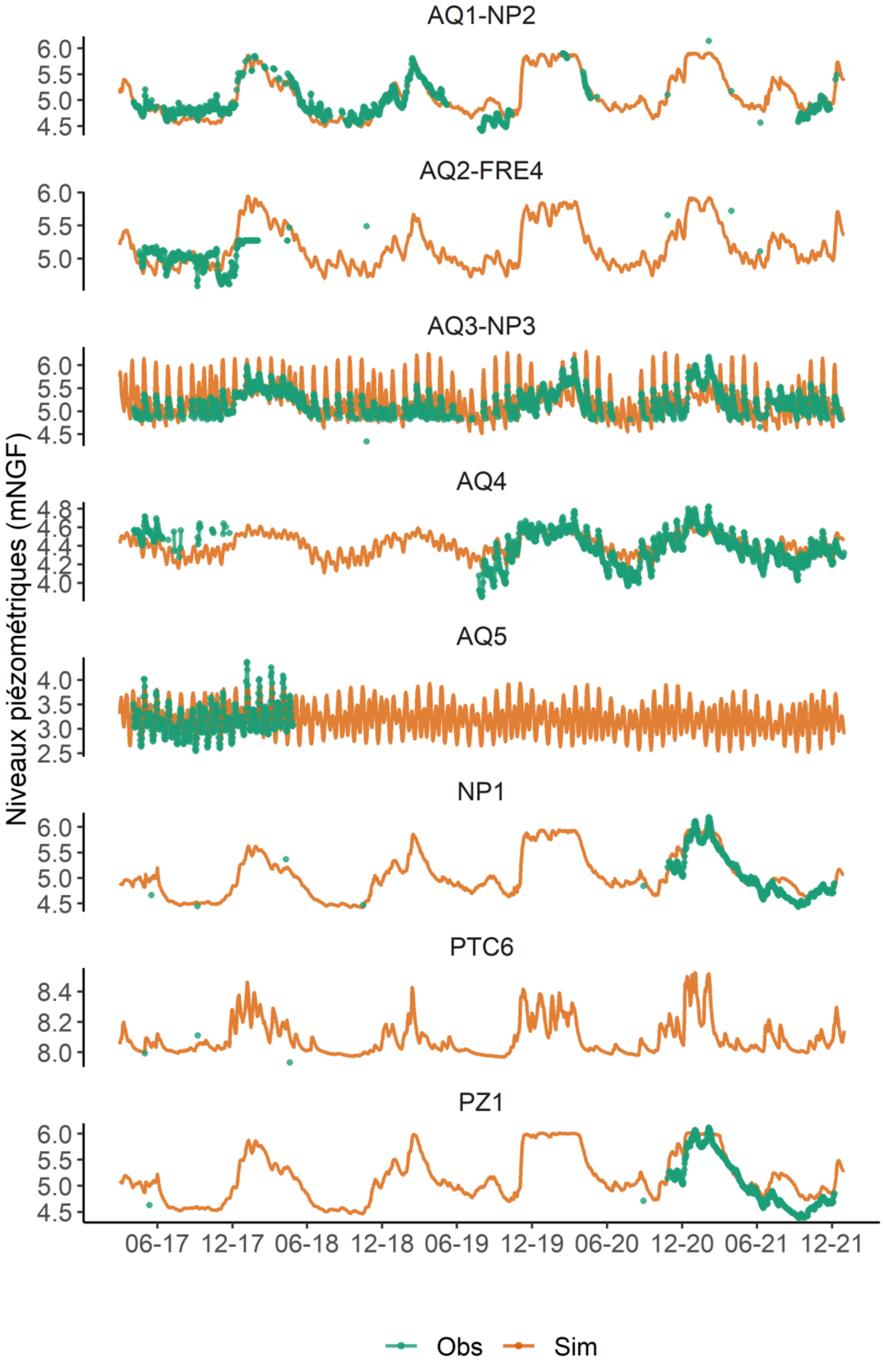

Figure 12 Time series of observed and simulated of piezometric levels over the period 2017 to 2021 at piezometers AQ1-NP2, AQ2-FRE4, AQ3-NP3, AQ4, AQ5, NP1, PTC6 and PZ1.

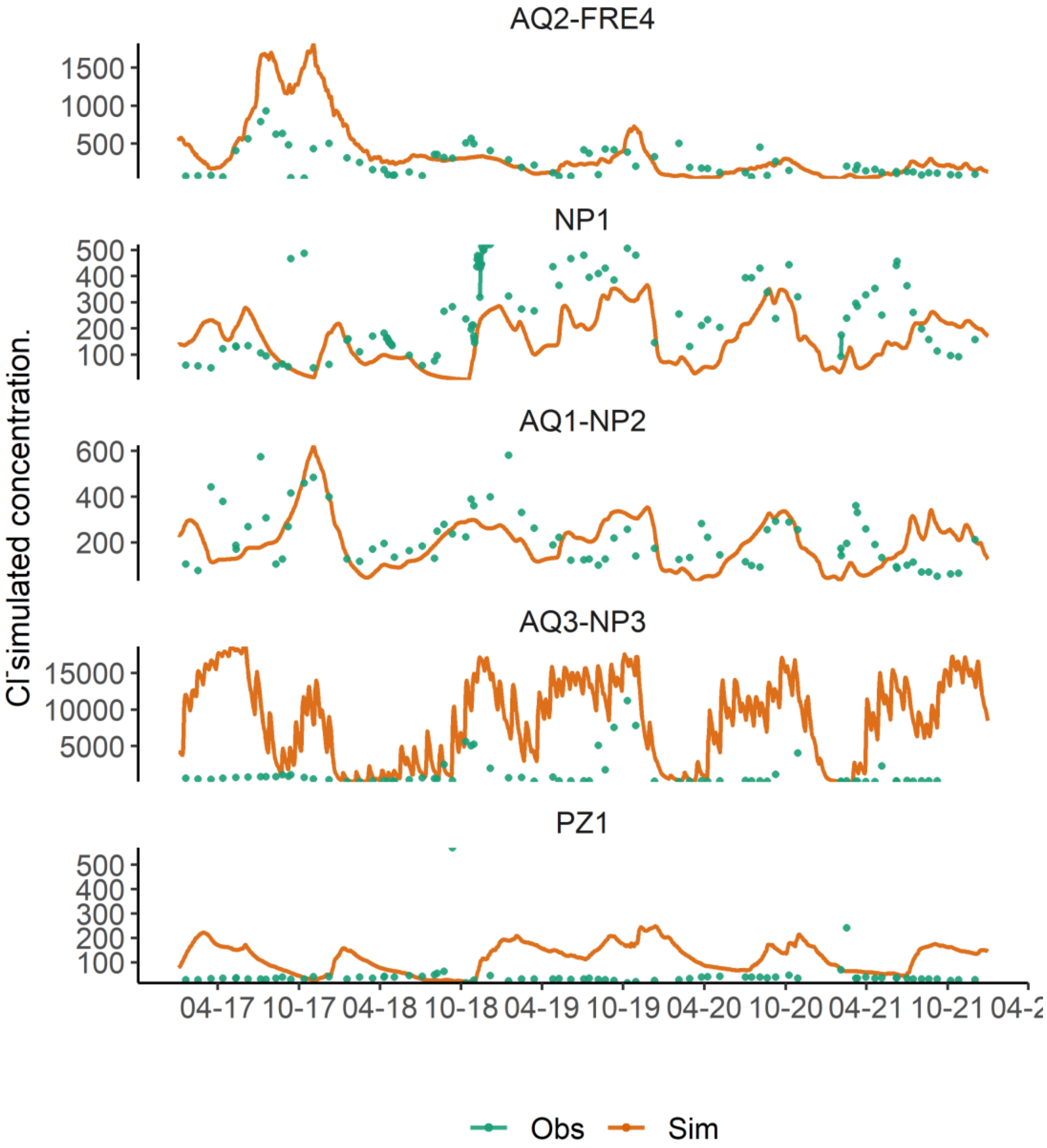

Figure 13 Time series of observed and simulated Cl^- concentrations (mg/L) over the period 2017 to 2021 in groundwater at piezometers AQ2-FRE4, NP1, AQ1-NP2, AQ3-NP3 and PZ1.

h) Hydrodynamic balances

The hydrodynamic balances over the period of 2017 and 2021 indicate the water exchanges between the influence zone of the SAT and its hydrodynamic environment. The area for the balance calculation (*Figure 14*), with an area of 0.6 km^2 is delimited by the bedrock outcrops and the coastline, excluding the Blainville Harbour to the north and the part of the Goulot upstream basin to the south.

The amounts of water entering the aquifer in the SAT zone of influence (*Figure 14*) are on average (from 2017 to 2021) 42.0% of STWW (0.57 Mm^3), to 29% of the water brought through groundwater-river exchanges (0.39 Mm^3), 29% of natural recharge water (14% of direct recharge of direct recharge equivalent to 0.20 Mm^3 and 14% of indirect recharge equivalent to 0.18 Mm^3) and 23% from outside the study area, mainly from the Blainville harbour (0.3 Mm^3). The different water inputs into the aquifer, via rivers, STWW, natural recharge and sea (harbor and coastal areas) result in water mixtures of variable chemical composition.

On average, 54% of the groundwater outflow from the balance area is provided by fixed hydraulic head boundaries at the sea (0.9 Mm^3) and 45% by groundwater overflows (0.7 Mm^3).

Natural recharge and STWW flows are lowest in the water year "2018-2019 with 0.28 Mm^3 and 0.37 Mm^3 compared to the "wet" water year 2020-2021 with 0.43 Mm^3 and 0.71 Mm^3 respectively. Given the low storage capacity of the aquifer, these “dry” and “wet” years have the same impact on the overflows and the volumes leaving the outlet towards the sea.

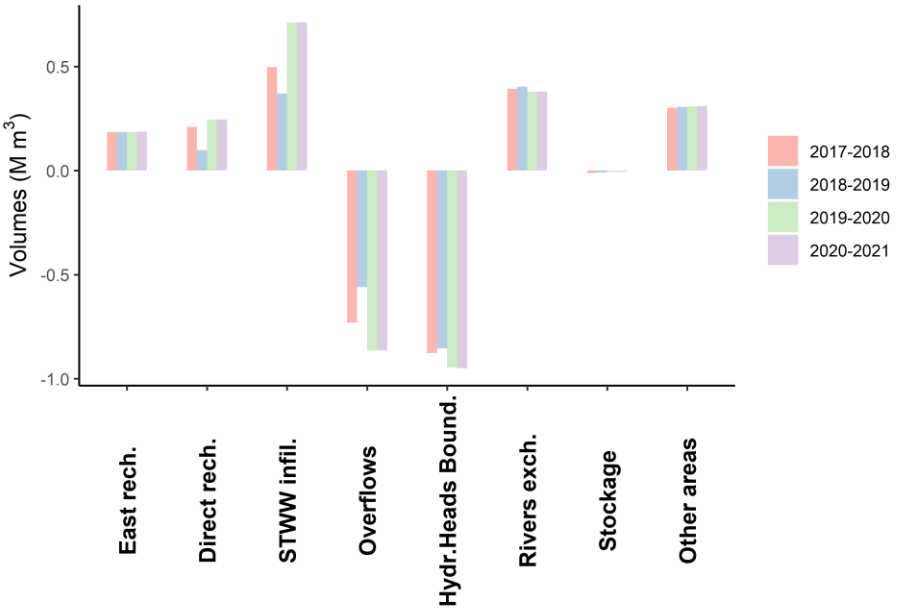

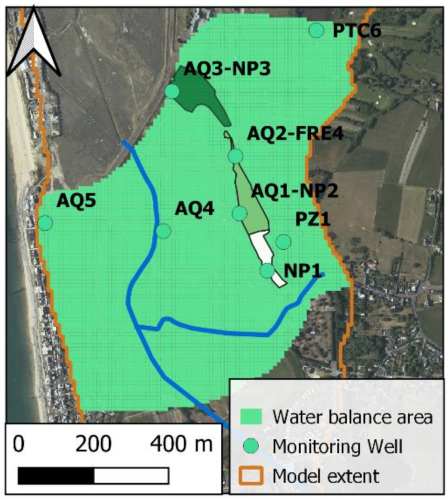

Figure 14 Hydrodynamic balances by hydrogeologic year (e.g., 2017-2018: Oct. 1, 2017-Oct. 1, 2018) on direct and indirect natural recharge, infiltrated STWW, overflows, fixed hydraulic heads at the western boundary of the model (sea boundary conditions), aquifer-river exchanges, aquifer storage, and volumes from other zones (balance area is shown on the right). Negative values indicate water outflow from the aquifer and positive values indicate water inflow into the aquifer.

i) Calculated piezometric maps and main flow lines

The simulated piezometric maps for May 2019 and May 2021 (*Figure 15*) represent the so-called high-water periods after poor winter recharge in 2018-2019 and heavy winter recharge in 2020-2021. The hydraulic heads on May 1, 2019 and 2021 vary between a minimum of 2.96 mASL west of the model and a maximum of 14.16 mASL east of the model. The main flow directions are NE-SW from the infiltration basins to the sea (East/West direction) crossing obliquely the downstream part of the Goulot stream and bending towards the sea perpendicular to the coastline. The flow directions at 3 different times (December, May, August) of the 2018-2019 and 2020-2021 years (*Figure 15*) show little change over the course of a hydrogeological year, except between the northernmost seepage basin (basin 3) and the Goulot stream where tidal conditions in the harbour play a significant role (e.g. May 2020, *Figure 15*).

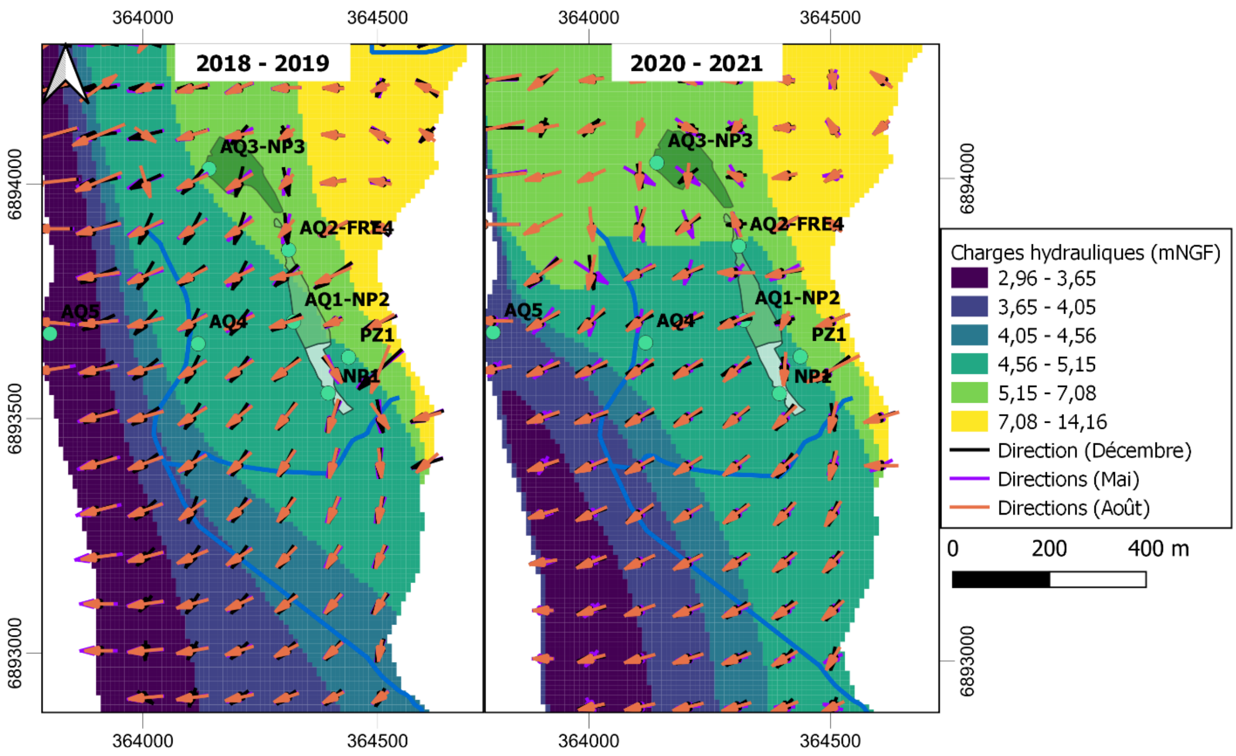

Figure 15 Calculated hydraulic loads on May 1, 2019 and May 1, 2021. The arrows represent groundwater flow directions for 3 periods: December (black), May (purple), and August (orange).

j) Spatialized variations of flow velocities and proportions of STWW

The mean values with coefficients of variation (CV) of flow velocities and STWW proportions are presented spatially for two extreme hydrogeological situations; in a low rainfall hydrogeological year (2018-2019) and in a high rainfall hydrogeological year (2020-2021). The calculation of averages and CVs is made from the real velocities calculated on two time steps per month (i.e. 24 time steps per year) by the numerical model.

k) Variations according to the flow lines of the flow velocities and proportions of STWW

The average velocities over the 2018-2019 and 2020-2021 hydrological years calculated by the model are between 0 and 80 m/d over the entire modelled area (*Figure 16*). The calculated velocities are located in a zone between the harbour and the coastline in a zone located upstream of the infiltration basins at the eastern limit of the model (10-80 m/d). The velocities in the harbour area are biased by the hydraulic head boundaries fixed in the harbour and on the coastline. As for the area upstream of the infiltration basins, the velocities are biased by the contribution of indirect recharge, in a zone of eolian sand of lower storage coefficient.

In the infiltration basins, the average velocities are 2 to 3 m/d and can reach maximum values of 3 to 5 m/d near basins #1 and #2. Between the infiltration basins and the sea, the average calculated velocities are between 2 and 5 m/d for a hydrogeological year of high or low natural recharge. A difference in velocity is calculated on both sides of the Goulot with higher velocities in the west (3 to 5 m/d) than in the east (2 to 3 m/d).

The CVs of the calculated average velocities, presented in *Figure 16*, are more important in the infiltration basins (27 to 58% variation in mean velocity). The CVs are lower between the Goulot stream and the sea, reaching higher variations of the average velocity of 12 à 23%. In the harbour, very important variations of average speeds are also calculated (variations of 58 to 27%) where the results are biased by the tidal boundary conditions.

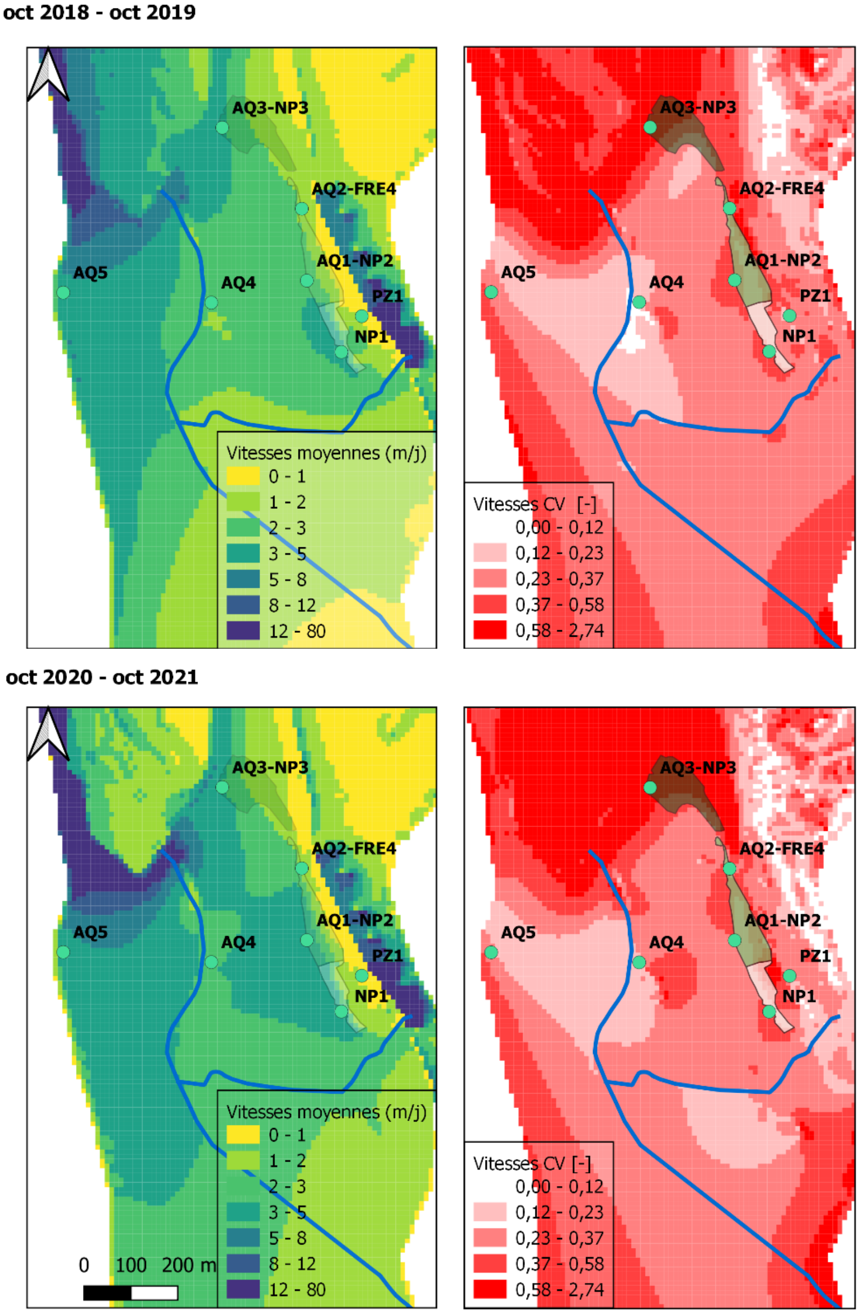

Figure 16 Average velocities and coefficients of variation CV calculated from the numerical model for two full hydrological years: 2018-2019 and 2020-2021.

The results of average proportions of STWW in groundwater over hydrogeological years 2018-2019 and 2020-2021 (Figure 17) range from 0% to 99% STWW over the entire modeled domain. The STWW plume extends from the infiltration basins to the coastline under the Goulot stream. The proportion of STWW systematically very important: from 90% to 99% between the infiltration basins n°1 and 2 and the Goulot. Between the Goulot and the coast, the proportion of STWW is decreased, reaching values around 40% to 80%. The plume of STWW coming from the infiltration basin n°3 extends southward with a proportion of 60% to 90%. The proportions of STWW are slightly modified over the year, with CVs reaching values of 0 to 10% between the infiltration basins and the Goulot stream (Figure 17). In the flow line of infiltration basin #3, larger variations (CVs up to 20%) in STWW are calculated by the model. The “dry” or “wet” situations of the 2018-2019 and 2020-2021 hydrogeological years do not generate significant differences in the proportions of STWW in the groundwater except for the extension of the plume (90-99% STWW) which is slightly larger by about 100 meters to the south for the period of heavy winter recharge (Figure 17).

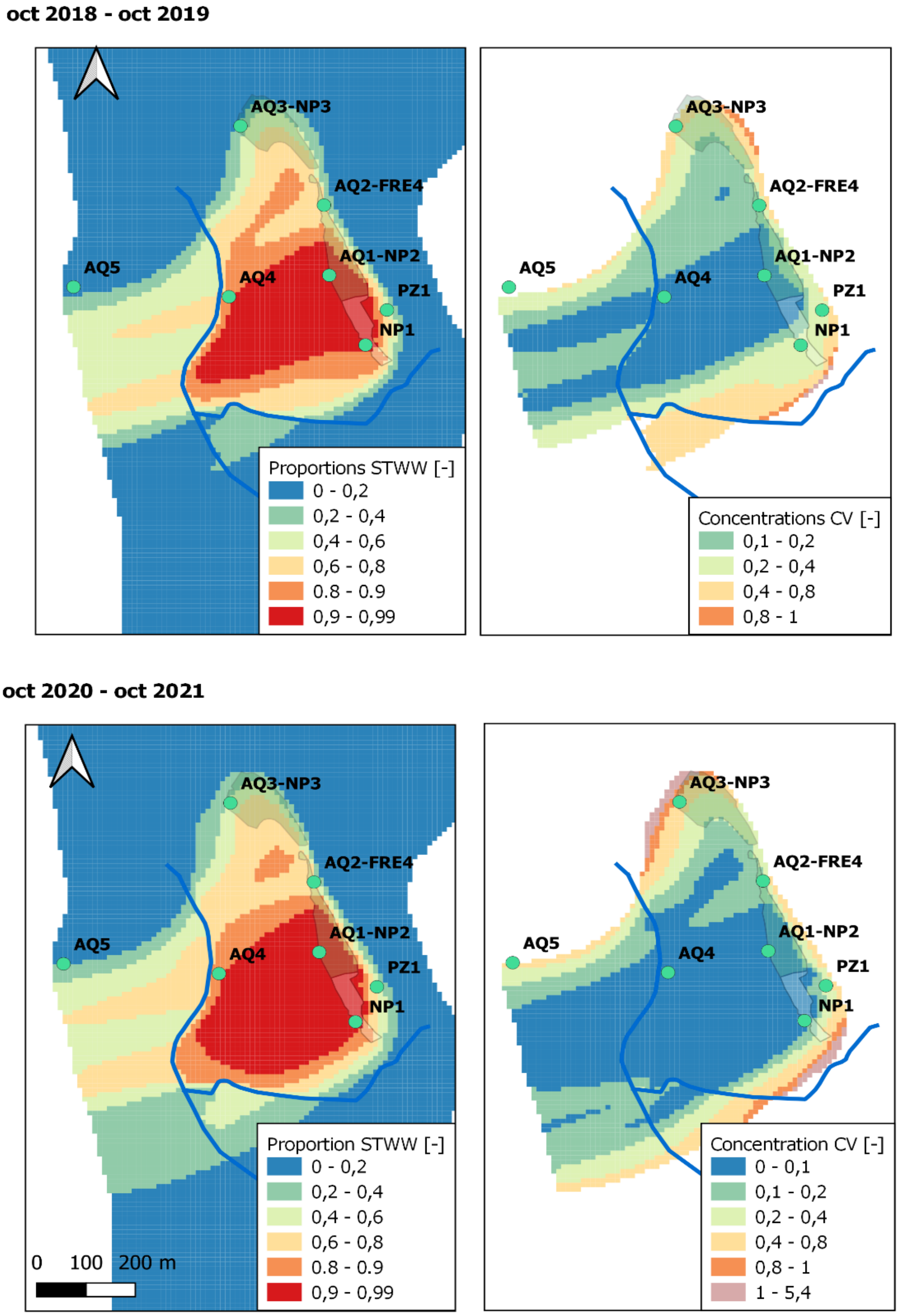

Figure 17 STWW concentrations (from 0 to 1) over the SAT area of influence and coefficient of variation (CV) calculated over two hydrogeological years: Oct 2018 - Oct 2019 and 2020 - Oct 2021.

Variations in flow velocities and STWW proportions in groundwater are analyzed over four segments (numbered #1 of 265 m, #2 of 325 m, #3 of 250 m, and #4 190 m, *Figure 18*) defined by the main flow lines from (1) the infiltration basins to the Goulot stream, the area with the highest STWW proportions (one line per basin), and (2) from the Goulot stream to the coast, an area with lower STWW proportions. Variations are calculated over the 2017-2021 period on a bi-monthly basis for each segment by averaging the simulated values across the segment's meshes.

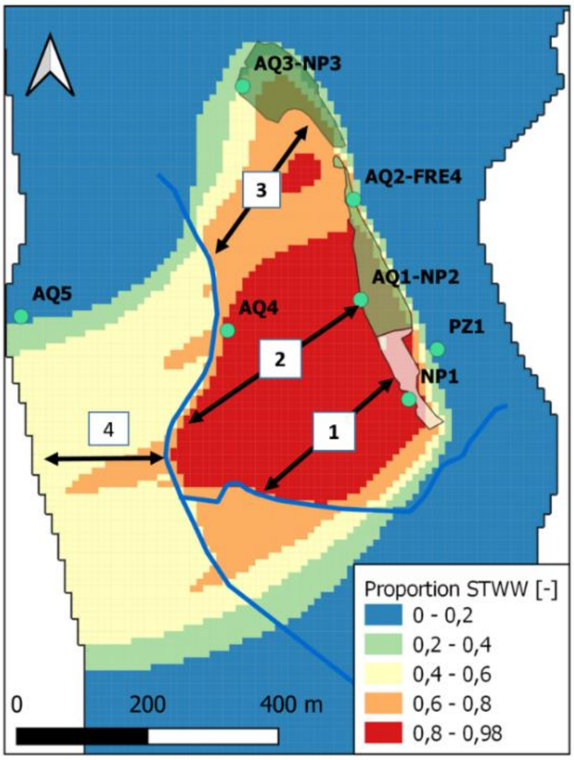

Figure 18 Selection of the main groundwater flow directions for the calculation of average velocities between average velocities between infiltration basins 1, 2, and 3 and between the Goulot and the sea. The lengths of flowlines are 265m for flowline #1, 325m for flowline #2, 250m for flowline #3 190m for flowline #4.

The average flow velocities calculated over all the meshes in segments #1, #2, #3, and #4 are 2.5 m/d, 2.7 m/d, 3.0 m/d, and 3.7 m/d, respectively (*Figure 19*). The highest velocities are calculated in winter period in February, March, April (4.6 m/d, 4.7 m/d, 5.5 m/d and 6.7 m/d). They are minimal during the summer periods in August, September and October (1.0 m/d, 1.3 m/d, 1.7 m/d and 0.9 m/d) indicating the seasonality of variations. The amplitude of the speed variations velocity is exacerbated on the flow lines n°3 and n°4 near the limit of the model that the sea which induces other variations of weaker amplitudes, 0.50 m/d approximately, caused by the approximately, caused by the daily tidal cycles.

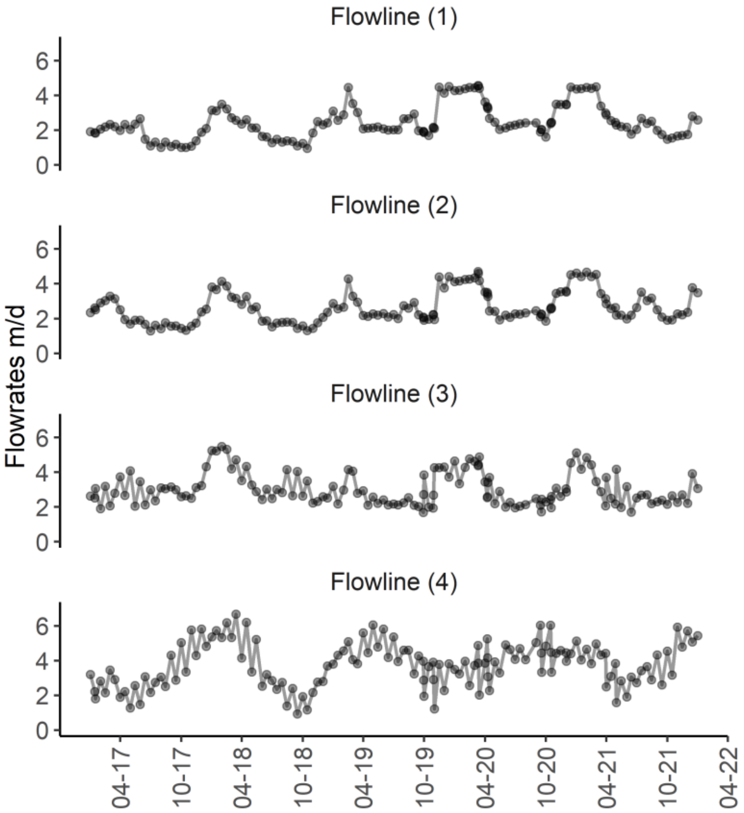

Figure 19 Variations of the average flow velocities calculated by the model according to the main flow lines identified at the departure of the different infiltration basins n°1, n°2, n°3 (Flowlines #1, #2, #3) and between the Goulot river and the sea (Flowline #4).

The mean residence times calculated from the flow velocity results and the length of the segments of lines #1, #2, #3, #4 (Table 5) are on average 107 d, 122 d, 82 d, 50 d respectively. In winter period, the mean residence times are shorter with minimum values of 28 to 69 days with the lowest values remaining on lines #3 and #4 near the sea. On the other hand, in summer period they are longer with maximum values of 148 d to 282 d always with this distinction of proximity of the conditions to the sea boundaries.

Table 5 Descriptive statistics of the average velocities calculated according to the main flow lines and associated and associated residence times (L is the length of the segments of each line).

Name	**Flowline #1**	**Flowline #2**	**Flowline #3**	**Flowline #3**
Length (m)	265	325	250	190
Velocity (m/d)				
Mean	**2.48**	**2.67**	**3.03**	**3.77**
Min	0.94	1.28	1.69	0.92
Max	4.55	4.69	5.48	6.67
Residence time (d)				
Mean	**107**	**122**	**82**	**50**
Min	58	69	46	28
Max	282	254	148	207

The cross-correlation function (CCF) applied to the time series of average flow velocities at each flowline and the different natural and anthropogenic forcings identifies their correlations with sometimes a time lag (k, equation (19)). The correlation coefficients, ρ (Table 6), show that velocities on flowlines #1 and #2 are primarily correlated with the volumes of STWW infiltrated into the basins and with natural recharge (ρ > 60). For flow line #3, the velocity variations are weakly correlated (0.2 > ρ > 0.33) with STWW infiltration, with natural recharge, and with tides on the coastline. Only flowline #4 has average velocities correlated mostly with tides (ρ = -0.82).

Table 6 Correlation coefficient ρ of the CCF function between the time series of natural and anthropogenic forcings natural and average flow velocities associated with the offset values (k) of the time series to obtain the highest correlation coefficients.

	Flowline #1	**Flowline #2**	**Flowline #3**	**Flowline #4**
Flow rate of infiltrated STWW	0.69	0.76	0.30	0.10
Direct natural recharge	0.63	0.68	0.25	0.13
Harbour boundary conditions	0.14	0.13	0.20	-0.13
Western coastal boundary conditions	0.14	0.08	0.33 (k = 1 d)	-0.82

The average proportions of STWW mixing in the aquifer calculated on flowlines #1 and #2 over the period 2017 to 2021 are on average 86% and 91% and vary significantly when the alternating discharge from one basin to the other is effective, prior to January 2019 (*Figure 20*). Prior to January 2019, the minimum and maximum values of proportions calculated for lines #1 and #2 are 45%-86% and 75%-93%, respectively whereas thereafter, after the release alternation is stopped, the average proportions of STWW on lines #1 and #2 reach a plateau of 86% and 97% and are only occasionally lowered by 10%. On flow line #3, the proportions of STWW vary more strongly with an average of 77% and higher minimum and maximum values (24% reached in May 2017, 98% achieved by January 2019). Large variations in proportions persist (e.g. 50% in November 2019) after this date. The STWW proportions for line #4 between the coast are relatively stable with an average of 60% regardless of the infiltration basins used.

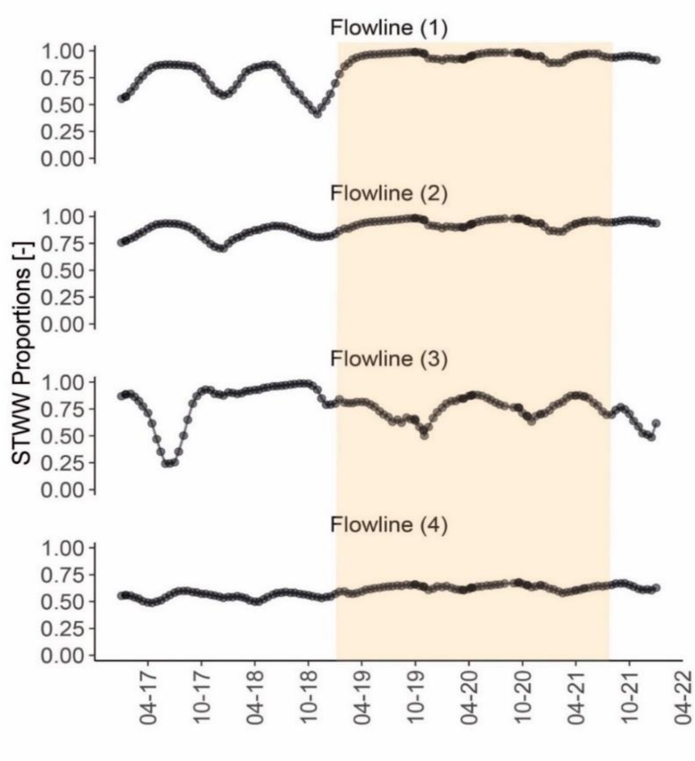

Figure 20 Variations in STWW proportions along the main flow lines identified between infiltration basins 1, 2, 3 (Flowlines #1, #2, #3) and the Goulot stream or the sea (Flowline #4). The orange area represents the period when the alternation of STWW discharges in the different infiltration basins is no longer assured.

l) Sensitivity

The sensitivity analysis presents the comparison of flow velocity and STWW proportion results between the calibrated model and different tests of boundary condition or hydrodynamic, hydrodispersive parameters changes. The sensitivity analysis shows that changes in stream boundary conditions (0.4 cm drop in water level and 1 m increase in stream bottom depth) and direct natural recharge (10% direct recharge) do not significantly the average flow velocities (-2 to 5%) and average STWW proportions (-1 to +5%) in the aquifer calculated on flowlines #1, #2, and #3 (Table 7). Only the proportions of STWW on the flowline #4 are lowered by 18% by the increase of the depth of the Goulot streambed. The simulations of changes in sea boundary conditions (Harbour not considered) modify the velocities (decrease up to 20% mainly on the flowline #3 and flowline #4) and modify the proportions of STWW (increase of 17% on the flowline #3 and decrease of 17% on the flowline #1 and flowline #4). For the modifications of the indirect natural recharge, the taking into account of the seasonalities of the inputs modifies slightly the speeds in the flowlines #1,#2,#3 and #4 (-2 to +8%) and the proportions of STWW in the flowlines #1,#2 an #3 (-4% to +8%) but more strongly in the flowline #4 (-19%). The modification of the indirect natural recharge by selecting a constant fixed hydraulic heads modifies more strongly the speeds (-10 to +29%) and the proportions of STWW (-30 to +12%).

Changes in hydrodynamic parameters strongly modify the velocities. The general decrease of the hydraulic conductivity in the dune aquifer from 2.0 10^{-3} $m.s^{-1}$ to 2.0 10^{-4} $m.s^{-1}$ induces a decrease of 85% compared to the velocities of the calibrated model. The assumption of a hydraulic conductivity considered homogeneous on the whole domain at 2.0 10^{-3} $m.s^{-1}$ (initially calibrated at 5 10^{-6} $m.s^{-1}$ for the eolian sands), induces an increase of the velocities mainly for the flowline #1 of 45% and for the flowline #2 of 26%. Few differences are observed for the flowline #3 and flowline #4.

The choice of a porosity of 20% for the whole domain (initially of 10% for the eolian sands), modifies very little the velocities and the proportions of STWW. Nevertheless, for a porosity of 35%, the calculated velocities undergo a decrease from 42% to 41% for the four flowlines. The longitudinal dispersivity parameter, αL - increased to 100 m (calibrated to 10 m) - decreases the proportion of STWW in the aquifer by 18%, 16%, 35% and 2% depending on the respective flowlines #1, #2, #3 and # 4.

Table 7 Average flow rates and average proportions of STWW in the aquifer from 2017 to 2021 for the baseline model and other models with different parameters for the main flowlines from the different infiltration basins 1, 2, 3 to the Goulot stream (Flowlines #1, #2, #3) and from the Goulot stream to the coastline (Flowline #4). Differences from the reference model results are indicated in percentage via the color scale (from +100% in blue to -100% in red).

	Groundwater velocities (m/d)				STWW proportions (-)			
Simulations	Flowline #1	Flowline #2	Flowline #3	Flowline #4	Flowline #1	Flowline #2	Flowline #3	Flowline #4
Base model	***2.48 ± 0.97***	***2.67 ± 0.91***	***3.03 ± 0.93***	***3.77 ± 1.27***	***0.86 ± 0.14***	***0.91 ± 0.07***	***0.77 ± 0.15***	***0.6 ± 0.05***
River 1 ; decreased water level	2.49 ± 0.98	2.71 ± 0.93	3.07 ± 0.90	3.67 ± 1.27	0.85 ± 0.15	0.91 ± 0.07	0.76 ± 0.16	0.63 ± 0.05
River 2 ; increased depth	2.45 ± 0.97	2.58 ± 0.90	3 ± 0.95	3.95 ± 1.26	0.88 ± 0.12	0.91 ± 0.06	0.78 ± 0.15	0.49 ± 0.06
Natural recharge 1 -10% recharge	2.48 ± 0.98	2.67 ± 0.91	3.01 ± 0.91	3.75 ± 1.26	0.87 ± 0.14	0.91 ± 0.06	0.78 ± 0.15	0.61 ± 0.05
Sea ; no harbour limit conditions	2.41 ± 1.00	2.48 ± 1.04	2.41 ± 1.01	3.2 ± 1.34	0.72 ± 0.26	0.89 ± 0.07	0.9 ± 0.04	0.5 ± 0.15
East recharge 1 ; Seasonal effects	2.52 ± 0.96	2.66 ± 0.89	3.06 ± 0.91	3.45 ± 1.32	0.93 ± 0.05	0.9 ± 0.07	0.74 ± 0.17	0.49 ± 0.12
East recharge 2 ; fixed head	3.21 ± 0.97	2.98 ± 0.91	2.52 ± 0.93	3.37 ± 1.27	0.97 ± 0.14	0.88 ± 0.07	0.76 ± 0.15	0.42 ± 0.05
K from $2 \cdot 10^{-3}$ to $2 \cdot 10^{-4}$ $m.s^{-1}$	0.39 ± 0.02	0.42 ± 0.03	0.55 ± 0.02	0.63 ± 0.13	0.49 ± 0.14	0.54 ± 0.05	0.67 ± 0.06	0.03 ± 0.00
Homogeneous K 2.10^{-3} $m.s^{-1}$	3.6 ± 1.35	3.37 ± 0.87	2.96 ± 0.75	3.56 ± 1.98	0.81 ± 0.17	0.72 ± 0.17	0.55 ± 0.2	0.45 ± 0.14
S_L, porosity 1 0.2	2.48 ± 0.97	2.67 ± 0.90	3.04 ± 0.91	3.77 ± 1.27	0.86 ± 0.14	0.9 ± 0.07	0.76 ± 0.16	0.6 ± 0.05
S_L, porosity 2 0.35	1.43 ± 0.54	1.54 ± 0.5	1.76 ± 0.5	2.22 ± 0.77	0.94 ± 0.08	0.91 ± 0.04	0.8 ± 0.15	0.55 ± 0.05
α_L 100m	2.48 ± 0.97	2.67 ± 0.91	3.03 ± 0.93	3.77 ± 1.27	0.71 ± 0.12	0.76 ± 0.05	0.5 ± 0.15	0.48 ± 0.06

Differences/base (%)	+100	+50	+25	0	-25	-50	-75	-100

2.1.5. DISCUSSION

The numerical model of flow and transport allows to calculate, in time and in any point of the aquifer of Agon-Coutainville of the flow velocities and the proportion of STWW in the groundwater but especially the trajectories followed by the STWW infiltrated through the three basins. This information, not known until now, is a key parameter to interpret the reactivity of TrOCs measured in the field. For this purpose, the developed model is based on a perception of the major flow and mixing processes integrating the dynamics of natural and anthropogenic forcings and on an acceptable calibration of the parameters with regard to the knowledge available. An iterative approach of new measurements on the field and the continuation of modeling efforts would improve the understanding of the coastal hydrosystem of Agon-Coutainville.

The identified limitations of the model are related to two modeling assumptions: (1) that of a homogeneous aquifer that does not take into account a probable stratification or diversity of facies within the porous medium and (2) that of flows without density effects that exist in these coastal environments (Bear et al., 1999). In the transition zone (freshwater-saltwater interface), fluid density varies in time and space as a function of temperature and salt concentration. As a result, variable density flow modeling is often performed to represent salt intrusion mechanisms (Dibaj et al., 2020; Simmons et al., 2001). These works show, possible effects are possible on the simulated flow velocities such as (1) decreases in groundwater flow velocities in the transition zone by increasing salinity concentration (2) increased STWW plume velocity by freshwater/saltwater stratification that would limit the aquifer thickness in which freshwater flows occur. Concerning the proportion of STWW, effects are also possible due to the modification of the progression of the STWW plume, which extends on a superficial part of the aquifer, less prone to dilution with sea water. These effects are nevertheless assumed to be negligible in the areas where the salt water wedge is not observed, close to the infiltration basins #1 and #2. In the areas closer to the coast and the harbour (basin #3), additional investigations, in particular by electrical conductivity profile measurements, or geophysical methods (e.g. electromagnetic induction tools, Vandenbohede et al., 2008) can be used to characterize the salt wedge and its extent at the Agon-Coutainville site.

The sensitivity analysis shows that the results of flow velocities and proportions of STWW presented are sensitive to permeability and porosity parameters and to the choices of conceptualization of indirect recharge. Additional in-situ measurements (e.g. pumping test) and (e.g. pumping test) and porosity (e.g. tracer test) can validate the choice of parameters for the calibration of the hydrodynamic model. Additional measurements to identify runoff to the east of the aquifer (e.g. flow measurements on upstream streams, use of isotope tracers) upstream, use of water isotope tracers) are also suggested.

m) Interaction between SAT and surrounding natural and anthropic dynamics

At the aquifer scale, STWW infiltrated in basins #1, 2, 3 flow toward the coast, its outlet, intersected perpendicularly by the hydrographic network. According to an interannual time scale over two distinct years of recharge conditions (over the hydrological years 2017-2018 and 2020-2021), the results show (1) the maintenance of a high proportion of STWW (60 to 99%) located between the infiltration basins and the stream and (2) velocities that vary between 2 and 5 m/d on an annual average between the infiltration basins and the stream.

Nevertheless, on an intra-annual time scale the calculations show that the SAT is subject to strong seasonal modifications of velocities and dilutions of STWW. Punctually, the velocities (along the main flowlines) vary between 0.9 and 5.5 m/d from the infiltration basins to the coast (equivalent residence time of 74 d and 489 d) and episodes of plume dilution may occur depending on the dynamic influence of natural and anthropogenic forcing. Particular dynamics are observed according to the spatial contribution of the different forcings from infiltration basins #1 and #2 (further from the harbour) to the stream, from infiltration basin #3 to the coast, then from the stream to the coast.

From the infiltration basins #1 and #2 to the stream, the flow velocities are modified by an important intra-annual seasonal dynamics. The general increase of piezometric levels linked to the volumes of water brought by the natural winter recharge and accentuated by the high infiltrated volumes of STWW (correlated to precipitation) doubles the flow velocities in the winter period compared to the summer period (4.7 m/d in winter to 2.6 m/d in summer). In this area with high proportions of STWW on average (>90%), the mean residence times of infiltrated STWW vary from 58 days in winter to 282 days in summer, without any influence of the natural recharge on the dilution as long as the supply of the basins is continuous (no alternation). When the basins are fed alternately, the natural recharge leads to a significant dilution of the STWW plume in the winter period up to 50% in basin #1 and 25% in basind #2. Even if the hypothesis of a correlation between BOD5 measurements and Cl^- concentrations to reconstruct the seasonal variations of Cl^- concentrations in STWW is based on only 9 measurements, we can have high confidence in the confidence in the velocities and proportions of STWW calculated from these flow directions, taking into account the quality of the calibration obtained at the observation points near the infiltration basins, both for the hydraulic heads and the Cl^- concentrations.

Between infiltration basin #3 and the sea along the Blainville Harbour, the proportions of STWW in the groundwater are of the same order of magnitude on average (77%) as those infiltration basins #1 and #2 with higher and more variable flow velocities. The variations in flow velocity (and mean residence time between 46 to 148 days) between basin #3 and the stream are caused by all factors: the sea, STWW and meteorology. The cyclicities of flow velocities are both seasonal (1.7 m/d minimum in summer to 5 m/d maximum in winter) and also monthly (of lesser amplitude) linked to the tidal cycles and spring tides. Occasional episodes of dilution of STWW plumes can up to 24%. These one-off events, particularly during the autumn equinoxes, are the result of the combination of (1) factors related to intense marine dynamics, in particular by (2) lower volumes of supply to basin #3 due to operational conditions (low supply of STW) and (3) higher groundwater levels during the winter recharge period. These important variations on both flow velocities and proportions of STWW, show that this area is strongly influenced by the sea. The piezometric calibration is well represented by the model on the basis of the assumptions made even if it could be improved. It is certain that the dynamics of harbour flooding is a major process that has a significant effect on the SAT during the equinox period. There are uncertainties related to some flow processes not taken into account (1) within surface meanders of the harbour and their interactions with underlying groundwater (2) meteorological effects on sea levels (3) effects related to changes in water density.

Between the stream and the sea, an increase in average flow velocities is calculated caused by the contribution of the stream and the exchanges with the groundwater that is identified by the calculation of the hydrodynamic balance (0.39 Mm^3/year of water exchanged from the river to the groundwater). Between the stream and the sea, the mean residence time varies from 28 to 207 days, very sensitive to seasonal dynamics, and to a lesser extent to sea dynamics (spring water); this brings to a mean residence time between 74 days and 489 days between the basins of infiltration and the coast. The stream smoothes the calculated STWW proportions, on average lower (60%), caused by the stream input. There are uncertainties in the calculation of dilution and flow velocities due to a less-than-robust estimate of water-river exchanges induced by the partial characterization of the stream. Even if the sensitivity analysis (stream geometry) confirms that the stream still induces an increase in velocity and high dilution in this area, it is not excluded that the flows can be reversed by considering a finer description of the dynamics of the stream then constraining the volumes exchanged with the groundwater. Additional investigations of flows, water levels, streambed geometry could be considered to verify this exchange dynamics, and finally, the role of the stream on the dynamics of the SAT as a new forcing element.

n) Effects of SAT variations on the fate of TrOCs at the scale of the hydrosystem

The most important mitigation mechanisms for TrOCs in SAT systems are degradation and sorption (Amy and Drewes, 2007; Maeng et al., 2011; Sharma and Kennedy, 2017). Sorption involves physical interactions that bind or slow down compounds in soil matrix materials (minerals, soil organic matter, dissolved organic matter...), which influences the mobility of TrOCs in the soil and aquifer.

The degradation of TrOCs involves microorganisms (such as bacteria and/or fungi) which assimilate them, and fungi) which assimilate them, via enzymes for the maintenance of the biomass. In general, under physico-chemical conditions favorable to degradation, TrOCs are more degraded when the residence time is higher. Nevertheless, some persistent compounds are not degraded even for long residence times (Amy and Drewes, 2007; Drewes et al., 2003). Degradation of persistent compounds may be zero, but under certain conditions their degradation can be enhanced. For example, the degradation of carbamazepine, identified as persistent, can be enhanced under specific conditions (redox conditions, availability of organic matter, Regnery et al., 2015). For compounds with low refractoriness, biodegradable (e.g., half-life of 1-10 days), there is little chance of finding these compounds at the outfall due to the high water residence times in the SAT. For compounds that are refractory compounds (e.g. 50 days), the residence time of 74 days and 489 days between the the infiltration basins and the coast calculated for the Agon-Coutainville SAT scheme would favour a decrease in their concentration of more than 50% amplified (by 40%) in the downstream parts of the aquifer by the dilution provided by the waters of the Goulot stream (implying that the stream water does not contain TrOCs) and/or by the water from the sea (saline intrusion and harbour flooding). For products of transformation products, this means residence time, associated with conditions allowing the degradation of molecules, would then conversely lead to an increase in their concentration (Muntau et al., 2017).

A quantification of the reactivity of TrOCs in the SAT of Agon-Coutainville has already been performed at the site by Guillemoto et al. (2022), at the scale of an infiltration basin and at the laboratory scale by Crampon et al. (2021). In our work, the modelling results show that this reactivity modeling results can be modified in time and space due to modifications of groundwater flow velocity and dilution.

Between the infiltration basins #1 and #2 and the Goulot stream, a variability of the reactivity of the SAT is expected due to the alternation of the infiltration basins and seasonal variations, and their effects on key factors that influence TrOC degradation (Regnery et al., 2017).

Microbial activity in SAT environments receiving STWW is highly related to the availability of dissolved biodegradable organic matter (DBOM) used as co-substrate to the metabolic transformations of TrOCs (Alidina et al., 2014; Hoppe-Jones et al., 2012; Rauch-Williams et al., 2009). Hoppe-Jones et al. (2012) and Rauch-Williams et al. also show that microbial adaptation to low BDOC conditions can strongly increase biodegradation of TrOCs. Alternating recharge of infiltration basins and dilution of groundwater can stimulate microbial diversity by decreasing available BDOC and therefore possibly the transformation of TrOCs.

The redox state of groundwater is also a key parameter that controls the degradation of TrOCs (Regnery et al., 2017). The degradation of many molecules is sensitive to the redox state of the system (Burke et al., 2014; Greskowiak et al., 2017). Often, zones of different redox conditions (oxic-penoxic-suboxic-anoxic zones, Burke et al., 2014; Henzler et al, 2016) are established in SAT systems, due to the high input of organic matter to the surface of the infiltration basins and the equilibrium with the atmosphere, which induces a lower availability oxygen availability along the flow. Stopping the alternation of infiltration between the basins would modify the redox zones installed along the flows in the system, and therefore possible degradation of redox-sensitive compounds. Seasonal variations strongly modify the dynamics of the SAT. From a reactive point of view seasonal temperature variations can strongly influence the degradation of TrOCs by the decrease of the microbial activity and the dynamics of the development of the various redox in the soil and aquifer (Greskowiak et al., 2006; Henzler et al., 2016). In the winter period, microbial activity can be reduced by decreases in temperature (Greskowiak et al., 2006). Over this same period, calculated mean residence times are shorter which contributes to a decrease in the overall reactive efficiency of the SAT. Nevertheless, the TrOCs concentrations in STWW are lower in winter (dilution by clear parasitic water) which reduces the impact of the reduced reactivity of the system. The temperature increase in summer, coupled with a higher input of biodegradable organic matter in the STWW creates conditions more favorable to the degradation of TrOCs (Massmann et al., 2006). These conditions, combined with increased summer mean residence time, would increase the overall efficiency of the SAT over this period compensating for the higher TrOCs concentration in STWW.

A change in the capacity of the aquifer is also considered. Indeed, the sorption of many TrOCs is related to the proportion of organic matter (Chefetz et al., 2008), to the hydrophobicity of the molecules (Chefetz et al., 2008; Schaffer et al., 2015) and the characteristics of the organic matter (Amy and Drewes, 2007; Huang et al., 2003; Laws et al., 2011; Maoz and Chefetz, 2010). The set of variations that concern organic matter; variation in dissolved organic matter, proportion of organic matter can therefore modify the mobility of TrOCs in the aquifer.

Close to the harbour (basin #3) and the sea, the plume of infiltrated STWW is subject to intrusions of marine water that could influence the reactivity of the TrOCs. There is little information on degradation of TrOCs in marine or estuarine environments. Benotti and Brownawell, 2009, for example, show that degradation rates in marine surface waters are lower than in freshwater. However, in groundwater, few studies have been able to verify the impact of the coastal environment on the reactivity of TrOCs. When seawater moves into a coastal aquifer, the modification of the chemical gradient can strongly modify the microbial activity and thus the degradation of TrOCs, as well as their mobility.

During the pathway, the molecules will encounter areas more conducive to degradation especially in the soil and aquifer, which also evolve according to the temperature, microbiological activity and the contribution of organic matter. On the Agon-Coutainville study site or any other SAT site, a higher reactivity of TrOCs is expected near of the basins (Stuyfzand, 2011) even if the transformation of more refractory molecules can continue after higher travel times, (Hoppe-Jones et al., 2012). Estimates of degradation are not easily extrapolated to an entire watershed or transposable to another site. At the scale of a SAT, spatialization and dynamics of reactivity of the TrOCs in perpetual feedback with that of the flows should be taken into account to hope to predict more precisely the degradation of TrOCs in such systems. The empirical formalisms established in the current literature on their degradation and sorption allow to bring a first characterization of the reactivity but are not necessarily adapted to this scale of study (Henzler et al., 2014; Sanz-Prat et al., 2020).

Spatially, the mobility of TrOCs is also influenced by organic matter content, higher at the beginning of infiltration, resulting in higher sorption to the first soil horizons (Chefetz et al., 2008). Along the runoff, in areas with lower organic matter the mobility of TrOCs may be increased, unless the presence of minerals (e.g. oxy-hydroxides, clays) in the aquifer can decrease the mobility of charged TrOCs (Schaffer and Licha, 2015).

2.1.6. CONCLUSION AND PRESPECTIVES

The numerical model developed addresses the need to assess flow velocities and STWW proportions from the infiltration basins to the aquifer outlet at the scale of the Agon-Coutainville coastal SAT site, information that was previously only available on an ad hoc and local infiltration basin (Guillemoto et al., 2022). Flow velocities and STWW proportions in the aquifer are quantified over time at any point in the aquifer.

The results show strong dynamics in the functioning of the SAT, including large variations in STWW mean residence time between infiltration basins to outfalls (~70 days and 500 days), mainly related to STWW discharge conditions and meteorological conditions. The dilution rates of STWWs vary depending on the operational (infiltration basins feeding) and according to the proximity of the coast (dilution by the saltwater dilution), the area near the harbour of Blainville and the Goulot stream (river dilution). The strong dynamics of the SAT could modifies the reactivity of the TrOCs during the passage in the SAT and put in perspective the quantifications of the reactivity of the TrOCs obtained by a local scale study based on the coefficients of the local scale study based on first order degradation coefficients (μ) and delay coefficients (R) at the Agon-Coutainville site, which can evolve at the hydrosystem scale and the annual scale.

Seasonality of STWW concentration variations, mean residence times, temperatures, could modify the reactivity of the SAT as a function of time. The conditions of reactivity of SAT in winter are less favorable to the degradation of TrOCs: shorter mean residence times, lower temperature. Nevertheless, the lower TrOC concentrations in STWW in winter compensate for this reduced reactivity and would still allow to reach low concentrations at the outlet of the aquifer. In summer, the SAT can respond to the higher TrOC concentrations in STWW, the reactivity of SAT is assumed to be higher with longer mean residence times, allowing to reach lower concentrations of TrOCs at the aquifer outlet.

Spatially, different dynamics identified allow to anticipate the modifications of reactivity in the SAT. In the area with higher stakes (STWW plume in groundwater), changes in redox conditions, organic matter availability, etc. can improve the purification capacity of the SAT with respect to TrOCs. Near the harbour, the reactive conditions are still very uncertain due to the uncertainties related to the flow and transport modeling (density effects, salt wedge position) and due to the saltwater intrusions that can have significant effects on SAT efficiency.

Additional measurements of TrOCs, with model support, may allow interpretation of effective SAT reactivity, depending on varying flow conditions and dynamic factors that influence the reactivity (redox conditions, organic matter availability temperature...) and thus deepen the knowledge about the key conditions that influence the degradation of TrOCs at the scale of an operational SAT site.

Finally, the developed hydrodynamic numerical model can be used to optimize the positions of STWW in the different infiltration basins, in order to optimise the mean residence time and thus the degradation of the organic trace molecules according to the conditions of tides, discharges, meteorological conditions at the Agon-Coutainville site. STWW infiltration scenarios on the different basins can be considered in order to obtain optimal conditions (residence time, dilution) so that the SAT can meet the challenges of TrOC concentrations at the aquifer outlet in order to protect coastal area.

Acknowledgement

This work has been performed in the frame of the EU Water JPI (Joint Programming Initiative "Water Challenges for a Changing World") within the research projects Eviban (evidence based assessment of NWRM for sustainable water management – ANR-18-WTW7-0008-ERA-NET Cofund WaterWorks – 2018) and AquaNES (Demonstrating synergies in combined natural and engineered processes for water treatment system under grant agreement no. 689450). We gratefully thank Eric Dufour, Mickaël Gosselin, Didier Alain (SAUR) and Denis Neyens (Imageau) for their field support and their data share as well as Yan Lefevre (BRGM) and the municipality of Agon-Coutainville who facilitated the implementation of the monitoring and modelling works.

2.1.7. SUPPLEMENTARY MATERIAL

o) SUPPLEMENTARY MATERIAL 1: GARDENIA CALCULATION CODE

The Rain—Evapotranspiration hydro-climatic balance and then the natural recharge is calculated from a global hydrological watershed model GARDENIA (Thiéry, 2009, 2010, 2014-2021, 2015) which simulates, through a succession of reservoirs (**Erreur ! Source du renvoi introuvable.**), the main mechanisms of the hydro-climatic balance in a watershed. The results of this balance are identical in all cells of the domain belonging to the same meteorological data and the same "soil" parameters. Transfers from one reservoir to another are governed by physical laws controlled by their parameters (soil retention capacity, transfer times, overflow thresholds, etc.) evaluated by adjustment on a series of observations (water flows in a stream, piezometric levels).

The standard GARDENIA code calls upon three reservoirs:

- A "soil" compartment: the "superficial" U reservoir submitted to evapotranspiration,
- An intermediate compartment (or Unsaturated Zone): the H reservoir (H as Hypodermic) that produces runoff,
- An underground compartment: The G reservoir, corresponding to groundwater.

When the GARDENIA module is coupled to an aquifer system, there is no underground compartment in GARDENIA as this compartment is replaced by MARTHE's aquifer cells.

The superficial reservoir (U) represents the first decimetres of soil subject to vegetation action and evaporation. The capacity of U is the reserve available for evapotranspiration. The soil reservoir is fed by rain (and snowmelt in winter). It is subject to PET (Potential Evapo-Transpiration) and allows calculating the actual evapotranspiration AET and the "Net Rainfall". This "progressive soil reservoir" is based on quadratic laws in terms of the saturation rate of the reservoir.

Satur = Filling of the reservoir / Capacity of the reservoir:

- If rainfall exceeds PET:
  Net Rainfall = (rainfall - PET) x Satur^2
- If PET exceeds rainfall:
  AET = (PET - rainfall) x Satur x (2 - Satur).

The Reservoir H represents the unsaturated zone. The water height it contains at a given moment is noted H. It is fed by “Net Rainfall” water coming from the near-surface reservoir, and it is emptied by two components:

- Percolation towards groundwater following a linear law (exponential draining) of a temporal constant THG (with dt = duration of time step):

$$ALIMG = \frac{H.dt}{THG}$$

- Runoff QH, following a non-linear law controlled by the RUIPER parameter; this parameter (RUIPER for "Runoff-PERcolation") is the water height in reservoir H, for which the percolation ALIMG is equal to runoff QH:

$$QH = \frac{H.dt}{THG.RUIPER/H}$$

Runoff QH predominates when reservoir H has a high filling ratio. However, the percolation ALIMG predominates when the reservoir H has a low filling ratio. The ratio QH / ALIMG is equal to the H / RUIPER ratio. The functioning of reservoir H thus resembles that of a progressive overflow sill at an average RUIPER height, but with a more realistic representation of the flow, in two components that are not mutually exclusive.

Reservoir H only serves for transferring water. It determines the distribution of net rainfall, coming from the near-surface reservoir, into runoff and recharge.

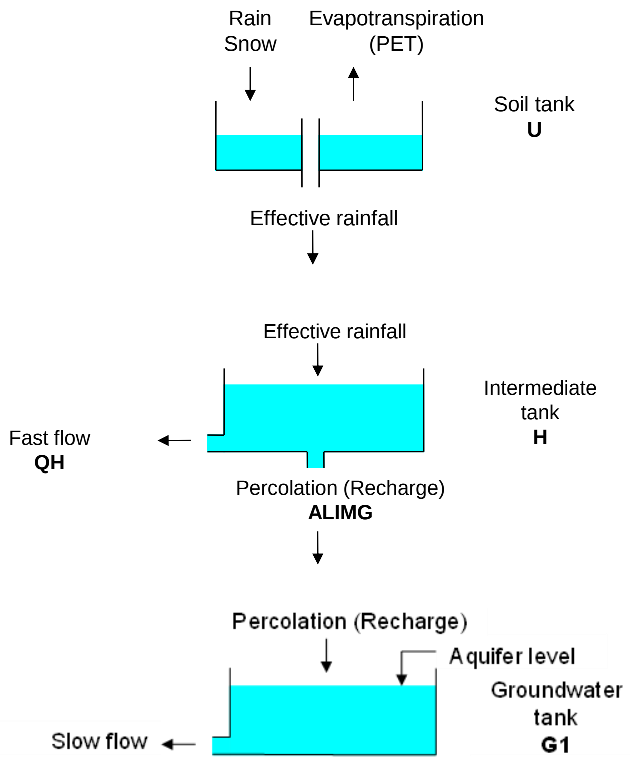

Figure A-2-21 : Complete GARDENIA hydro-climatic balance scheme (Thiéry, 2014)

The G1 groundwater reservoir produces the slow flow. It generally represents the aquifer. The level of water it contains at any given time is noted as G1. It is supplied with recharge by the intermediate reservoir H. It is emptied at a basin outlet in the form of a slow flow QG1, following an exponential emptying law of time constant TG1 :

$$QG1 = .\frac{G1\,dt}{TG1}$$

Table A-1: Gardenia parameters applied in the calculation of natural recharge in Agon-Coutainville

Recharge area	Capacity (reservoir U)	RUIPER parameter (Reservoir H)	THG parameter (Reservoir H)
Indirect recharge from the Estern watershed	600 mm	2 mm	3 months
Direct recharge on the sand dune aquifer	196 mm	9995 mm	3.8 days

p) SUPPLEMENTARY MATERIAL 2: CATHERINE AND TIDAL LEVEL SIMULATION

The Catherine software (Thiéry, 2012) allows the calculation of piezometric level variations at a point of a groundwater table whose diffusivity is known and which is bordered by a boundary (river, lake, sea) whose temporal variations in water level are known. The variations in recorded levels and tides allow the parameter $Di = T/S$ to be optimised, with T the transmissivity and S the storage coefficient, so that the tidal signal at the limits of the model allows a modelled time series to be obtained via the diffusivity of the aquifer. The optimisation is done by dichotomy method. The correlation coefficient between modelled and observed is calculated by the square root of the Nash coefficient (Nash and Sutcliffe, 1970).

As the Agon-Coutainville site does not have a tide gauge in place, the coastal water level data for this site are reconstructed, following a method already used at the Gâvres site in the Morbihan (Idier et al., 2020). This method is based on the joint use of the FES2014 tidal component database (Lyard et al., 2021), which has a global coverage with a spatial resolution of 1/16°, and altimetry reference data (RAM, 2020).

The FES2014 database was used to reconstruct and predict the tidal signal (relative to the mean level) at about 3 km from the Agon-Coutainville site over the period 2010-2021, at a time step of 10 minutes. The water levels thus obtained include only the tide, without taking into account either the effects of rises or the effects of waves. In order for these data to be positioned in the same vertical datum (mASL) as the piezometric and topographic data, they are then converted into altitude (mASL) in relation to the French IGN69 datum from the Maritime Altimeter References (RAM, 2020) at the Granville tide gauge (located approximately 25 km to the south), the closest tide gauge where the average level information in relation to the IGN69 datum is available.

The correlation coefficient (square root of the Nash coefficient) with the observed piezometric levels obtained is 0.85 with a diffusivity parameter calibrated at 1.5 10^{-2} $m^2.s^{-1}$. The diffusivity parameter is higher than expected (3.0 10^{-3} m^2/s) with the hydrodynamic parameters of the dune aquifer with a conductivity of 10^{-3} $m.s^{-1}$, an aquifer thickness of 10 m and a porosity of 0.3.

2.2. SYSTEM MONITORING DEVICE (SMD) AND THE ENVIRONMENTAL MONITORING INTERFACE (EMI) (IMAGEAU)

2.2.1. Technical Description

SMD (Subsurface Monitoring Device) is an automatic geophysical tool installed in a piezometer used to constantly record water's electrical conductivity along the aquifer's vertical axis. It provides a real-time picture of the position and evolution of the saltwater intrusion. In costal environments, the saltwater intrusion can penetrate several kilometers inland after a drop in the piezometric level caused by excessive pumping and/or droughts. If uncontrolled, this phenomenon can compromise the region's drinking water supply and economic activity.

The SMD includes a cable loaded with electrodes which is deployed in a borehole and provides a profile of the resistivity of the rock formation around the borehole. A surface data acquisition box injects a known current between electrodes and measures the induced potential difference between two other electrodes (Figure 1). Bulk resistivity is obtained using Ohm's law, corrected by a geometric factor. This process is repeated from the top to the bottom of the electrode cable, allowing the measurement of bulk resistivity profiles. Bulk resistivity, which is affected by the water salinity, porosity and rock type, is converted into EC of the liquid, using the Waxman–Smits equation. This conversion considers the formation factor (F), and the surface conductivity term (Cs), which are determined using a reduced set of logging measurements (gamma ray, resistivity and sonic for porosity).

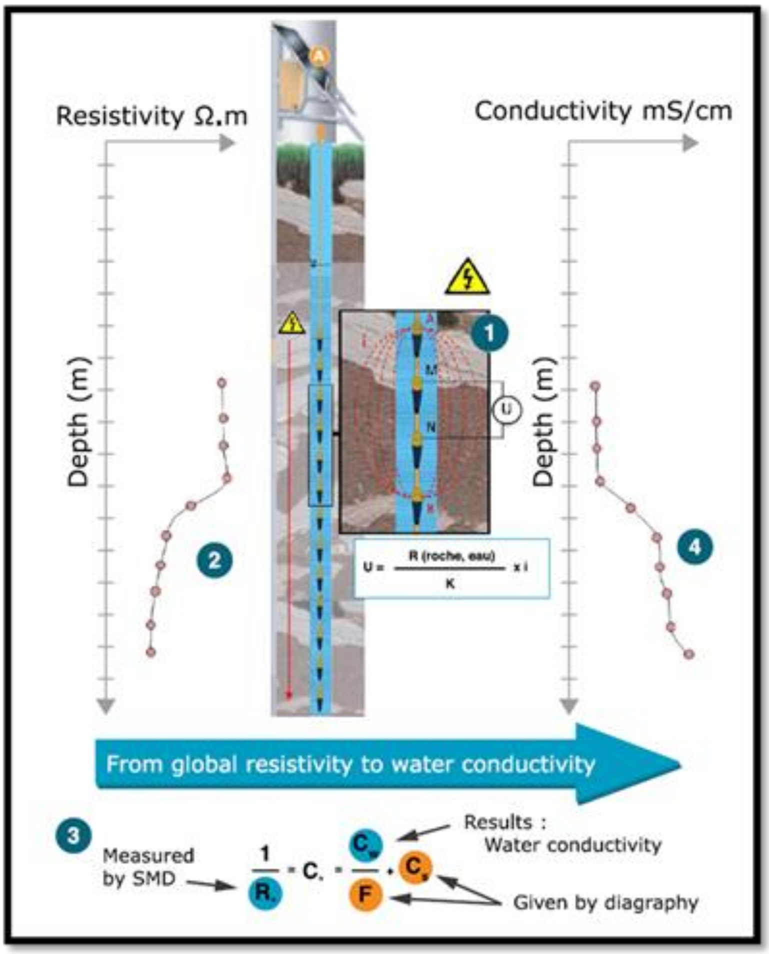

*Figure 1: the SMD principle: (1) Current (i) between two electrodes (A and B) measure the induced potential difference between two other electrodes (M and N). According to Ohm's law corrected by a geometric factor, bulk resistivity (R) is thus obtained (U =R (formation, pore) * (i)/k. U is the tension (Volt) and K the formation factor (2) This process is repeated from the top of the electrodes cable to its bottom allowing the measurement of bulk resistivity profiles. (3) According to the Waxman–Smits equation, bulk resistivity is converted in to ECw20. This conversion needs to know the formation factor (F), and the surface conductivity term (Cs), which are determined using a reduced set of logging measurement (gamma ray, resistivity and sonic for porosity). (4) Finally, ECw20 profiles are obtained. The ECw20 profiles are corrected from borehole effect and normalized in temperature.*

The electrodes are made of a cupro-aluminium allowing reduction of the corrosion process. The energizing power was 12 V (battery or solar type), with the possibility of being plugged to the mains.

The radial resolution in the SMD is 40% to 50% of the spacing between electrodes, namely: For 1 m spacing, the radial resolution is 40–50 cm. The measured resistivity mostly represents salinity of groundwater outside the well, avoiding the well vertical flow effect.

The data is transferred by telecommunication and may be visible on an internet interface the Environmental Monitoring Interface (EMI). Online software platform (using an Internet browser), the EMI has been developed to collate and display information about the aquifer. It includes full description of water dynamics and has specific tools for salt-water intrusion data management. Current and historic data are available 24/7.

Each SMD installed on the site is connected to a secure extranet where data can be downloaded and visualized.

EMI application is based on two identities:

- A database where all the data coming from sensors installed in different sites is stored. Different processes to import data are available (several format files, API…)
- A web application allowing viewing and processing data

EMI can accept and integrate data from every monitoring tools already installed on the well field (whatever the tool and the manufacturing), such as flow meters, water level sensors, water quality sensors, pluviometers, ...

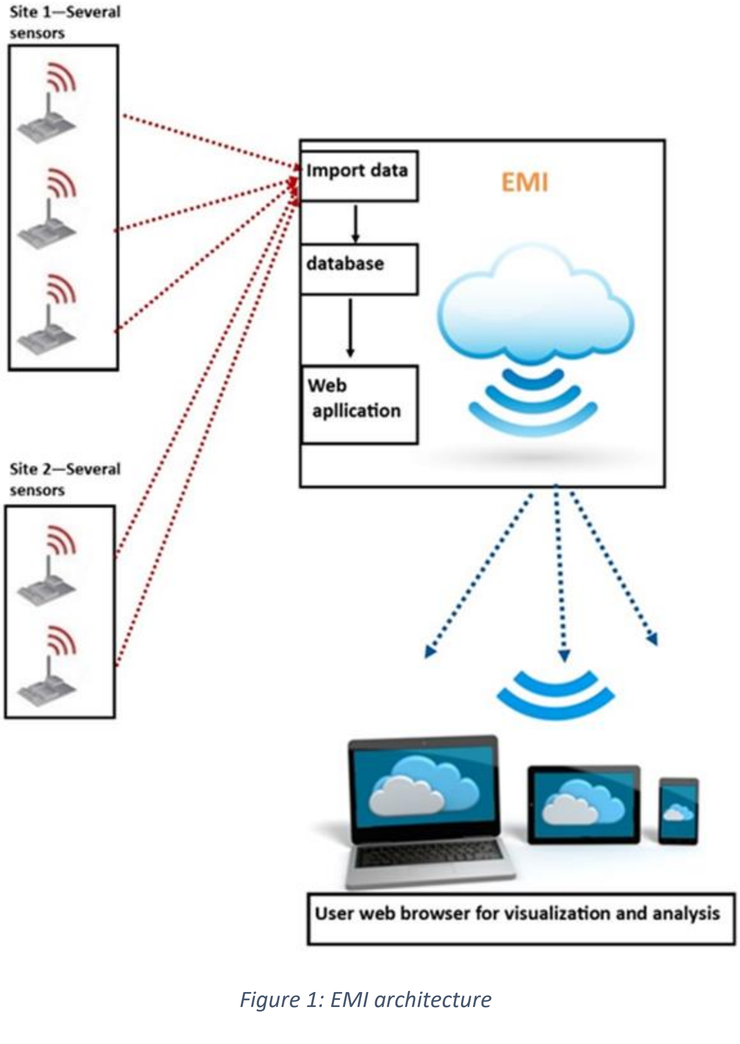

Figure 1: EMI architecture

To enable accessing to the data online, an interface has been developed allowing to:

- viewing data on graphs (value parameter versus time)
- processing the data
    - calculate hydrogeological parameters
    - have statistics on data
    - interpolate the data on 3D graphs
- export, if necessary, a large samples of preformatted data in order to use it in other programs
- setting alerts and thresholds on some parameters (water level…)

EMI organization is based on tree architecture. For each defined site, several monitoring stations can be associated; and for each station, several sensors with several measured parameters can be defined.

The site overview can be used to locate the monitoring tools connected to EMI.

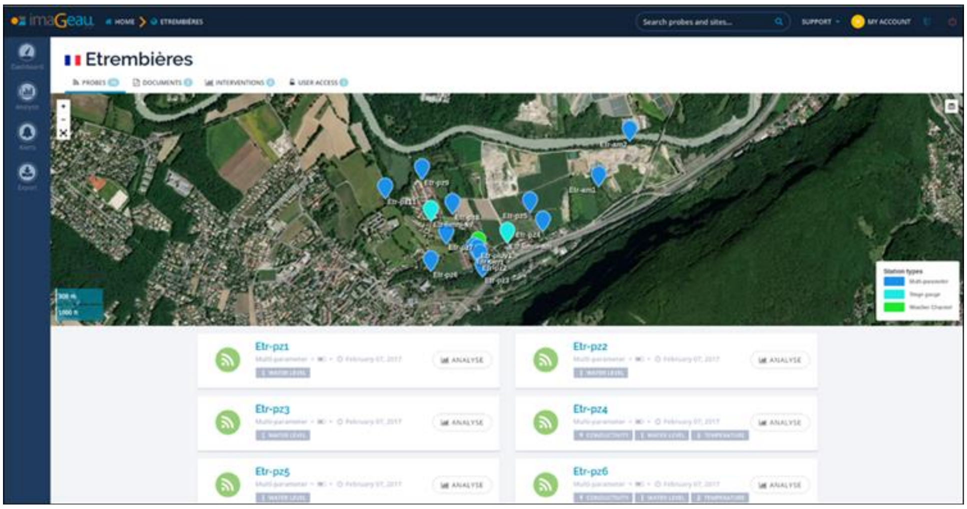

Figure 2: Site overview with different monitoring stations (dark blue: multi-parameters sensors (Cw, water level T°); light green: rain gauge; blue: water level sensor)

This organization allows having all the data associated to the same site in a same place in order to visualise and analyse it with different process. For example, on a site with several boreholes equipped with water level elevation sensors, all the water level elevation curves can be plotted on the same graph. If a rain gauge is installed on the site, the water level can be plotted in front of this rain gauge allowing having data cross-correlation.

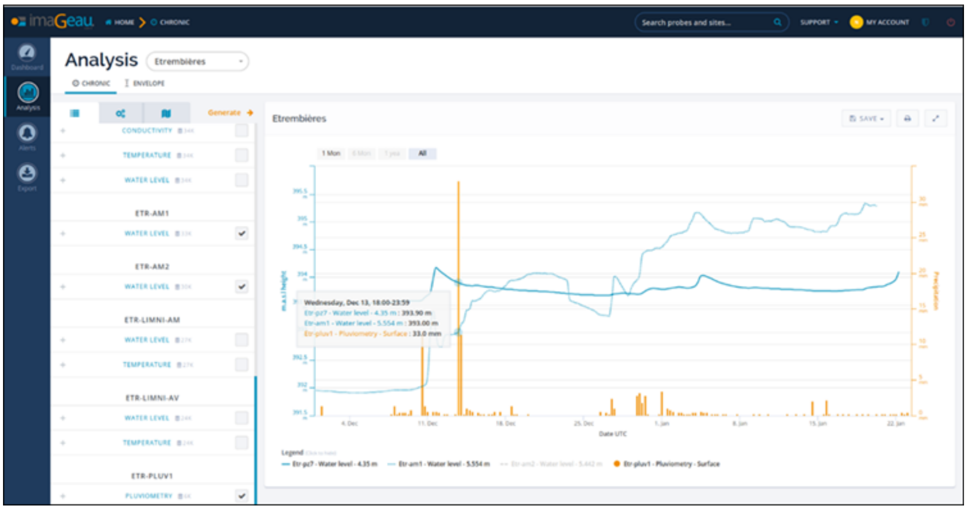

Figure 3: Site overview with different monitoring stations (dark blue: multi-parameters sensors (Cw, water level T°); light blue: rain gauge; green: water level sensor)

Different viewing/analysis tools are available in order to better analyze the data. Depending on the sensor type, different analyses are available. For single point sensor (i.e. water level sensor, quality sensor…), data can be plotted with:

- "Temporal Chronic": Used to view environmental data changes in graph form. Up to ten curves can be added to the graph and multiple parameters can be viewed through linked graphs.
- “Envelop”: used to plot actual data relative to historic data (i.e. mean to see the evolution of the water level relative to anterior years)

When multiple parameters are measured at the same measurement station, it is possible to display them simultaneously on superimposed graphs with the same timescales. The browser's cursor can be used to directly compare different parameters at the same "T time."

Figure 4: Mutli-parameters curves displaying on the same graph with different colours and scales depending of the parameter (black: T°, blue: conductivity, orange: water level)

For multi-points sensors (i.e. SMD), in addition, other analyses are available:

- "Interpolation": Used to interpolate multi-point data in order to create temporary iso-value maps, example: display the map of water conductivity changes over the whole aquifer block over a one-year period,

- "Log": Used to view multi-point data in the form of a profile at a given date or over a given time interval,
- "Saltwater intrusion interface": In the case of a conductivity profile measured using imaGeau systems (SMD), the saltwater intrusion interface can be used to follow over time the depth of an interface defined by the user, e.g.: change in depth of the fresh water/salt water interface (limit 5000 µS/cm). If multiple conductivity sensors are measuring changes over the entire vertical of a piezometer, it is useful to track the evolution of the depth of the interface between two masses of water of differing salinities. In the case of saltwater intrusion tracking, the depth of the saltwater intrusion (freshwater/saltwater interface) is an essential parameter for understanding the evolution of the saltwater intrusion.

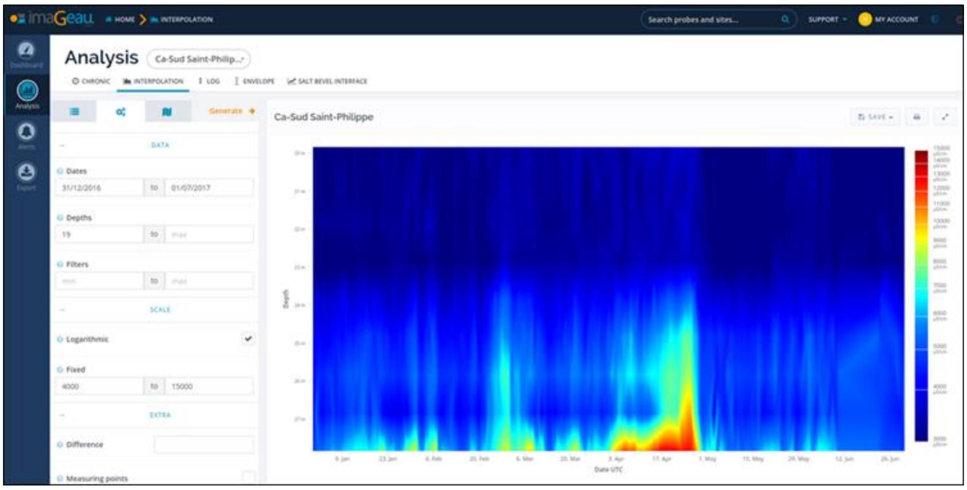

Figure 5: 3D interpolation generated from multi point data over vertical and time, example of SMD monitoring a salt water intrusion

2.2.2. Objectives

In case of quifer recharge, the SMD monitoring allows to determine the impact of the recharge in terms of water quality and potential benefit of this recharge to struggle against the saltwater intrusion.

2.2.3. Works in Eviban

Analysis of conductivity acquired by SMD tools at various locations, at different depth during several years provides a new perspective on the impact of wastewater spreading on saltwater intrusion. The SMD technologies in the EVIBAN project provides evidence of the potential benefit of MAR practices and management to a larger scale of aquifer recharge, particularly in coastal areas to struggle saltwater intrusion.

As part of the European project named AquaNES, imaGeau has proposed to install SMD technology in order to record the saltwater intrusion into a sandy coastal aquifer where a Managed Aquifer Recharge (MAR) is performed.

Three SMD tools and a level sensor has been installed in 2017 names Aq1, AQ3 et AQ4 (red point, Figure 2).

Figure 2: location of the Three SMD tools and picture of final installation

Since April 2017, the SMD tools are continuously measuring water conductivity evolutions between coastline and water treatment at different locations and depths (Figure 3).

SMD	AQ1	AQ3	AQ4
GPS coordinates	N 49°3’19.256” O 1°21’32.086”	N 49°3’28.922” O 1°35’52.641”	N 49°3’22.922” O 1°28’22.41”
Instrumented depth	2,44 – 6,44 m	2,4 – 6,4 m	1,96 – 5,96 m
Electrode spacing	0,3 m	0,3 m	0,3 m
Number of depths with EC measures	11	11	11
Time range of system ON	24/24h Every day	Once per hour Every day	Once per hour Every day
Automatic acquisition routine	Yes	Yes	Yes
Automatic data transfer	Yes	Yes	Yes
Remote control	OK	OK	OK
Local data storage	Yes	Yes	Yes
Power source	230 VAC	Solar panels and battery	Solar panels and battery

Figure 3: SMD features installed on site

For EviBan project, the three SMD systems have been maintained to continuously acquire EC data. In this purpose, field survey and remote diagnostics have been performed in order to continuously have data (Figure 4).

date	Intervention type	Monitoring system	tasks
23 July 2019	Field visit	SMD-AQ4	• Changing the electrical box • Replacing the battery (out of order due to water) • Removal of the battery box • Soft update and build • FTP update • Raising of the solar panel and housing Changing the orientation of the box (placed under the solar panel) • Update of COM port
23 July 2019	Field visit	CPT-AQ5	• Replacing batteries • Data recovery. • Changing FTP uploads from 1x/day to 1x/3 days.
23 July 2019	Field visit	SMD-AQ3	• Soft update and build • FTP update
24 July 2019	Field visit	SMD-AQ1	• Change of box and orientation (back to the direction of the rains). • Power cable unplugged at the gym. • Test carried out on the mains, • FTP update • Update of COM port • Waiting for main supply (230 V) from the municipality
10 Sept. 2020	remote diagnostic	SMD-AQ1	• Power supply 12V HS (no led on) Circuit breaker OK Time switch OK • Replacement of the power supply by the Saur technician.

Figure 4: table of maintenance operations

2.2.4. Results

Water level and local flow

The regional water flow is oriented East-West (land to sea) (bottom right, Figure 5)

The water level measured at different locations on the site during several years () allows to determine that (Figure 5):

- The water table on site is influenced by high tides
- a flow can be set up according to the volumes infiltrated on the reedbed (water table on Aq1 coming higher to water table on Aq3, January 2019 and February 2022) during high water level periods

- These located flows could have an impact on the saltwater intrusion

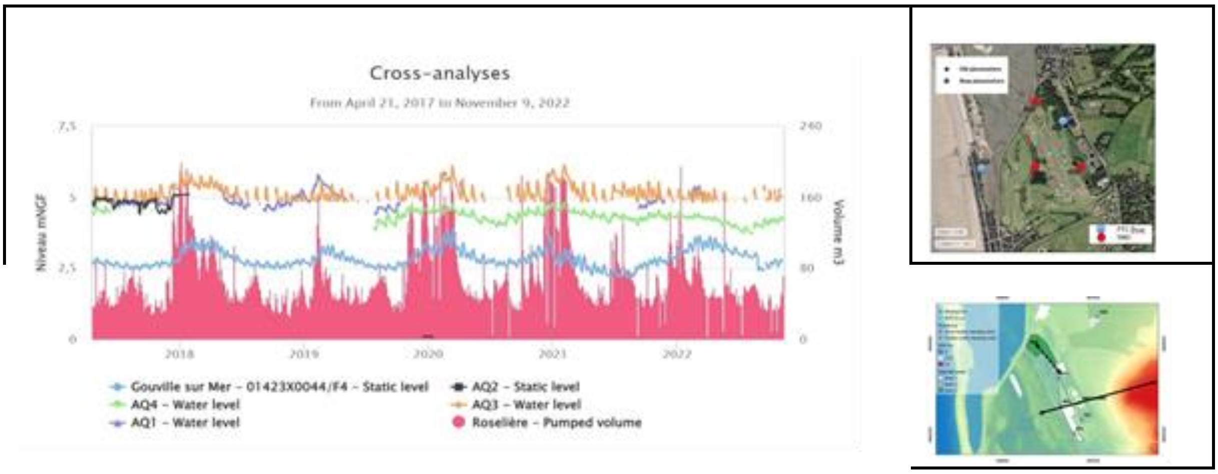

Figure 5: Water table on different locations (blue: regional water table, black: AQ2 location, orange: AQ3 location, purple: AQ1 location, green: AQ4 location) Vs wastewater hourly volume spread in the reedbed (pink) from 2017 to 2022

Conductivity (salinity) evolution

Aq3 location (north of the site, between sea and reedbed)

The electrical conductivity of the aquifer water measured at different depths by the SMD tools AQ3 allows to determine that (Figure 6, Figure 7):

- Conductivity increases with depth (aquifer bottom) at the end of each summer, reaching 20,000 µS/cm;
- Conductivity is very dependant of the tides;
- conductivity becomes lower and decreases during autumn each year;
- conductivity decreases when wastewater is spread during autumn.

This analysis allows us to assume that recharge limits the salt arrivals. The water recharge has two components:

- the natural recharge;
- the infiltration recharges du to wastewater spreading.

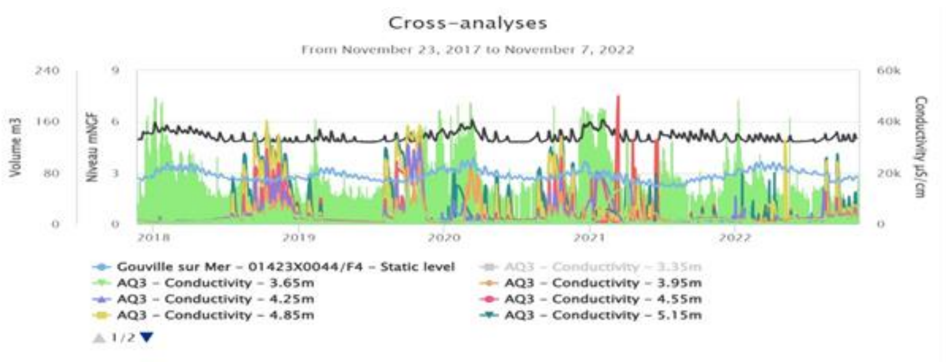

Figure 6: Evolution of conductivity (colours) at different depths measured by the SMD tools at AQ3 location VS water level on site (black and blue) and wastewater volume spread in the reedbed (green) – 2018-2022

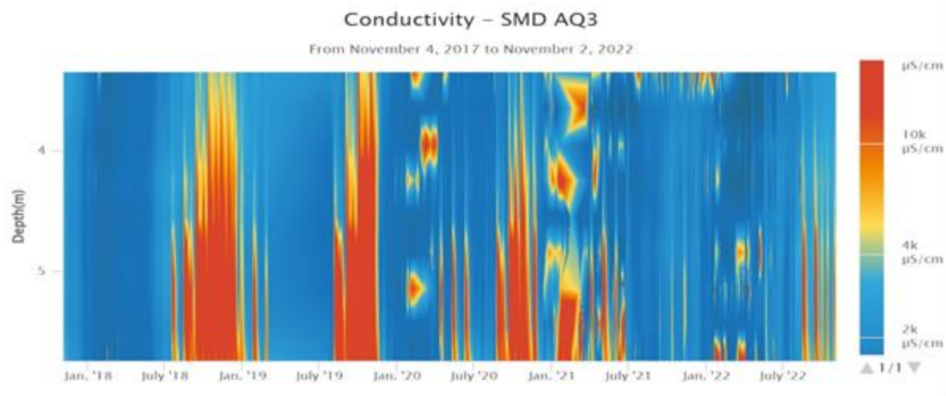

Figure 7 : Evolution of conductivity measured by the AQ3 SMD tool during time (x axis) and depth (y axis), showing the arrivals of salt in depth each year – 2018-2022

<u>Aq4 location (center of the site, between sea and reedbed in the golf field)</u>

The electrical conductivity of the aquifer water measured at different depths by the SMD tools AQ4 allows to determine that (Figure 8, Figure 9):

- Conductivity increases with depth (aquifer bottom) at the end of each summer, reaching 30,000 µS/cm in 2019;
- Conductivity is dependant of the tides;
- conductivity becomes lower and decreases during autumn each year;
- conductivity decreases when wastewater is spread during autumn;
- the salt intrusion becomes lower with years (impact of a higher wastewater volume in summer?).

A real impact of the period and volume of wastewater spread in the reedbed can be outlined. The salt intrusion is lower year after year while volume of wastewater spread in summer becomes higher (volume in July 2021 greater than 2020.

This analysis allows us to assume that recharge limits the salt arrivals (like for AQ3 location), and the water recharge has two components:

- the natural recharge;
- the infiltration recharge du to wastewater spreading.

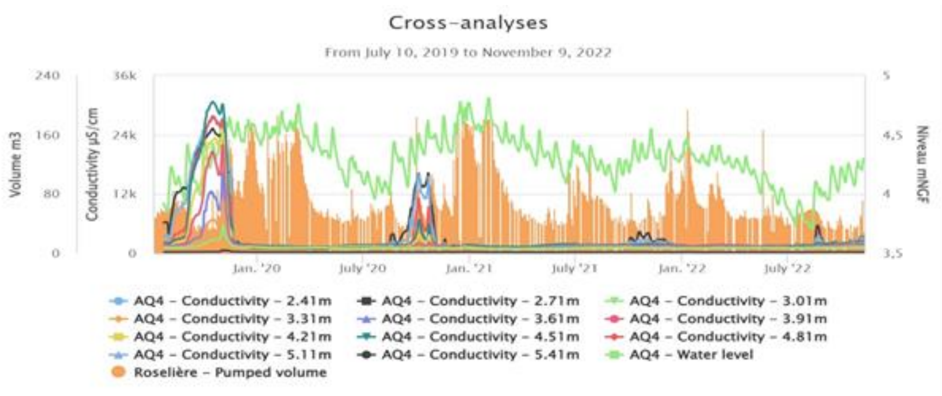

Figure 8: Evolution of conductivity (colours) at different depths measured by the SMD tools at AQ4 location VS water level on site (green) and wastewater volume spread in the reedbed (orange) – 2019-2022

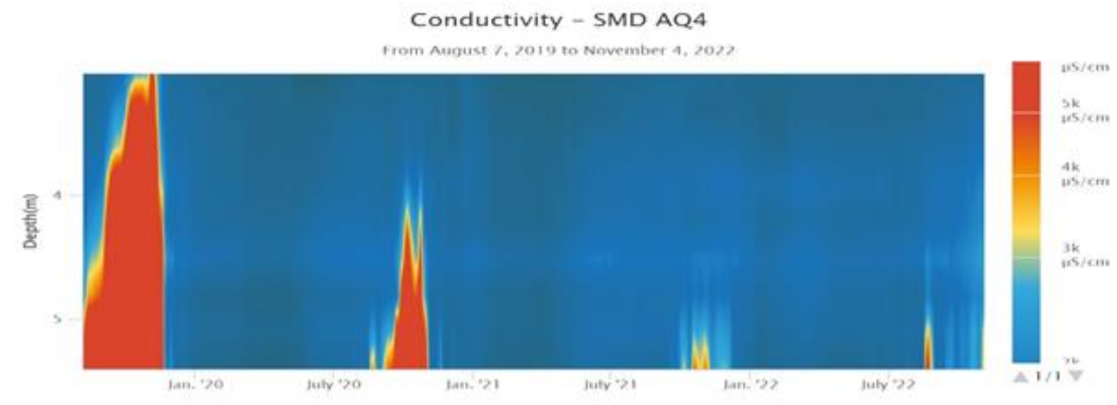

Figure 9: Evolution of conductivity measured by the AQ4 SMD tool during time (x axis) and depth (y axis), showing the arrivals of salt in depth each year – 2019-2022

<u>*Aq1 location (into the reedbed)*</u>

The electrical conductivity of the aquifer water measured at different depths by the SMD tools AQ1 shows same phenomena than observed at AQ3 and AQ4 location but with lower intensity.

Data acquired allows to determine that (Figure 10):

- Conductivity increases with depth (aquifer bottom) at the end of each summer, reaching only 3,500 µS/cm in 2018;
- Conductivity is little influenced by tides;
- conductivity becomes lower and decreases during autumn each year;
- conductivity decreases when volume of wastewater becomes higher;
- the salt intrusion becomes lower with years (impact of a higher wastewater volume in summer?).

As for AQ3 and AQ4 location, the recharge limits the salt arrivals and infiltration of wastewater in this location (piezometer close to the water treatment plant) has a real impact on water conductivity.

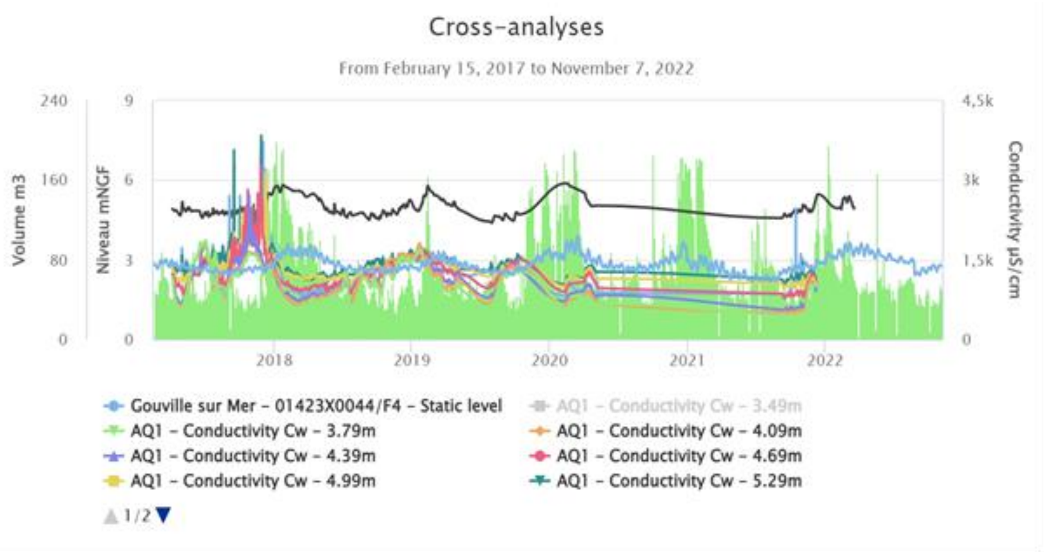

Figure 10: Evolution of conductivity (colours) at different depths measured by the SMD tools at AQ1 location VS water level on site (blue and black) and wastewater volume spread in the reedbed (green) – 2017-2022

A focus of conductivity evolution at 4-5 m depth at AQ1 and Aq3 locations allows to determine that (Figure 11):

- the water level at AQ1 location (into the reedbed) increases when wastewater infiltration occurs during wastewater spreading (red arrow);
- the water table at AQ1 location becomes higher than water level on AQ3 location. The consequence of this change in water level is a change in the orientation of the local flow (Figure 12).

This change in the orientation of local flow allows:

- a decrease of water salinity at AQ1 location (red arrow, Figure 11)
- a decrease of water salinity at AQ3 location (red arrow, Figure 11), from 20,000 to 500 microS/cm.

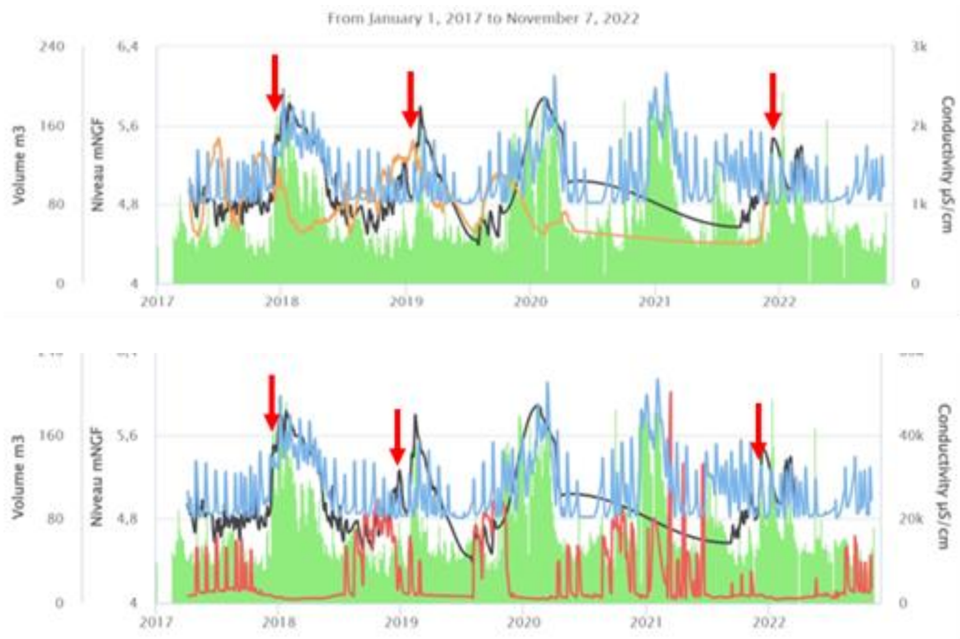

Figure 11: Evolution of water conductivity at 4 m depth at AQ1 location (orange, upper graph), water conductivity at 5,5 m depth at AQ3 location (red, lower graph), VS water table at AQ1 location (black, both graph) and water table at AQ3 location (blue, both graph) and hourly volume of wastewater spreading (green, both graph)

Figure 12: change of orientation of local flow during wastewater spreading

A focus of conductivity evolution at 4 m depth at AQ4 location (golf field) allows to determine that the recharge due to wastewater infiltration results in an increase of local water table AQ1. This results in an increase of piezometric gradient between AQ1 location (reed bed) and AQ4 location (AQ4 golf field)-and a decrease in salinity (red arrow, Figure 13).

The wastewater spreading allows to create a hydraulic barrier to saltwater intrusion.

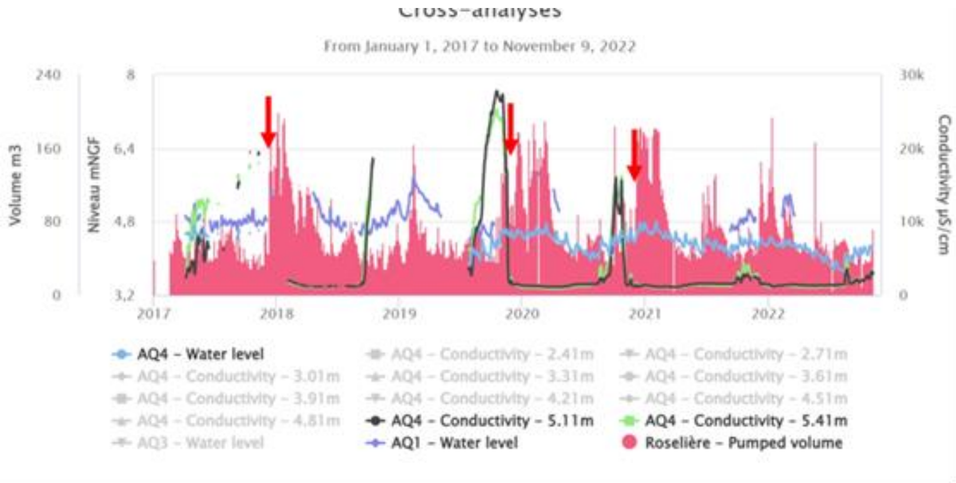

Figure 13: Evolution of water conductivity at 5 m depth at AQ4 location (green, black), VS water table at AQ1 location (purple) and water table at AQ4 location (blue) and hourly wastewater volume (pink)

Analysis of evolution of conductivity at 5m depth at AQ3 and AQ4 location (Figure 14) allows to link the decrease of conductivity to the:

1. natural recharge
2. wastewater infiltration

The rapid and sharp decrease of salinity (i.e conductivity) seems due to infiltration when the released wastewater volume is higher than 100 m3/h. (red arrow, Figure 14)

A hydraulic barrier to saltwater intrusion can be thus created when volume of wastewater is higher this limit (100 m3/h).

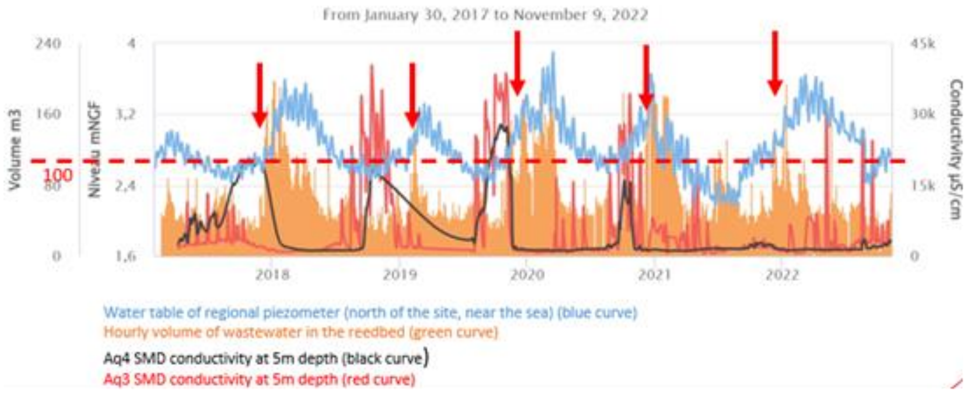

Figure 14:Evolution of water conductivity at 5 m depth at AQ3 and AQ4 locations (red, black), VS water table (blue) and hourly wastewater volume (orange)

2.2.5. Discussion

Analysis of conductivity acquired by SMD tools at various locations, at different depth during several years provides a new perspective on the impact of wastewater spreading on saltwater intrusion.

In resume, the infiltration of wastewater can locally alter the water flow and have an impact on saltwater intrusion. It is difficult to distinguish the impact of natural recharge and infiltration, but when the volume of released wastewater is higher than 100 m3/h, a sharp and rapid decrease in conductivity occurs.

The distance of wastewater effect on saltwater intrusion is not determined but greater than the distance between Aq1 location and Aq4 location (>250m)

A hydraulic barrier can be created with wastewater preventing the saltwater intrusion if wastewater volume is sufficient.

To provide accurate impact of wastewater on salt intrusion, an accurate monitoring of wastewater physical parameters (such as salinity, conductivity) should be implemented allowing to discriminate salinity coming from the sea (saltwater intrusion) and salinity coming from the wastewater.

The implementation of the SMD technologies in the EVIBAN project provides evidence of the potential benefit of MAR practices and management to a larger scale of aquifer recharge, particularly in coastal areas to struggle saltwater intrusion.

2.3. NORRMAN MAR/SAT

2.3.1. Overview of the software

The NORRMAN software (**N**ormes et **O**bjectifs de **R**éduction des **R**ejets pour les **MA**sses d'eau **N**aturelles : Standards and Discharge Reduction Targets for Natural Water Resources) simulates the impacts of polluting emissions in rivers at the scale of the water body. It helps to evaluate emission limit values and thus to determine discharge permits in compliance with good status objectives. NORRMAN has been published since 2008 by Antea Group after an initial collaboration with the Loire-Bretagne Water Agency.

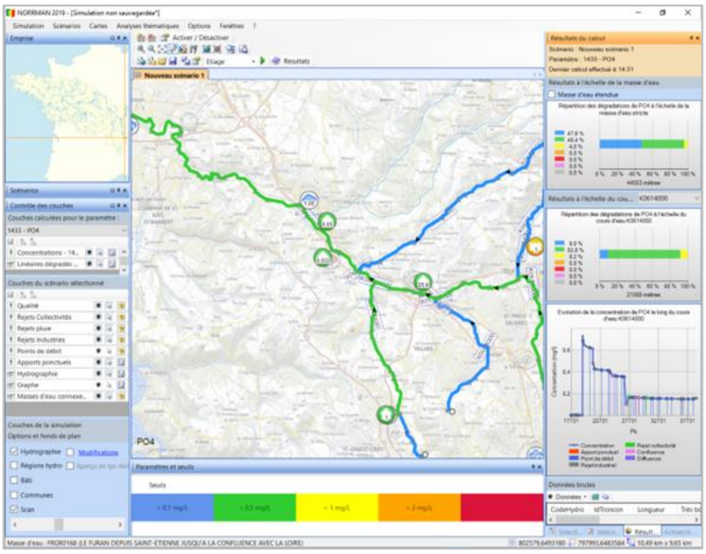

The operating principle of NORRMAN is to create and edit simulations of the impact of discharges at the scale of a body of water. The user selects a geographical footprint (water body), initial conditions (low water or modulus, rainy or dry weather, discharges: maximum, average...). NORRMAN then uploads the data from a web service published by Antea Group and initiates the simulation. Before performing the calculations of his simulation, the user can create, modify, parameterize, or move different objects on his map: Wastewater treatment plants (public or industrial), weirs, lateral inputs of watercourses, runoff, water flows and speed, kinetics by river section.

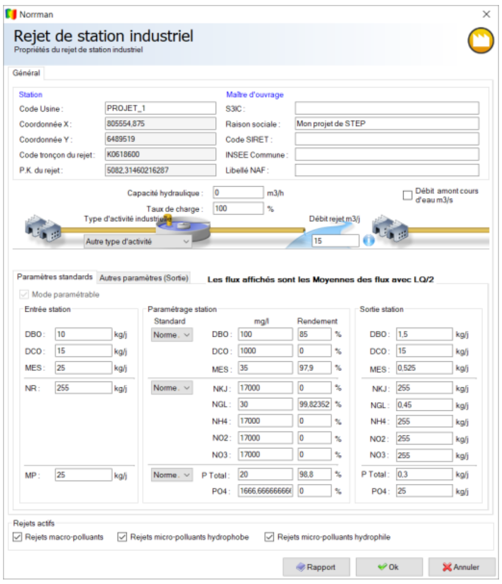

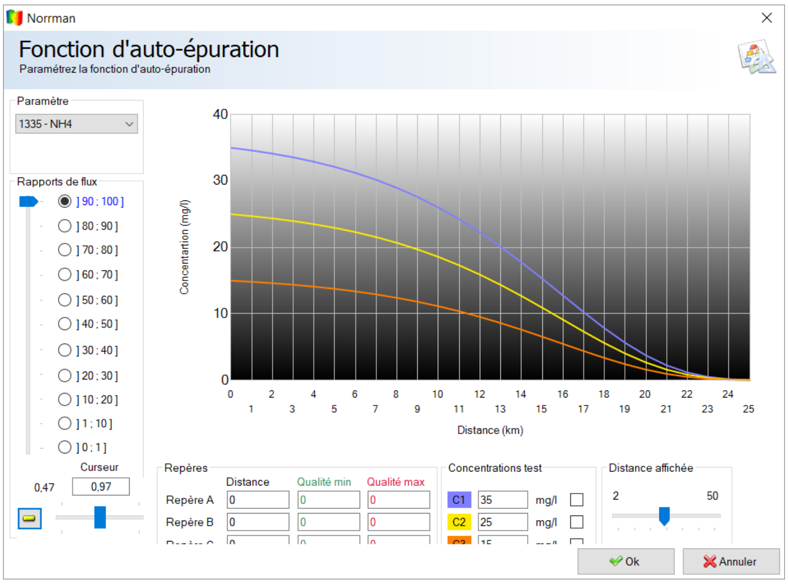

For these calculations, NORRMAN relies on self-purification kinetics parameterized according to hydrophilic micropollutants (DT50), hydrophobic micropollutants, macropollutants, flow rates and velocities. The results are rendered in the form of distribution graphs, graphs of profiles in length, GIS layers of degraded shelves, list of downgrading discharges...

Project Objectives

The NORRMAN software deals with the impact of wastewater treatment plants on the environment at the scale of the water body. It is a relevant decision-making tool for the wastewater treatment plant manager who wishes to assess the impact on surface water of an existing site or a construction project. The business field and the scale of work constitute a very relevant basis for integrating the Managed Aquifer Recharge (MAR) / Soil Aquifer Treatment (SAT) issue that is studied within the EviBAN project.

The aim was therefore to provide NORRMAN users with additional functionality to assess the feasibility of soil treatment of wastewater. Presented in the form of a geographical layer projected on the study territory, the module should make it possible to determine whether the area where the treatment plant is located is favourable to the implementation of an MAR/SAT system.

2.3.2. Work done for the project

NORRMAN simulation data

The first step in the work carried out by Antea Group was to collect baseline data on the study area. It turns out that the current version of NORRMAN only disseminates data from the Loire-Bretagne watershed. However, the Agon-Coutainville site is located on the Seine-Normandy basin. It was therefore necessary to contact the data managers of Seine-Normandie watershed to get authorization and obtain the river network divided into sections. Secondary work was then carried out by our geomatics specialists to prepare these data and integrate them into the NORRMAN database model. A specific web service was then published to connect to this new data.

Creating MAR/SAT decision layers

The second and not least step was to prepare the decision support data layer. To begin with, it was necessary to determine what information was needed to define the feasibility of a MAR/SAT system. To this end, Antea Group worked with the BRGM through several workshops to obtain expert advice.

- **GIS approach**

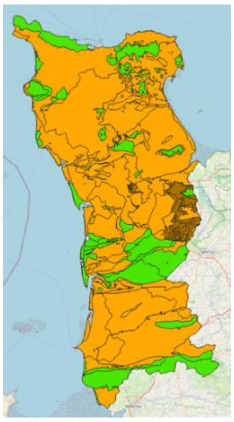

Following these workshops, it was agreed to rely on a BRGM publication that had carried out a similar assessment at the scale of the Rhône-Méditerranée-Corse watershed (*Analysis of the feasibility of artificial recharge in the RMC basin – BRGM-67534-FR*). This method was applied to the geographical area of the Agon-Coutainville study site by constraining the input data to the Cotentin region (Normandy) so as not to be dependent on too long processing times facing an approach that was intended to be iterative. Four GIS layers were used as input to the calculation: Slope (calculated on the 25m DEM), Soil Permeability Index (IDPR), Not saturated zone (NSZ) and BdLisa (Groundwater bodies). The result of the treatment was obtained at the scale of groundwater bodies according to the division of the BdLisa data.

- **AI approach**

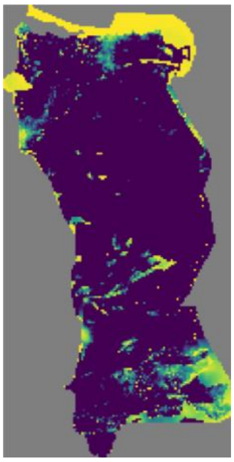

A second approach based on statistical analysis and artificial intelligence algorithms was studied during the project to compare the results obtained with the first method. The SIMCA (Soft Independent Modelling of Class Analogies) method was used. This method is based on three types of data; i) context data as input to the model (Protected zones, surface water bodies, River basins, ICPE, Biotopes, Geology, UNESCO, Slope, IDPR, Non saturated zone, Groundwater bodies) ii) the business data that determine the areas that are NOT favorable to the implementation of a MAR/SAT system, iii) the grid defining the scale of the result (here 500 meters grids). The algorithm then defined mesh by mesh the probability of "non-favorability". The model is trained on part of the data and then tested on the rest of the data. When the data scientist validates the right level of performance then the model is played on all the data. The result of the treatment produced a raster grid with for each cell a result between 0 and 1. 0 indicating 0% "not favorable" (which does not necessarily mean "favorable".), 1 indicating 100% "not favorable".

NORRMAN Software Update

The layers produced using both GIS and AI methods were published on a geographic server operated by Antea Group. The source code of the NORRMAN software has been updated to integratethese new layers and allow them to appear in the background of the simulations.

2.3.3. Results

Two different approaches were investigated. The GIS approach based on a methodology described in a BRGM paper on the one hand and the statistical approach based on AI algorithms on the other. The two approaches produce different interpretations.

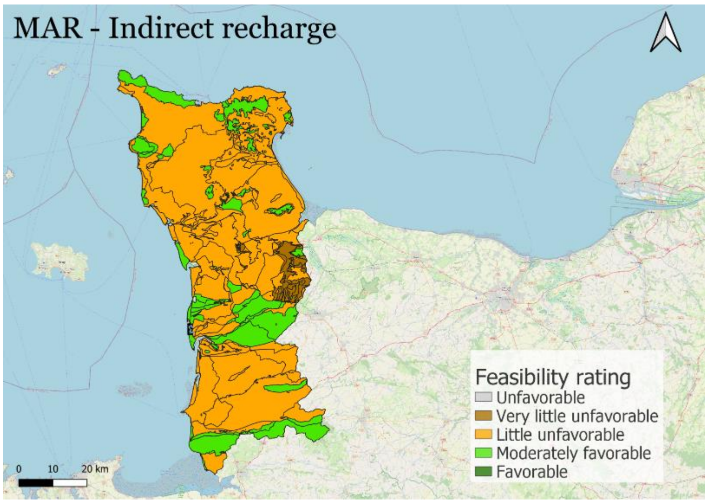

GIS treatment result

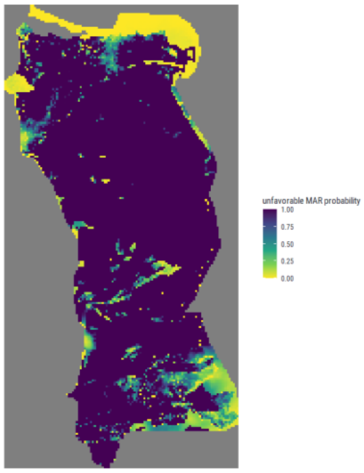

AI treatment result

The **GIS approach** was based on 4 geographical layers as input to the treatment. This seems too little for the scale of the study. The results define favorable and unfavorable zones for MAR/SAT at the scale of the groundwater body and too large. An expert eye cannot be expressed at the scale of a wastewater treatment plant site on a body of surface water. The scale of work on a large French watershed as proposed in the BRGM publication has therefore proved to be far too large compared to the study area of the EviBAN project.

On the other hand, the **AI approach** offers a much more adapted scale by proposing results on cells of 500 meters side. In addition, the input data was much more complete with 11 layers compared to 4 in the GIS cross-referencing method. The model gave quite satisfactory results with a level of accuracy of 95%. This level can be further improved by removing certain errors such as false positives located at sea north of the study area. This problem could be solved by, for example, adding the coastline in the input data.

The SIMCA method restores levels of "non-favorability" based on the principle that the algorithm produces classifications based on expert statements defining areas for which it is certain that the MAR/SAT is unfavorable. It will then be a question of testing the algorithm by indicating favorable areas. But this implies an unsure expert commitment and potentially questionable results.

2.3.4. Conclusion

The NORRMAN software is aimed at managers and decision-makers concerned about the impact of discharges from their installations. It is therefore an excellent support for integrating the concept of water treatment by means of natural based solutions such as MAR/SAT. Without saying precisely where and how to implement this solution, NORRMAN is an excellent entry point to make its users aware of this type of solution, which is still very little common in France.

However, it is essential to communicate reliable information to the user. For this, we studied two different approaches that we confronted with the study area of Agon-Coutainville. On the one hand the GIS approach which consisted in crossing different geographical information layers and on the other hand the statistical approach with the implementation of an artificial intelligence algorithm.

At the end of the project, the results of the second approach using AI algorithms seem to us to be the most relevant and promising for an analysis of the river water body scale. However, the results need to be deepened with business experts and tested on other geographical areas (lowland areas, mountainous areas, etc.). before being released in the major version of NORRMAN.

On the other hand, publishing this service also involves certain technical considerations that cannot be dismissed. On the one hand the need to have a layer of watercourses throughout the whole French territory. It also implies to get all input data at the national scale to produce the result layer from AI processing.

Finally, it must be taken into consideration that the NORRMAN software is only dedicated to the French territory. Its data are standardized according to French directives and the interfaces are not available in other languages. The prospect of internationalizing this product is currently difficult to envisage without a complete overhaul of the software.

3. Applicability of French model to South Africa

The MARTHE model is being set up for the Melkhoutfontein area 4km north of Stilbaai.

The Melkhoutfontein aquifer is the highest yielding of the coastal aquifers and supplies Melkhoutfontein, Stilbaai and Jongensfontein with drinking water. A low-cost housing development with 550 houses has been approved in the Melkhoutfontein village. An earlier hydrocensus and modelling exercise to investigate water security of Stilbaai with these additional houses showed that the spring is does not yield enough water during the summer months to adequately supply residents and holiday makers with water, should the additional houses be built (Du Plessis & Steenekamp, 2015).

Also as part of the Melkhoutfontein expansion project, the existing wastewater treatment works is being upgraded to a 0.45Ml/d facility. The treated effluent could potentially be used to recharge the aquifer to ensure constant supply during the dry summer months when tourism is also at its peak and demand outstrips supply. Melkhoufontein is situated on the same geology as the area described above in section xx, where springs discharge into the river. The Wankoe formation of the Bredasdorp group overlays the De Hoopvlei formation (also Bredasdorp Group) that comprises calcarenite and calcareous sandstone with pebbles, forming the aquifer. The aquifer is situated on an aquiclude of Bokkeveld shale. The Bokkeveld shale aquiclude is above sea level and as such saline intrusion is not an issue for the aquifer.

Some initial modelling work has been done to investigate the use of treated effluent as irrigation water for smallholder farmer development and it was recommended that farming be moved far away from the abstraction borehole to avoid contamination of the drinking water supplies (Du Plessis & Steenekamp, 2020). Modflow software was used for this. This situation in Melkhoutfontein closely resembles that of the MAR-SAT system of Agon-Countainville in France, where treated effluent is being used to water the golf course. Setting up the MARTHE model in Melkhoutfontein will therefore be a good comparison with the French case study.

The MARTHE model in Melkhoutfontein will build on the existing work that was done by Du Plessis and Steenekamp (2020) and incorporate their recommendations. However, we want to create a scenario where agricultural run-off can be treated through a reed bed or similar nature-based solution before recharging the aquifer, and/or the implementation of organic agriculture to avoid contamination altogether. The MARTHE model will enable the project team to better capture the complexities of the system than earlier simpler modelling efforts.

4. Applicability of South Africa model to French model

The Pitman model (through SPATSIM) could add value to the French modelling efforts by providing a better understanding of the hydrology of the river Sienne River. The MARTHE model requires hydrological catchment data as an input measure, which at this stage are mostly assumptions. Applying SPATSIM to the catchment should provide a better understanding of the hydrology of the river and will thereby improve the quality of the results produced in the MARTHE model (serving as the management tool). It will also provide valuable additional information to the municipality in terms of water management in the catchment to ensure sustainable environmental flows during peak holiday seasons, which is becoming a management challenge here and in other areas in France. The municipality will further benefit from the newly established relationship with the Hessequa Municipality through learning from their tough lessons learned through numerous droughts, extreme events and management of peak holiday seasons.

5. References

Aemig, Q., Hélias, A., Patureau, D., 2021. Impact assessment of a large panel of organic and inorganic micropollutants released by wastewater treatment plants at the scale of France. Water Res. 188, 116524. https://doi.org/10.1016/j.watres.2020.116524

Aeschbach-Hertig, W., Gleeson, T., 2012. Regional strategies for the accelerating global problem of groundwater depletion. Nat. Geosci. 5, 853–861. https://doi.org/10.1038/ngeo1617

Ahmed, K.M., Sultana, S., Chowdhury, T., Islam, R., Delwaruzzaman, M., Mahtab-ul Alam, S.M., Ravenscroft, P., Tuinhof, A., Onabolu, B., Akhter, N., Mahmud, M.N., Rahman, M.S., Ghosh, S.K., Zheng, Y., 2020. Case Study 1: A resilient drinking water supply using aquifer storage and recovery for coastal communities in Batiaghata, Khulna, Bangladesh, in: MANAGING AQUIFER RECHARGE A Showcase for Resilience and Sustainability. Yan Zheng, Andrew Ross, Karen Villholth and Peter Dillon (eds), Paris, UNESCO., pp. 82–89.

Ajjur, S.B., Baalousha, H.M., 2021. A review on implementing managed aquifer recharge in the Middle East and North Africa region: methods, progress and challenges. Water Int. 46, 578–604. https://doi.org/10.1080/02508060.2021.1889192

Alidina, M., Li, D., Ouf, M., Drewes, J.E., 2014. Role of primary substrate composition and concentration on attenuation of trace organic chemicals in managed aquifer recharge systems. J. Environ. Manage. 144, 58–66. https://doi.org/10.1016/j.jenvman.2014.04.032

Amy, G., Drewes, J., 2007. Soil Aquifer Treatment (SAT) as a Natural and Sustainable Wastewater Reclamation/Reuse Technology: Fate of Wastewater Effluent Organic Matter (EfOM) and Trace Organic Compounds. Environ. Monit. Assess. 129, 19–26. https://doi.org/10.1007/s10661-006-9421-4

Anderson, W.P., Emanuel, R.E., 2009. Effect of interannual climate oscillations on rates of submarine groundwater discharge 13. https://doi.org/doi:10.1029/2009WR008212

ANSES, 2016. Risques sanitaires liés à la recharge artificielle de nappes d'eau souterraine. Avis de l'Anses. Rapport d'expertise collective. ANSES.

Appelo, C.A.J., Postma, D., 2005. Geochemistry, groundwater and pollution, 2nd edition. ed. CRC Press, Taylor & Francis Group, Boca Raton London New York.

AQUASTAT, 2022. AQUASTAT Core Database. Food and Agriculture Organization of the United Nations.

Arrêté du 22 juin 2007, n.d. Arrêté du 22 juin 2007 relatif à la collecte, au transport et au traitement des eaux usées des agglomérations d'assainissement ainsi qu'à la surveillance de leur fonctionnement et de leur efficacité, et aux dispositifs d'assainissement non collectif recevant une charge brute de pollution organique supérieure à 1,2 kg/j de DBO5.

Arrêté du 25 janvier 2010, 2010. Arrêté du 25 janvier 2010 établissant le programme de surveillance de l'état des eaux en application de l'article R. 212-22 du code de l'environnement. MINISTÈRE DE L'ÉCOLOGIE, DE L'ÉNERGIE, DU DÉVELOPPEMENT DURABLE ET DE LA MER.

Artimo, A., Puurunen, O., Sami, S., 2020. Case Study 2: Managed Aquifer Recharge for Drinking Water Supply, Turku Region, Southwestern Finland, in: MANAGING AQUIFER RECHARGE A Showcase for Resilience and Sustainability. Yan Zheng, Andrew Ross, Karen Villholth and Peter Dillon (eds), Paris, UNESCO.

Arye, G., Dror, I., Berkowitz, B., 2011. Fate and transport of carbamazepine in soil aquifer treatment (SAT) infiltration basin soils. Chemosphere 82, 244–252. https://doi.org/10.1016/j.chemosphere.2010.09.062

Assises de l'eau, 2020. Bilan des Assises de l'eau du Comité national de l'eau du 16 juillet 2020.

Ayuso-Gabella, N., Page, D., Masciopinto, C., Aharoni, A., Salgot, M., Wintgens, T., 2011. Quantifying the effect of Managed Aquifer Recharge on the microbiological human health risks of irrigating crops with recycled water. Agric. Water Manag. 99, 93–102. https://doi.org/10.1016/j.agwat.2011.07.014

Baulon, L., Massei, N., Allier, D., Fournier, M., Bessiere, H., 2022. Influence of low-frequency variability on high and low groundwater levels: example of aquifers in the Paris Basin. Hydrol. Earth Syst. Sci. 26, 2829–2854. https://doi.org/10.5194/hess-26-2829-2022

Bear, J., Cheng, A., Sorek, S., Ouazar, D., Herrera, I., 1999. Seawater intrusion in coastal aquifers : concepts, methods, and practices.

Bekele, E., Toze, S., Patterson, B., Higginson, S., 2011. Managed aquifer recharge of treated wastewater: Water quality changes resulting from infiltration through the vadose zone. Water Res. 45, 5764–5772. https://doi.org/10.1016/j.watres.2011.08.058

Bailey, A.K & Pitman, WV. 2016. Water Resources of South Africa, 2012 study (WR2012). Volume 7: WRSM/Pitman User's Manual. WRC Report No. TT 689/16, Pretoria, South Africa.

BellotJ-P., Neyens D., Pezard P.A, Cazaux D. Battelle Chlorinated Conference in Monterey. Nineth international conference on remediation of chlorinated and recalcitrant compounds, May 19–22, 2014 Monterey, California, Dynamic monitoring of pure phase chlorinated solvents in aquifer by in situ electrical resistivity,

Bellot J-P., Neyens D., Pezard P.A, Depraz O., Barry S.,De Mezzo B., Henry G., Depraz L., Baqué L. A new dowhole real time and near field hydrogophysical observatory of grounwater quality, European Meeting of Environmental and Engineering Geophysics of the Near Surface Geoscience, Paris, September 3-5,2012,

Bellot J-P., Depraz O., Neyens D., Barry S., De Mezzo B., Baqué L., Henry G., Depraz L., Pezard P.A. The imaGeau observatory: moving towards the innovative management of coastal aquifers. TIAC'12: International Conference on Technology Seawater Intrusion in Coastal Aquifers, Alicante, Spain, April 24-27, 2012,

Benotti, M.J., Brownawell, B.J., 2009. Microbial degradation of pharmaceuticals in estuarine and coastal seawater. Environ. Pollut. 157, 994–1002. https://doi.org/10.1016/j.envpol.2008.10.009

Bertelkamp, C., Reungoat, J., Cornelissen, E.R., Singhal, N., Reynisson, J., Cabo, A.J., van der Hoek, J.P., Verliefde, A.R.D., 2014. Sorption and biodegradation of organic micropollutants during river bank filtration: A laboratory column study. Water Res. 52, 231–241. https://doi.org/10.1016/j.watres.2013.10.068

Biel-Maeso, M., Corada-Fernández, C., Lara-Martín, P.A., 2018. Monitoring the occurrence of pharmaceuticals in soils irrigated with reclaimed wastewater. Environ. Pollut. 235, 312–321. https://doi.org/10.1016/j.envpol.2017.12.085

Bierkens, M.F.P., Wada, Y., 2019. Non-renewable groundwater use and groundwater depletion: a review. Environ. Res. Lett. 14, 063002. https://doi.org/10.1088/1748-9326/ab1a5f

Blanc, P., Devau, N., Pettenati, M., Picot, G., Mauffret, A., 2016. FRAME :Treatment process and contaminant behavior in porous media models considering the most relevant factors determining CEC attenuation 45.

Brunsch, A.F., ter Laak, T.L., Rijnaarts, H., Christoffels, E., 2018. Pharmaceutical concentration variability at sewage treatment plant outlets dominated by hydrology and other factors. Environ. Pollut. 235, 615–624. https://doi.org/10.1016/j.envpol.2017.12.116

Bunting, S.Y., 2021. Emerging organic compounds in European groundwater. Environ. Pollut. 13.

Burke, V., Greskowiak, J., Asmuß, T., Bremermann, R., Taute, T., Massmann, G., 2014. Temperature dependent redox zonation and attenuation of wastewater-derived organic micropollutants in the hyporheic zone. Sci. Total Environ. 482–483, 53–61. https://doi.org/10.1016/j.scitotenv.2014.02.098

Burke, V., Greskowiak, J., Grünenbaum, N., Massmann, G., 2017a. Redox and Temperature Dependent Attenuation of Twenty Organic Micropollutants - A Systematic Column Study. Water Environ. Res. 89, 155–167. https://doi.org/10.2175/106143016X14609975746000

Burke, V., Greskowiak, J., Grünenbaum, N., Massmann, G., 2017b. Redox and Temperature Dependent Attenuation of Twenty Organic Micropollutants - A Systematic Column Study. Water Environ. Res. 89, 155–167. https://doi.org/10.2175/106143016X14609975746000

Burke, V., Treumann, S., Duennbier, U., Greskowiak, J., Massmann, G., 2013. Sorption behavior of 20 wastewater originated micropollutants in groundwater — Column experiments with pharmaceutical residues and industrial agents. J. Contam. Hydrol. 154, 29–41. https://doi.org/10.1016/j.jconhyd.2013.08.001

Burnett, W.C., Bokuniewicz, H., Huettel, M., Moore, W.S., Taniguchi, M., 2003. Groundwater and pore water inputs to the coastal zone. Biogeochemistry 66, 3–33. https://doi.org/10.1023/B:BIOG.0000006066.21240.53

Cabeza, Y., Ahrens, L., Ronenb, D., Teijona, G., 2012. Monitoring the occurrence of emerging contaminants in treated wastewater and groundwater between 2008 and 2010. The Baix Llobregat (Barcelona, Spain). J. Hazard. Mater. 8. https://doi.org/10.1016/j.jhazmat.2012.07.032

Cary, L., Casanova, J., Gaaloul, N., Guerrot, C., 2013. Combining boron isotopes and carbamazepine to trace sewage in salinized groundwater: A case study in Cap Bon, Tunisia. Appl. Geochem. 34, 126–139. https://doi.org/10.1016/j.apgeochem.2013.03.004

Casanova, J., Cagnimel, M., Devau, N., Pettenati, M., 2013. Recharge artificielle des eaux souterraines : état de l'art et perspectives 227.

Chapelle, F. (Geological S., Columbia, SC (United States)), 1993. Ground-water microbiology and geochemistry. New York, NY (United States); John Wiley and Sons, United States.

Chefetz, B., Mualem, T., Ben-Ari, J., 2008. Sorption and mobility of pharmaceutical compounds in soil irrigated with reclaimed wastewater. Chemosphere 73, 1335–1343. https://doi.org/10.1016/j.chemosphere.2008.06.070

Clara, M., Strenn, B., Kreuzinger, N., 2004. Carbamazepine as a possible anthropogenic marker in the aquatic environment: investigations on the behaviour of Carbamazepine in wastewater treatment and during groundwater infiltration. Water Res. 38, 947–954. https://doi.org/10.1016/j.watres.2003.10.058

Code de l'environnement, 2022. Section 1 : Sites Natura 2000 (Articles L414-1 à L414-7).

Code de l'environnement R122-2, 2022. Code de l'environnement. Article Annexe à l'article R122-2.

Code de l'environnement R214-1, 2021. Code de l'environnement Article R214-1, Version en vigueur depuis le 14 février 2021.

Code de l'environnement R214-3, 2020. Code de l'environnement Article R214-3, Version en vigueur depuis le 14 février 2021.

Commune d'Agon-Coutainville, 2013. Profil de vulnérabilité. Rapport technique.

Cowpertwait, P.S.P., Metcalfe, A.V., 2009. Introductory time series with R, Use R! Springer, Dordrecht Heidelberg London New York.

Crampon, M., Soulier, C., Sidoli, P., Hellal, J., Joulian, C., Charron, M., Guillemoto, Q., Picot-Colbeaux, G., Pettenati, M., 2021. Dynamics of Soil Microbial Communities During Diazepam and Oxazepam Biodegradation in Soil Flooded by Water From a WWTP. Front. Microbiol. 12, 742000. https://doi.org/10.3389/fmicb.2021.742000

Cruz-Ayala, M.B., Megdal, S.B., 2020. An Overview of Managed Aquifer Recharge in Mexico and Its Legal Framework. Water 12, 474. https://doi.org/10.3390/w12020474

Dalton, H., Stirling, D.I., Quayle, J.R., 1982. Co-metabolism [and discussion].

Dashora, Y., Dillon, P., Maheshwari, B., Soni, P., Mittal, H.K., Dashora, R., Singh, P.K., Purohit, R.C., Katara, P., 2020. Case Study 4: Recharge structures in ephemeral streams in Dharta watershed, Rajasthan, India, in: MANAGING AQUIFER RECHARGE A Showcase for Resilience and Sustainability. Yan Zheng, Andrew Ross, Karen Villholth and Peter Dillon (eds), Paris, UNESCO., pp. 105–112.

de. Marsily, G., 1983. Hydrogéologie Quantitative. 216 pp., 11 p1. Paris, New York, Milan, Mexico, Rio de Janeiro: Masson. ISBN 2 225 75504 3 (paperback). Geol. Mag. 120, 94–94. https://doi.org/10.1017/S0016756800025127

Décret du 10 mars 2022, 2022. Journal officiel électronique authentifié n° 0059 du 11/03/2022 Décret n° 2022-336 du 10 mars 2022 relatif aux usages et aux conditions de réutilisation des eaux usées traitées.

Department of Water Affairs (South Africa), 2010. The Atlantis Water Resource Management Scheme : 30 years of Artificial Groundwater Recharge. (No. PRSA 000/00/11609/10 Activity 17 (AR5.1)), Strategy and Guideline Development for National Groundwater Planning Requirements.

Dibaj, M., Javadi, A.A., Akrami, M., Ke, K.-Y., Farmani, R., Tan, Y.-C., Chen, A.S., 2020. Modelling seawater intrusion in the Pingtung coastal aquifer in Taiwan, under the influence of sea-level rise and changing abstraction regime. Hydrogeol. J. 28, 2085–2103. https://doi.org/10.1007/s10040-020-02172-4

Dillon, P., 2005. Future management of aquifer recharge. Hydrogeol. J. 13, 313–316. https://doi.org/10.1007/s10040-004-0413-6

Dillon, P., Alley, W., Zheng, Y., Vanderzalm, J., Ward, J., Megdal, S., Hipke, W., Thomas, P., Tuthill, D., Carlson, R., 2022. Managed Aquifer Recharge: Overview and Governance.

Dillon, P., Fern, E., Massmann, G., 2020. Managed Aquifer Recharge for Water Resilience 11.

Dillon, P., Stuyfzand, P., Grischek, T., Lluria, M., Pyne, R.D.G., Jain, R.C., Bear, J., Schwarz, J., Wang, W., Fernandez, E., Stefan, C., Pettenati, M., van der Gun, J., Sprenger, C., Massmann, G., Scanlon, B.R., Xanke, J., Jokela, P., Zheng, Y., Rossetto, R., Shamrukh, M., Pavelic, P., Murray, E., Ross, A., Bonilla Valverde, J.P., Palma Nava, A., Ansems, N., Posavec, K., Ha, K., Martin, R., Sapiano, M., 2019. Sixty years of global progress in managed aquifer recharge. Hydrogeol. J. 27, 1–30. https://doi.org/10.1007/s10040-018-1841-z

Dimitrov, S., Pavlov, T., Dimitrova, N., Georgieva, D., Nedelcheva, D., Kesova, A., Vasilev, R., Mekenyan, O., 2011. Simulation of chemical metabolism for fate and hazard assessment. II CATALOGIC simulation of abiotic and microbial degradation. SAR QSAR Environ. Res. 22, 719–755. https://doi.org/10.1080/1062936X.2011.623322

Directive 2000/60/CE, 23 octobre. Directive 2000/60/CE du Parlement européen et du Conseil du 23 octobre 2000 établissant un cadre pour une politique communautaire dans le domaine de l'eau.

Directive 2006/7/CE, 15 février. DIRECTIVE 2006/7/CE DU PARLEMENT EUROPÉEN ET DU CONSEIL du 15 février 2006 concernant la gestion de la qualité des eaux de baignade et abrogeant la directive 76/160/CEE.

Directive 2006/118/CE, 12 décembre. DIRECTIVE 2006/118/CE DU PARLEMENT EUROPÉEN ET DU CONSEIL du 12 décembre 2006 sur la protection des eaux souterraines contre la pollution et la détérioration.

Directive 2008/105/CE, 16 décembre. PARLEMENT EUROPÉEN ET DU CONSEIL du 16 décembre 2008.

Directive 2013/39/UE, 12 août. DIRECTIVE 2013/39/UE DU PARLEMENT EUROPÉEN ET DU CONSEIL du 12 août 2013 modifiant les directives 2000/60/CE et 2008/105/CE en ce qui concerne les substances prioritaires pour la politique dans le domaine de l'eau.

Dörfliger, N., Crochet, P., Guerrin, R., Jozja, N., Marsaud, B., Mondain, P.H., Muet, P., Plagnes, V., 2010. Guide méthodologique Les outils de l'hydrogéologie karstique pour la caractérisation de la structure et du fonctionnement des systèmes karstiques et l'évaluation de leur ressource 224.

Drewes, J.E., Heberer, T., Rauch, T., Reddersen, K., 2003. Fate of Pharmaceuticals During Ground Water Recharge. Groundw. Monit. Remediat. 23, 64–72. https://doi.org/10.1111/j.1745-6592.2003.tb00684.x

Drewes, J.E., Heberer, T., Reddersen, K., 2002. Fate of pharmaceuticals during indirect potable reuse. Water Sci. Technol. 46, 73–80. https://doi.org/10.2166/wst.2002.0058

Drillia, P., Stamatelatou, K., Lyberatos, G., 2005. Fate and mobility of pharmaceuticals in solid matrices. Chemosphere 60, 1034–1044. https://doi.org/10.1016/j.chemosphere.2005.01.032

Du, B., Price, A.E., Scott, W.C., Kristofco, L.A., Ramirez, A.J., Chambliss, C.K., Yelderman, J.C., Brooks, B.W., 2014. Comparison of contaminants of emerging concern removal, discharge, and water quality hazards among centralized and on-site wastewater treatment system effluents receiving common wastewater influent. Sci. Total Environ. 466–467, 976–984. https://doi.org/10.1016/j.scitotenv.2013.07.126

Dulio, V., van Bavel, B., Brorström-Lundén, E., Harmsen, J., Hollender, J., Schlabach, M., Slobodnik, J., Thomas, K., Koschorreck, J., 2018. Emerging pollutants in the EU: 10 years of NORMAN in support of environmental policies and regulations. Environ. Sci. Eur. 30, 5. https://doi.org/10.1186/s12302-018-0135-3

Dupret, L., Poncet, J., Lautribou, J.P., Hommeril, P., 1987. Notice explicative de la feuille coutances à 1/50 000.

DWS. 2014. Development of reconciliation strategies for all towns in the southern planning region: Riversdale, Hessequa LM (WSA), Eden DM Western Cape Province Version 2. Department of Water and Sanitation, Pretoria, South Africa.

Elkayam, R., Negev, I., Lev, O., 2020. Case Study 6: Soil Aquifer Treatment of Secondary Effluent for Irrigation in the Negev desert area, Israel, in: MANAGING AQUIFER RECHARGE A Showcase for Resilience and Sustainability. Yan Zheng, Andrew Ross, Karen Villholth and Peter Dillon (eds), Paris, UNESCO., pp. 124–130.

European Commission, 2014. Commission Directive 2014/80/EU, amending Annex II to Directive 2006/118/EC of the European Parliament and of the Council on the protection of groundwater against pollution and deterioration. Off. J. Eur. Union L 182.

Famiglietti, J.S., 2014. The global groundwater crisis. Nat. Clim. Change 4, 945–948. https://doi.org/10.1038/nclimate2425

Fent, K., Weston, A.A., Caminada, D., 2006. Ecotoxicology of human pharmaceuticals. Aquat. Toxicol. 76, 122–159. https://doi.org/10.1016/j.aquatox.2005.09.009

Feranec, J., 2016. Project CORINE land cover, in: European Landscape Dynamics. CRC Press, pp. 39–44.

Ferguson, G., Gleeson, T., 2012. Vulnerability of coastal aquifers to groundwater use and climate change. Nat. Clim. Change 2, 342–345. https://doi.org/10.1038/nclimate1413

Ferguson, G., McIntosh, J.C., Warr, O., Sherwood Lollar, B., Ballentine, C.J., Famiglietti, J.S., Kim, J., Michalski, J.R., Mustard, J.F., Tarnas, J., McDonnell, J.J., 2021. Crustal Groundwater Volumes Greater Than Previously Thought. Geophys. Res. Lett. 48. https://doi.org/10.1029/2021GL093549

Fernández-Escalante, E., Henao Casas, J.D., Vidal Medeiros, A.M., San Sebastián Sauto, J.S.S.S., 2020. Regulations and guidelines on water quality requirements for Managed Aquifer Recharge. International comparison. Acque Sotter. - Ital. J. Groundw. https://doi.org/10.7343/as-2020-462

Fernández-Escalante, E., Sauto, J.S.S., Gil, R.C., 2019. Sites and Indicators of MAR as a Successful Tool to Mitigate Climate Change Effects in Spain. Water 11, 1943. https://doi.org/10.3390/w11091943

Ferreira, J.P.L., Oliveira, M., Diamantino, C., João Moinante, M., Medeiros, A., 2007. DELIVERABLE 31 - Inventory of alternative water sources for each Test site, G A B A R D I N E groundwater artificial recharge based on alternative sources of water: advanced integrated technologies and management.

Franco, A., Trapp, S., 2008. ESTIMATION OF THE SOIL–WATER PARTITION COEFFICIENT NORMALIZED TO ORGANIC CARBON FOR IONIZABLE ORGANIC CHEMICALS. Environ. Toxicol. Chem. 27, 1995. https://doi.org/10.1897/07-583.1

Gale, I., 2005. Strategies for Managed Aquifer Recharge (MAR) in semi-arid areas. UNESCO's International Hydrological Programme (IHP) IHP/2005/GW/MAR, 33.

Garceran, R., 2017. Installation report of three imaGeau "Subsurface Monitoring Device" (SMD) and two data loggers in Agon-Coutainville, littoral of Manche department in France., Aquanes. IMAGEO.

Geissen, V., Mol, H., Klumpp, E., Umlauf, G., Nadal, M., van der Ploeg, M., van de Zee, S.E.A.T.M., Ritsema, C.J., 2015. Emerging pollutants in the environment: A challenge for water resource management. Int. Soil Water Conserv. Res. 3, 57–65. https://doi.org/10.1016/j.iswcr.2015.03.002

Gelhar, L.W., Welty, C., Rehfeldt, K.R., 1992. A critical review of data on field-scale dispersion in aquifers. Water Resour. Res. 28, 1955–1974. https://doi.org/10.1029/92WR00607

Ghil, M., Allen, M.R., Dettinger, M.D., Ide, K., Kondrashov, D., Mann, M.E., Robertson, A.W., Saunders, A., Tian, Y., Varadi, F., Yiou, P., 2002. ADVANCED SPECTRAL METHODS FOR CLIMATIC TIME SERIES: CLIMATIC TIME SERIES ANALYSIS. Rev. Geophys. 40, 3-1-3–41. https://doi.org/10.1029/2000RG000092

Giger, W., Schaffner, C., Kohler, H.-P.E., 2006. Benzotriazole and Tolyltriazole as Aquatic Contaminants. 1. Input and Occurrence in Rivers and Lakes †. Environ. Sci. Technol. 40, 7186–7192. https://doi.org/10.1021/es061565j

Gleeson, T., Wada, Y., Bierkens, M.F.P., van Beek, L.P.H., 2012. Water balance of global aquifers revealed by groundwater footprint. Nature 488, 197–200. https://doi.org/10.1038/nature11295

Golovko, O., Örn, S., Sörengård, M., Frieberg, K., Nassazzi, W., Lai, F.Y., Ahrens, L., 2021. Occurrence and removal of chemicals of emerging concern in wastewater treatment plants and their impact on receiving water systems. Sci. Total Environ. 754, 142122. https://doi.org/10.1016/j.scitotenv.2020.142122

Greskowiak, J., Hamann, E., Burke, V., Massmann, G., 2017. The uncertainty of biodegradation rate constants of emerging organic compounds in soil and groundwater – A compilation of literature values for 82 substances. Water Res. 126, 122–133. https://doi.org/10.1016/j.watres.2017.09.017

Greskowiak, J., Prommer, H., Massmann, G., Nützmann, G., 2006. Modeling Seasonal Redox Dynamics and the Corresponding Fate of the Pharmaceutical Residue Phenazone During Artificial Recharge of Groundwater. Environ. Sci. Technol. 40, 6615–6621. https://doi.org/10.1021/es052506t

Guillemoto, Q., Picot-Colbeaux, G., Valdes, D., Devau, N., Mathurin, F.A., Pettenati, M., Kloppmann, W., Mouchel, J.-M., 2022. Transfer of trace organic compounds in an operational soil-aquifer treatment system assessed through an intrinsic tracer test and transport modelling. Sci. Total Environ. 836, 155643. https://doi.org/10.1016/j.scitotenv.2022.155643

Hart, D.S., Davis, L.C., Erickson, L.E., Callender, T.M., 2004. Sorption and partitioning parameters of benzotriazole compounds. Microchem. J. 77, 9–17. https://doi.org/10.1016/j.microc.2003.08.005

Heberer, T., Massmann, G., Fanck, B., Taute, T., Dünnbier, U., 2008. Behaviour and redox sensitivity of antimicrobial residues during bank filtration. Chemosphere 73, 451–460. https://doi.org/10.1016/j.chemosphere.2008.06.056

Hebig, K.H., Groza, L.G., Sabourin, M.J., Scheytt, T.J., Ptacek, C.J., 2017. Transport behavior of the pharmaceutical compounds carbamazepine, sulfamethoxazole, gemfibrozil, ibuprofen, and naproxen, and the lifestyle drug caffeine, in saturated laboratory columns. Sci. Total Environ. 590–591, 708–719. https://doi.org/10.1016/j.scitotenv.2017.03.031

Hellauer, K., Karakurt, S., Sperlich, A., Burke, V., Massmann, G., Hübner, U., Drewes, J.E., 2018. Establishing sequential managed aquifer recharge technology (SMART) for enhanced removal of trace organic chemicals: Experiences from field studies in Berlin, Germany. J. Hydrol. 563, 1161–1168. https://doi.org/10.1016/j.jhydrol.2017.09.044

Hellauer, K., Martínez Mayerlen, S., Drewes, J.E., Hübner, U., 2019. Biotransformation of trace organic chemicals in the presence of highly refractory dissolved organic carbon. Chemosphere 215, 33–39. https://doi.org/10.1016/j.chemosphere.2018.09.166

Henzler, A.F., Greskowiak, J., Massmann, G., 2016. Seasonality of temperatures and redox zonations during bank filtration – A modeling approach. J. Hydrol. 535, 282–292. https://doi.org/10.1016/j.jhydrol.2016.01.044

Henzler, A.F., Greskowiak, J., Massmann, G., 2014. Modeling the fate of organic micropollutants during river bank filtration (Berlin, Germany). J. Contam. Hydrol. 156, 78–92. https://doi.org/10.1016/j.jconhyd.2013.10.005

Hoppe-Jones, C., Dickenson, E.R.V., Drewes, J.E., 2012. The role of microbial adaptation and biodegradable dissolved organic carbon on the attenuation of trace organic chemicals during groundwater recharge. Sci. Total Environ. 437, 137–144. https://doi.org/10.1016/j.scitotenv.2012.08.009

Hoppe-Jones, C., Oldham, G., Drewes, J.E., 2010. Attenuation of total organic carbon and unregulated trace organic chemicals in U.S. riverbank filtration systems. Water Res. 44, 4643–4659. https://doi.org/10.1016/j.watres.2010.06.022

Hough, J.J.H. & Rudolph, D.C. 2017. Geohydrological assessment report towns of Hessequa Municipality, Western Cape Province. GHT Consulting Engineers.

Howard, K.W.F., Gelo, K.K., 2002. Intensive groundwater use in urban areas: the case of megacities. Intensive Use Groundw. Chall. Oppor. 484.

Huang, W., Peng, P., Yu, Z., Fu, J., 2003. Effects of organic matter heterogeneity on sorption and desorption of organic contaminants by soils and sediments. Appl. Geochem. 18, 955–972. https://doi.org/10.1016/S0883-2927(02)00205-6

Hübner, U., Miehe, U., Jekel, M., 2012. Optimized removal of dissolved organic carbon and trace organic contaminants during combined ozonation and artificial groundwater recharge. Water Res. 46, 6059–6068. https://doi.org/10.1016/j.watres.2012.09.001

Hübner, U., Wurzbacher, C., Helbling, D.E., Drewes, J.E., 2022. Engineering of managed aquifer recharge systems to optimize biotransformation of trace organic chemicals. Curr. Opin. Environ. Sci. Health 27, 100343. https://doi.org/10.1016/j.coesh.2022.100343

Huet, S., Bouvier, A., Poursat, M.-A., Jolivet, E., 2004. Statistical tools for nonlinear regression: a practical guide with S-PLUS and R examples, 2nd ed. ed, Springer series in statistics. Springer, New York.

Huggins, X., Gleeson, T., Kummu, M., Zipper, S.C., Wada, Y., Troy, T.J., Famiglietti, J.S., 2022. Hotspots for social and ecological impacts from freshwater stress and storage loss. Nat. Commun. 13, 439. https://doi.org/10.1038/s41467-022-28029-w

IAH MAR, 2022. IAH Commission on Managing Aquifer Recharge.

Idier, D., Bertin, X., Thompson, P., Pickering, M.D., 2019. Interactions Between Mean Sea Level, Tide, Surge, Waves and Flooding: Mechanisms and Contributions to Sea Level Variations at the Coast. Surv. Geophys. 40, 1603–1630. https://doi.org/10.1007/s10712-019-09549-5

Idier D., Rohmer J., Pedreros R. *et al.* Coastal flood: a composite method for past events characterisation providing insights in past, present and future hazards—joining historical, statistical and modelling approaches. Nat Hazards (2020). https://doi.org/10.1007/s11069-020-03882-4.

IGRAC, 2022. IGRAC, 2016. Global MAR inventory (online). Consulté le 15/10/2022.

Imig, A., Szabó, Z., Halytsia, O., Vrachioli, M., Kleinert, V., Rein, A., 2022. A review on risk assessment in managed aquifer recharge. Integr. Environ. Assess. Manag. ieam.4584. https://doi.org/10.1002/ieam.4584

IPCC, 2022. Climate change 2022 :impacts, adaptation, and vulnerability (No. [H.-O. Pörtner, D.C. Roberts, M. Tignor, E.S. Poloczanska, K. Mintenbeck, A. Alegría, M. Craig, S. Langsdorf, S. Löschke, V. Möller, A. Okem, B. Rama (eds.)] Cambridge

University Press. Cambridge University Press, Cambridge, UK and New York, NY, USA, 3056 pp.,). Intergovernmental Panel on Climate Change, [Geneva] :

Jalón-Rojas, I., Schmidt, S., Sottolichio, A., 2016. Evaluation of spectral methods for high-frequency multiannual time series in coastal transitional waters: advantages of combined analyses: Tests of spectral analysis on coastal time series. Limnol. Oceanogr. Methods 14, 381–396. https://doi.org/10.1002/lom3.10097

Janna, H., Scrimshaw, M.D., Williams, R.J., Churchley, J., Sumpter, J.P., 2011. From Dishwasher to Tap? Xenobiotic Substances Benzotriazole and Tolyltriazole in the Environment. Environ. Sci. Technol. 45, 3858–3864. https://doi.org/10.1021/es103267g

Jasechko, S., Birks, S.J., Gleeson, T., Wada, Y., Fawcett, P.J., Sharp, Z.D., McDonnell, J.J., Welker, J.M., 2014. The pronounced seasonality of global groundwater recharge. Water Resour. Res. 50, 8845–8867. https://doi.org/10.1002/2014WR015809

Jia, Y., Aagaard, P., Breedveld, G.D., 2007. Sorption of triazoles to soil and iron minerals. Chemosphere 67, 250–258. https://doi.org/10.1016/j.chemosphere.2006.10.021

Jin, Q., Bethke, C.M., 2005. Predicting the rate of microbial respiration in geochemical environments. Geochim. Cosmochim. Acta 69, 1133–1143. https://doi.org/10.1016/j.gca.2004.08.010

Jin, S., Feng, G., 2013. Large-scale variations of global groundwater from satellite gravimetry and hydrological models, 2002–2012. Glob. Planet. Change 106, 20–30. https://doi.org/10.1016/j.gloplacha.2013.02.008

Karickhoff, S., Brown, D., Scott, T., 1979. Sorption of hydrophobic pollutants on natural sediments. Water Res. 13, 241–248. https://doi.org/10.1016/0043-1354(79)90201-X

Kiecak, A., Breuer, F., Stumpp, C., 2019a. Column Experiments on Sorption Coefficients and Biodegradation Rates of Selected Pharmaceuticals in Three Aquifer Sediments. Water 12, 14. https://doi.org/10.3390/w12010014

Kiecak, A., Sassine, L., Boy-Roura, M., Elsner, M., Mas-Pla, J., Le Gal La Salle, C., Stumpp, C., 2019b. Sorption properties and behaviour at laboratory scale of selected pharmaceuticals using batch experiments. J. Contam. Hydrol. 225, 103500. https://doi.org/10.1016/j.jconhyd.2019.103500

Kim, J.-H., Lee, J., Cheong, T.-J., Kim, R.-H., Koh, D.-C., Ryu, J.-S., Chang, H.-W., 2005. Use of time series analysis for the identification of tidal effect on groundwater in the coastal area of Kimje, Korea. J. Hydrol. 11.

Kirk, R.W.V., Contor, B.A., Morrisett, C.N., Null, S.E., Loibman, A.S., 2020. Potential for Managed Aquifer Recharge to Enhance Fish Habitat in a Regulated River. Water 12, 673. https://doi.org/10.3390/w12030673

Kloppmann, W., 2015. Traçages multi-isotopiques : des égouts aux cathédrales. Habilitation à diriger des recherches,. Université d'Orléans.

Kloppmann, W., Aharoni, A., Chikurel, H., Dillon, P., Gaus, I., Guttman, J., Kraitzer, T., Kremer, S., Masciopinto, C., Pavelic, P., Picot-Colbeaux, G., Pettenati, M., Miotlinski, K., 2012. Use of groundwater models for prediction and optimisation of the behaviour of MAR sites, in: Water Reclamation Technologies for Safe Managed Aquifer Recharge. pp. 311–349.

Kloppmann, W., Chikurel, H., Picot, G., Guttman, J., Pettenati, M., Aharoni, A., Guerrot, C., Millot, R., Gaus, I., Wintgens, T., 2009. B and Li isotopes as intrinsic tracers for injection tests in aquifer storage and recovery systems. Appl. Geochem. 24, 1214–1223. https://doi.org/10.1016/j.apgeochem.2009.03.006

Kløve, B., Ala-Aho, P., Bertrand, G., Gurdak, J.J., Kupfersberger, H., Kværner, J., Muotka, T., Mykrä, H., Preda, E., Rossi, P., Uvo, C.B., Velasco, E., Pulido-Velazquez, M., 2014. Climate change impacts on groundwater and dependent ecosystems. J. Hydrol. 518, 250–266. https://doi.org/10.1016/j.jhydrol.2013.06.037

Laperche, D., 2021. Aquifer : un projet européen pour mieux gérer les eaux souterraines. Actu-Environnementcom.

Lapworth, D.J., Baran, N., Stuart, M.E., Ward, R.S., 2012. Emerging organic contaminants in groundwater: A review of sources, fate and occurrence. Environ. Pollut. 163, 287–303. https://doi.org/10.1016/j.envpol.2011.12.034

Lapworth, D.J., Lopez, B., Laabs, V., Kozel, R., Wolter, R., Ward, R., Vargas Amelin, E., Besien, T., Claessens, J., Delloye, F., Ferretti, E., Grath, J., 2019. Developing a groundwater watch list for substances of emerging concern: a European perspective. Environ. Res. Lett. 14, 035004. https://doi.org/10.1088/1748-9326/aaf4d7

Lartigaut, C., 2019. Rapport de Stage BRGM.

Laws, B.V., Dickenson, E.R.V., Johnson, T.A., Snyder, S.A., Drewes, J.E., 2011. Attenuation of contaminants of emerging concern during surface-spreading aquifer recharge. Sci. Total Environ. 409, 1087–1094. https://doi.org/10.1016/j.scitotenv.2010.11.021

Le Gaudu, M., Thiebault, T., Quénéa, K., Alliot, F., Guigon, E., Le Callonnec, L., 2022. Trace organic contaminants within solid matrices along an anthropized watercourse: Organo-mineral controls on their spatial distribution. Sci. Total Environ. 822, 153601. https://doi.org/10.1016/j.scitotenv.2022.153601

Leibundgut, C., Seibert, J., 2011. Tracer Hydrology, in: Treatise on Water Science. Elsevier, pp. 215–236. https://doi.org/10.1016/B978-0-444-53199-5.00036-1

Li, W.-L., Zhang, Z.-F., Ma, W.-L., Liu, L.-Y., Song, W.-W., Li, Y.-F., 2018. An evaluation on the intra-day dynamics, seasonal variations and removal of selected pharmaceuticals and personal care products from urban wastewater treatment plants. Sci. Total Environ. 640–641, 1139–1147. https://doi.org/10.1016/j.scitotenv.2018.05.362

Lithologic, 2014. Mise en place de trois nouveaux piézomètres de contrôle au sein de la roselière de la station d'épuration d'Agon-Coutainville.

Liu, Y.-S., Ying, G.-G., Shareef, A., Kookana, R.S., 2013. Biodegradation of three selected benzotriazoles in aquifer materials under aerobic and anaerobic conditions. J. Contam. Hydrol. 151, 131–139. https://doi.org/10.1016/j.jconhyd.2013.05.006

Liu, Y.-S., Ying, G.-G., Shareef, A., Kookana, R.S., 2011. Biodegradation of three selected benzotriazoles under aerobic and anaerobic conditions. Water Res. 45, 5005–5014. https://doi.org/10.1016/j.watres.2011.07.001

LYXEA, Public presentation of the tool developed by Antea Group http://www.lyxea.fr/geo-hyd/nos-references

Löffler, D., Römbke, J., Meller, M., Ternes, T.A., 2005. Environmental Fate of Pharmaceuticals in Water/Sediment Systems. Environ. Sci. Technol. 39, 5209–5218. https://doi.org/10.1021/es0484146

Loizeau, S., Rossier, Y., Gaudet, J.-P., Refloch, A., Besnard, K., Angulo-Jaramillo, R., Lassabatere, L., 2017. Water infiltration in an aquifer recharge basin affected by temperature and air entrapment. J. Hydrol. Hydromech. 65, 222–233. https://doi.org/10.1515/johh-2017-0010

Lomb, N.R., 1976. Least-squares frequency analysis of unequally spaced data. Astrophys. Space Sci. 39, 447–462. https://doi.org/10.1007/BF00648343

Lopez, B., Ollivier, P., Togola, A., Baran, N., Ghestem, J.-P., 2015. Screening of French groundwater for regulated and emerging contaminants. Sci. Total Environ. 518–519, 562–573. https://doi.org/10.1016/j.scitotenv.2015.01.110

Lovrinović, I., Bergamasco, A., Srzić, V., Cavallina, C., Holjević, D., Donnici, S., Erceg, J., Zaggia, L., Tosi, L., 2021. Groundwater Monitoring Systems to Understand Sea Water Intrusion Dynamics in the Mediterranean: The Neretva Valley and the Southern Venice Coastal Aquifers Case Studies. Water 13, 561. https://doi.org/10.3390/w13040561

Lyard, F.H., Allain, D.J., Cancet, M., Carrère, L., Picot, N., 2021. FES2014 global ocean tide atlas: design and performance. Ocean Sci. 17, 615–649. https://doi.org/10.5194/os-17-615-2021

Maeng, S.K., Ameda, E., Sharma, S.K., Grützmacher, G., Amy, G.L., 2010. Organic micropollutant removal from wastewater effluent-impacted drinking water sources during bank filtration and artificial recharge. Water Res. 44, 4003–4014. https://doi.org/10.1016/j.watres.2010.03.035

Maeng, S.K., Sharma, S.K., Lekkerkerker-Teunissen, K., Amy, G.L., 2011. Occurrence and fate of bulk organic matter and pharmaceutically active compounds in managed aquifer recharge: A review. Water Res. 45, 3015–3033. https://doi.org/10.1016/j.watres.2011.02.017

Maoz, A., Chefetz, B., 2010. Sorption of the pharmaceuticals carbamazepine and naproxen to dissolved organic matter: Role of structural fractions. Water Res. 44, 981–989. https://doi.org/10.1016/j.watres.2009.10.019

Mardhel, V., Pinson, S., Allier, D., 2020. Description of an indirect method (IDPR) to determine spatial distribution of infiltration and runoff and its hydrogeological applications to the French territory. J. Hydrol. 592, 125609. https://doi.org/10.1016/j.jhydrol.2020.125609

Margat, J., Collin, J.-J., 1992. L'avenir de l'eau souterraine : la gestion active des aquifères. 22e Journ. Hydraul. 9.

Masciopinto, C., Carrieri, C., 2002. Assessment of Water Quality After 10 Years of Reclaimed Water Injection: The Nardò Fractured Aquifer (Southern Italy). Ground Water Monit. Remediat. 22 (1), 88–87.

Massmann, G., Greskowiak, J., Dünnbier, U., Zuehlke, S., Knappe, A., Pekdeger, A., 2006. The impact of variable temperatures on the redox conditions and the behaviour of pharmaceutical residues during artificial recharge. J. Hydrol. 328, 141–156. https://doi.org/10.1016/j.jhydrol.2005.12.009

Massmann, G., Sültenfuß, J., Dünnbier, U., Knappe, A., Taute, T., Pekdeger, A., 2008. Investigation of groundwater residence times during bank filtration in Berlin: a multi-tracer approach. Hydrol. Process. 22, 788–801. https://doi.org/10.1002/hyp.6649

Millero, F.J., Feistel, R., Wright, D.G., McDougall, T.J., 2008. The composition of Standard Seawater and the definition of the Reference-Composition Salinity Scale. Deep Sea Res. Part Oceanogr. Res. Pap. 55, 50–72. https://doi.org/10.1016/j.dsr.2007.10.001

Miotlinski, K., Barry, K., Breton, M., 2010. Alice Springs SAT Project Hydrological and Water Quality Monitoring Report 2008-2009 (Report of the NWC Raising National Water Standards project: Facilitating recycling of stormwater and reclaimed water via aquifers. No. Water for a Healthy Country Flagship Report series ISSN: 1835-095X).

Monod, J., 1949. The Growth of Bacterial Cultures. Annu Rev Microbiol 371–393.

Muntau, M., Schulz, M., Jewell, K.S., Hermes, N., Hübner, U., Ternes, T., Drewes, J.E., 2017. Evaluation of the short-term fate and transport of chemicals of emerging concern during soil-aquifer treatment using select transformation products as intrinsic redox-sensitive tracers. Sci. Total Environ. 583, 10–18. https://doi.org/10.1016/j.scitotenv.2016.12.165

Nash, J.E., Sutcliffe, J.V., 1970. River flow forecasting through conceptual models part I — A discussion of principles. J. Hydrol. 10, 282–290. https://doi.org/10.1016/0022-1694(70)90255-6

Négrel, P., Guerrot, C., Millot, R., 2007. Chemical and strontium isotope characterization of rainwater in France: influence of sources and hydrogeochemical implications. Isotopes Environ. Health Stud. 43, 179–196. https://doi.org/10.1080/10256010701550773

Nelson, E.D., Do, H., Lewis, R.S., Carr, S.A., 2011. Diurnal Variability of Pharmaceutical, Personal Care Product, Estrogen and Alkylphenol Concentrations in Effluent from a Tertiary Wastewater Treatment Facility. Environ. Sci. Technol. 45, 1228–1234. https://doi.org/10.1021/es102452f

Nguyen, F., Benoit, S., Gommers, K., Ghysels, G., Hermans, T., Huysmans, M., 2017. Characterization of riverbed sediments hydraulic conductivity using slug tests and electrical resistivity tomography and induced polarization tomogrpahy., in: AGU Fall Meeting Abstracts. pp. H21A-1436.

Nham, H.T.T., Greskowiak, J., Nödler, K., Rahman, M.A., Spachos, T., Rusteberg, B., Massmann, G., Sauter, M., Licha, T., 2015. Modeling the transport behavior of 16 emerging organic contaminants during soil aquifer treatment. Sci. Total Environ. 514, 450–458. https://doi.org/10.1016/j.scitotenv.2015.01.096

NORRMAN, a referenced tool for the assessment of the Loire Bretagne https://sdage-sage.eau-loire-bretagne.fr/files/live/mounts/midas/Donnees-et-documents/PUBLI_EDL2019-HD.pdf (p. 165) and basin applied for Self-Purification Assessment https://www.ille-et-vilaine.gouv.fr/content/download/35160/255420/file/010-B-resume.pdf (§6.1.1.2)

NRMMC, EPHC, and NHMRC, 2009. Australian Guidelines for water recycling, managing health and environmental risks, vol 2C: managed aquifer recharge. Natural Resource Management Ministerial Council, Environment Protection and Heritage Council National Health and Medical Research Council.

OFB, 2020, 2020. Eau et milieux aquatiques - Les chiffres clés - Édition 2020 128.

OMS, 2003. State of the art report health risks in aquifer recharge using reclaimed water. World Health Organization.

Organisation des Nations Unies, 2022. Rapport mondial des Nations Unies sur la mise en valeur des ressources en eau 2022 : Eaux souterraines : rendre visible l'invisible. UNESCO, Paris.

Ousrhire, A., Ghafiri, A., 2022. Artificial aquifer recharge: systematic mapping study. Water Pract. Technol. 17, 1706–1727. https://doi.org/10.2166/wpt.2022.082

Palmer, M., Liu, J., Matthews, J., Mumba, M., D'Odorico, P., 2015. Water Security: Gray or Green? Science.

Parker, J., Van Genuchten, M., 1984. Determining Transport Parameters from Laboratory and Field Tracer Experiments. Va Agric Exp Sin Bull 84–3.

Parkhurst, D.L., Appelo, C.A.J., 2013. Description of input and examples for PHREEQC version 3: a computer program for speciation, batch-reaction, one-dimensional transport, and inverse geochemical calculations (Report No. 6-A43), Techniques and Methods. Reston, VA. https://doi.org/10.3133/tm6A43

Patterson, B.M., Shackleton, M., Furness, A.J., Bekele, E., Pearce, J., Linge, K.L., Busetti, F., Spadek, T., Toze, S., 2011. Behaviour and fate of nine recycled water trace organics during managed aquifer recharge in an aerobic aquifer. J. Contam. Hydrol. 122, 53–62. https://doi.org/10.1016/j.jconhyd.2010.11.003

Patterson, B.M., Shackleton, M., Furness, A.J., Pearce, J., Descourvieres, C., Linge, K.L., Busetti, F., Spadek, T., 2010. Fate of nine recycled water trace organic contaminants and metal(loid)s during managed aquifer recharge into a anaerobic aquifer: Column studies. Water Res. 44, 1471–1481. https://doi.org/10.1016/j.watres.2009.10.044

Pêches et Océans Canada, 2022. À propos des marées et des courants | Pêches et Océans Canada. Les plus grandes marées du monde : Baie de Fundy et baie d'Ungava.

Pereira, L.C., de Souza, A.O., Bernardes, M.F.F., Pazin, M., Tasso, M.J., Pereira, P.H., Dorta, D.J., 2015. A perspective on the potential risks of emerging contaminants to human and environmental health. Environ. Sci. Pollut. Res. 22, 13800–13823. https://doi.org/10.1007/s11356-015-4896-6

Petrie, B., Barden, R., Kasprzyk-Hordern, B., 2015. A review on emerging contaminants in wastewaters and the environment: Current knowledge, understudied areas and recommendations for future monitoring. Water Res. 72, 3–27. https://doi.org/10.1016/j.watres.2014.08.053

Pettenati, M., Dörfliger, N., 2019. Des solutions fondées sur la nature pour s'adapter au changement climatique. Rapport au Premier ministre et au Parlement. Chapitre D. Eau et biodiversité. Observatoire national sur les effets du réchauffement climatique 306.

Pettenati, M., Picot-Colbeaux, G., Mathurin, F., Soulier, C., Togola, A., Devau, N., Lartigaut, C., Thomas, L., Aurouet, A., Thierion, C., Wissocq, A., Baïsset, M., Neyens, D., 2019. Novel monitoring- modelling systems to manage qualitative and quantitative status of coastal aquifers (Deliverable H2020-WATER No. D2.3.1), AquaNES, Demonstrating synergies in combined natural and engineered processes for wastertreatment systems.

Pezard P.A, Perroud H., Lofi J., Gautier S., Henry G., Geeraert M., Deleau A., Neyens D., Barry S., Levannier A. A new downhole geophysical observatory for near-field monitoring and real-time subsurface management, XIV IWRA World Water Congress, Porto de Galinhas, Brazil, September 25-29, 2011,

Pezard P., Henry G., Hebert V., Garing C., Lofi J., Barry S., Perroud H., Rousset D., Neyens D., Depraz O.. A new kind of high-resolution downhole hydrogeophysical observatory for real-time salt intrusion management, SWIM21 - 21st Salt Water Intrusion Meeting, Azores, Portugal, June 21 - 26, 2010.

Pezard P.A , Gouze P. , Perroud H. , Lofi J. , Denchik N. , Henry H. , Geeraert M. , Neyens D. , Bellot J-P. ,Levannier A. Coastal aquifer monitoring and management from high frequency and autonomous downhole hydrogeophysical observatories, Salt Water Intrusion Meeting, Husum, June 16-20, 2014,

Picot-Colbeaux, G., Devau, N., Pettenati, M., Akrour, R., Blanc, P., Thiéry, D., 2018. D3.2 Developments of a multi-scale modeling tool to describe the fate and transport of CECs, TPs and pathogens through IPR strategies (No. WaterJPI2013-FRAME Report), Water Challenges for a Chalenging World – Joint Programming initiative –.

Picot-Colbeaux, G., Mathurin, F., Pettenati, M., Nakache, F., Guillemoto, Q., Baïsset, M., Devau, N., Gosselin, M., Allain, D., Neyens, D., Lartigaut, C., Dufour, E., Togola, A., Depraz, O., Nauleau, F., 2020. Sustainable Managed Aquifer Recharge (MAR) – Soil Aquifer Treatment system to protect coastal ecosystem in Agon-Coutainville (Normandy), France, in: Zheng, Y., Ross, A., Villholth, K., Dillon, P. (Eds.), Exemplary Case Studies of Sustainable and Economic Managed Aquifer Recharge., UNESCO-IAH-GRIPP Publication. A UNESCO-IAH-GRIPP Publication.

Pouvreau, N., 2008. Trois cents ans de mesures marégraphiques en France : outils, méthodes et tendances des composantes du niveau de la mer au port de Brest. (THÈSE DE DOCTORAT DE L'UNIVERSITE DE LA ROCHELLE).

Préfecture de la Manche, 2001. Arrêté préfectoral autorisant et reglementant la station d'épuration et l'épandage des boues de la commune de Agon-Coutainville.

Prudhomme, C., Giuntoli, I., Robinson, E.L., Clark, D.B., Arnell, N.W., Dankers, R., Fekete, B.M., Franssen, W., Gerten, D., Gosling, S.N., Hagemann, S., Hannah, D.M., Kim, H., Masaki, Y., Satoh, Y., Stacke, T., Wada, Y., Wisser, D., 2014. Hydrological droughts in the 21st century, hotspots and uncertainties from a global multimodel ensemble experiment. Proc. Natl. Acad. Sci. 111, 3262–3267. https://doi.org/10.1073/pnas.1222473110

Ptak, T., Piepenbrink, M., Martac, E., 2004. Tracer tests for the investigation of heterogeneous porous media and stochastic modelling of flow and transport—a review of some recent developments. J. Hydrol. 294, 122–163. https://doi.org/10.1016/j.jhydrol.2004.01.020

Pyne, R.D.G., 1995. Groundwater Recharge and Wells: A Guide to Aquifer Storage Recovery.

Qi, Y., Yu, H., Fu, Q., Chen, Q., Ran, J., Yang, Z., 2022. Future Changes in Drought Frequency Due To Changes in the Mean and Shape of the PDSI Probability Density Function Under RCP4.5 Scenario. Front. Earth Sci. 10, 857885. https://doi.org/10.3389/feart.2022.857885

RAM, 2020. Références Altimétriques Maritimes, Ports de France métropolitaine et d'outre-mer Cotes du zéro hydrographique et niveaux caractéristiques de la marée. SHOM.

Rauch-Williams, T., Hoppe-Jones, C., Drewes, J.E., 2009. The role of organic matter in the removal of emerging trace organic chemicals during managed aquifer recharge. Water Res. 44, 449–460. https://doi.org/10.1016/j.watres.2009.08.027

Ravenscroft, P. 2019. Personal communication

Reemtsma, T., Miehe, U., Duennbier, U., Jekel, M., 2010. Polar pollutants in municipal wastewater and the water cycle: Occurrence and removal of benzotriazoles. Water Res. 44, 596–604. https://doi.org/10.1016/j.watres.2009.07.016

Refsgaard, J.C., Henriksen, H.J., 2004. Modelling guidelines––terminology and guiding principles. Adv. Water Resour. 27, 71–82. https://doi.org/10.1016/j.advwatres.2003.08.006

Regnery, J., Gerba, C.P., Dickenson, E.R.V., Drewes, J.E., 2017. The importance of key attenuation factors for microbial and chemical contaminants during managed aquifer recharge: A review. Crit. Rev. Environ. Sci. Technol. 47, 1409–1452. https://doi.org/10.1080/10643389.2017.1369234

Regnery, J., Wing, A.D., Alidina, M., Drewes, J.E., 2015. Biotransformation of trace organic chemicals during groundwater recharge: How useful are first-order rate constants? J. Contam. Hydrol. 179, 65–75. https://doi.org/10.1016/j.jconhyd.2015.05.008

Réseau31, 2021. Lancement du projet R'Garonne, partenariat phare entre le BRGM et Réseau31.

Richert, J.G., 1900. On Artificial Underground Water, . C. E. Fritze's Royal Book-Store. ed. Stockholm.

Rodríguez-Escales, P., Barba, C., Sanchez-Vila, X., Jacques, D., Folch, A., 2020. Coupling Flow, Heat, and Reactive Transport Modeling to Reproduce *In Situ* Redox Potential Evolution: Application to an Infiltration Pond. Environ. Sci. Technol. acs.est.0c03056. https://doi.org/10.1021/acs.est.0c03056

Sabljić, A., Güsten, H., Verhaar, H., Hermens, J., 1995. QSAR modelling of soil sorption. Improvements and systematics of log KOC vs. log KOW correlations. Chemosphere 31, 4489–4514. https://doi.org/10.1016/0045-6535(95)00327-5

Sanz-Prat, A., Greskowiak, J., Burke, V., Rivera Villarreyes, C.A., Krause, J., Monninkhoff, B., Sperlich, A., Schimmelpfennig, S., Duennbier, U., Massmann, G., 2020. A model-based analysis of the reactive transport behaviour of 37 trace organic compounds during field-scale bank filtration. Water Res. 173, 115523. https://doi.org/10.1016/j.watres.2020.115523

SAUR, 2014. Bilan annuel du système d'assainissement. STEP d'Agon Coutainville.

Scanlon, B.R., Healy, R.W., Cook, P.G., 2002. Choosing appropriate techniques for quantifying groundwater recharge. Hydrogeol. J. 22.

Scargle, J.D., 1982. Studies in astronomical time series analysis. II - Statistical aspects of spectral analysis of unevenly spaced data. Astrophys. J. 263, 835. https://doi.org/10.1086/160554

Schaffer, M., Boxberger, N., Börnick, H., Licha, T., Worch, E., 2012. Sorption influenced transport of ionizable pharmaceuticals onto a natural sandy aquifer sediment at different pH. Chemosphere 87, 513–520. https://doi.org/10.1016/j.chemosphere.2011.12.053

Schaffer, M., Kröger, K.F., Nödler, K., Ayora, C., Carrera, J., Hernández, M., Licha, T., 2015. Influence of a compost layer on the attenuation of 28 selected organic micropollutants under realistic soil aquifer treatment conditions: Insights from a large scale column experiment. Water Res. 74, 110–121. https://doi.org/10.1016/j.watres.2015.02.010

Schaffer, M., Licha, T., 2015. A framework for assessing the retardation of organic molecules in groundwater: Implications of the species distribution for the sorption-influenced transport. Sci. Total Environ. 524–525, 187–194. https://doi.org/10.1016/j.scitotenv.2015.04.006

Scheytt, T., Mersmann, P., Lindstädt, R., Heberer, T., 2005. Determination of sorption coefficients of pharmaceutically active substances carbamazepine, diclofenac, and ibuprofen, in sandy sediments. Chemosphere 60, 245–253. https://doi.org/10.1016/j.chemosphere.2004.12.042

Scheytt, T.J., Mersmann, P., Heberer, T., 2006. Mobility of pharmaceuticals carbamazepine, diclofenac, ibuprofen, and propyphenazone in miscible-displacement experiments. J. Contam. Hydrol. 83, 53–69. https://doi.org/10.1016/j.jconhyd.2005.11.002

Schulze-Makuch, D., 2005. Longitudinal dispersivity data and implications for scaling behavior. Groundwater 43, 443–456. https://doi.org/10.1111/j.1745-6584.2005.0051.x

Seguin, J.-J., 2015. Méthodes d'évaluation de la recharge des nappes (No. BRGM/RP-65635-FR). BRGM.

Seilmayer, M., 2019. spectral: Common Methods of Spectral Data Analysis.

Sengar, A., Vijayanandan, A., 2022. Human health and ecological risk assessment of 98 pharmaceuticals and personal care products (PPCPs) detected in Indian surface and wastewaters. Sci. Total Environ. 807, 150677. https://doi.org/10.1016/j.scitotenv.2021.150677

Shammas, M.I., 2008. The effectiveness of artificial recharge in combating seawater intrusion in Salalah coastal aquifer, Oman. Environ. Geol. 55, 191–204. https://doi.org/10.1007/s00254-007-0975-4

Shamsudduha, M., Taylor, R.G., 2020. Groundwater storage dynamics in the world’s large aquifer systems from GRACE: uncertainty and role of extreme precipitation. Earth Syst. Dyn. 11, 755–774. https://doi.org/10.5194/esd-11-755-2020

Sharma, L., Greskowiak, J., Ray, C., Eckert, P., Prommer, H., 2012. Elucidating temperature effects on seasonal variations of biogeochemical turnover rates during riverbank filtration. J. Hydrol. 428–429, 104–115. https://doi.org/10.1016/j.jhydrol.2012.01.028

Sharma, S.K., Kennedy, M.D., 2017. Soil aquifer treatment for wastewater treatment and reuse. Int. Biodeterior. Biodegrad. 119, 671–677. https://doi.org/10.1016/j.ibiod.2016.09.013

Shiklomanov, I.A., 2000. Appraisal and Assessment of World Water Resources. Water Int. 25, 11–32. https://doi.org/10.1080/02508060008686794

Shubo, T., Fernandes, L., Montenegro, S.G., 2020. An Overview of Managed Aquifer Recharge in Brazil. Water 12, 1072. https://doi.org/10.3390/w12041072

Shumway, R.H., Stoffer, D.S., 2017. Time Series Analysis and Its Applications. With R Examples, Fourth Edition. ed. Springer Texts in Statistics, New York, NY.

Siebert, S., Burke, J., Faures, J.M., Frenken, K., Hoogeveen, J., Döll, P., Portmann, F.T., 2010. Groundwater use for irrigation – a global inventory. Hydrol. Earth Syst. Sci. 14, 1863–1880. https://doi.org/10.5194/hess-14-1863-2010

Simmons, C.T., Fenstemaker, T.R., Sharp, J.M., 2001. Variable-density groundwater flow and solute transport in heterogeneous porous media: approaches, resolutions and future challenges. J. Contam. Hydrol. 52, 245–275. https://doi.org/10.1016/S0169-7722(01)00160-7

Simon, B., 2007. La marée océanique côtière, Collection “Synthèses.” Institut océanographique, Paris.

Sprenger, C., Hartog, N., Hernández, M., Vilanova, E., Grützmacher, G., Scheibler, F., Hannappel, S., 2017. Inventory of managed aquifer recharge sites in Europe: historical development, current situation and perspectives. Hydrogeol. J. 25, 1909–1922. https://doi.org/10.1007/s10040-017-1554-8

Srzić, V., Lovrinović, I., Racetin, I., Pletikosić, F., 2020. Hydrogeological Characterization of Coastal Aquifer on the Basis of Observed Sea Level and Groundwater Level Fluctuations: Neretva Valley Aquifer, Croatia. Water 12, 348. https://doi.org/10.3390/w12020348

Stefan, C., Ansems, N., 2018. Web-based global inventory of managed aquifer recharge applications. Sustain. Water Resour. Manag. 4, 153–162. https://doi.org/10.1007/s40899-017-0212-6

Stein, K., Ramil, M., Fink, G., Sander, M., Ternes, T.A., 2008. Analysis and Sorption of Psychoactive Drugs onto Sediment. Environ. Sci. Technol. 42, 6415–6423. https://doi.org/10.1021/es702959a

Stuart, M., Lapworth, D., Crane, E., Hart, A., 2012. Review of risk from potential emerging contaminants in UK groundwater. Sci. Total Environ. 416, 1–21. https://doi.org/10.1016/j.scitotenv.2011.11.072

Stuyfzand, P.J., 2011. Hydrogeochemical Processes During Riverbank Filtration and Artificial Recharge of Polluted Surface Waters: Zonation, Identification, and Quantification, in: Shamrukh, M. (Ed.), Riverbank Filtration for Water Security in Desert Countries. Springer Netherlands, Dordrecht, pp. 97–128.

Tal, Adi, Yishai Weinstein, Matthieu Baïsset, Arik Golan, and Yoseph Yechieli. 2019. "High Resolution Monitoring of Seawater Intrusion in a Multi-Aquifer System-Implementation of a New Downhole Geophysical Tool" Water 11, no. 9: 1877. https://doi.org/10.3390/w11091877

Tang, G., Mayes, M.A., Parker, J.C., Jardine, P.M., 2010. CXTFIT/Excel–A modular adaptable code for parameter estimation, sensitivity analysis and uncertainty analysis for laboratory or field tracer experiments. Comput. Geosci. 36, 1200–1209. https://doi.org/10.1016/j.cageo.2010.01.013

Teijon, G., Candela, L., Tamoh, K., Molina-Díaz, A., Fernández-Alba, A.R., 2010. Occurrence of emerging contaminants, priority substances (2008/105/CE) and heavy metals in treated wastewater and groundwater at Depurbaix facility (Barcelona, Spain). Sci. Total Environ. 408, 3584–3595. https://doi.org/10.1016/j.scitotenv.2010.04.041

Ternes, T.A., 1998. Occurrence of drugs in German sewage treatment plants and rivers1Dedicated to Professor Dr. Klaus Haberer on the occasion of his 70th birthday.1. Water Res. 32, 3245–3260. https://doi.org/10.1016/S0043-1354(98)00099-2

Thiebault, T., Fougère, L., Destandau, E., Réty, M., Jacob, J., 2019. Impact of meteorological and social events on human-excreted contaminant loads in raw wastewater: From daily to weekly dynamics. Chemosphere 230, 107–116. https://doi.org/10.1016/j.chemosphere.2019.04.221

Thiéry, 2021. Modélisation 3D du transport de masse et du transfert thermique avec le code de calcul MARTHE version 7.5 (No. BRGM/RP-64765-FR).

Thiéry, D., 2020. Code de calcul MARTHE version 7.8 Modélisation 3D des écoulements et des transferts dans les hydrosystèmes. BRGMRP-69541-FR 344.

Thiéry, D. (2014-2021) – Logiciel GARDÉNIA, version 8.2 - Mise à jour version v8.8. Guide d'utilisation. Rapport BRGM/RP-62797-FR, 140 p., 74 fig., 2 ann. http://infoterre.brgm.fr/rapports/RP-62797-FR.pdf. (Access January 2020).

Thiéry D. (2015) - Validation du code de calcul GARDÉNIA par modélisations physiques comparatives. Rapport BRGM/RP-64500-FR, 48 p., 28 fig.

Thiéry, D., 2012. Code de calcul CATHERINE - Principe et mode d'emploi. (No. BRGM/RP-61430-FR).

Thiéry, D. (2010) – Modélisation des Ecoulements Souterrains en Milieu Poreux avec MARTHE. in Traité d'hydraulique environnementale – Volume 9 – Logiciels d'ingénierie du cycle de l'eau. Tanguy J.M. (Ed.) - Éditions Hermès - Lavoisier. Chapitre 4 pp. 77-94. ISBN 978-2-7462-2339-4.

Thiéry, D. (2009) – Modèles à Réservoirs en Hydrogéologie. in Traité d'hydraulique environnementale – Volume 4 - Modèles mathématiques en hydraulique maritime et modèles de transport. Tanguy J.M. (Ed.) - Éditions Hermès - Lavoisier. Chapitre 7 pp. 239-249. ISBN 978-2-7462-2006-5.

Thiéry, D., 1977. calcul de pluie efficace au pas journalier avec les sous-programmes climat et clidat.

Thornthwaite, C.W., 1948. An Approach toward a Rational Classification of Climate. Geogr. Rev. 38, 55. https://doi.org/10.2307/210739

Todd, D.K., 1959. Annotated bibliography on artificial recharge of ground water through 1954 (Report No. 1477), Water Supply Paper. https://doi.org/10.3133/wsp1477

Togola, A., Baran, N., Coureau, C., 2014. Advantages of online SPE coupled with UPLC/MS/MS for determining the fate of pesticides and pharmaceutical compounds. Anal. Bioanal. Chem. 406, 1181–1191. https://doi.org/10.1007/s00216-013-7248-8

Toride, N., Leij, F., Van Genuchten, M., 1995. The CXTFIT Code for Estimating Transport Parameters from Laboratory or Field Tracer Experiments. Salin. Lab. 137.

Tran, N.H., Reinhard, M., Gin, K.Y.-H., 2018. Occurrence and fate of emerging contaminants in municipal wastewater treatment plants from different geographical regions-a review. Water Res. 133, 182–207. https://doi.org/10.1016/j.watres.2017.12.029

Tran, N.H., Urase, T., Ngo, H.H., Hu, J., Ong, S.L., 2013. Insight into metabolic and cometabolic activities of autotrophic and heterotrophic microorganisms in the biodegradation of emerging trace organic contaminants. Bioresour. Technol. 146, 721–731. https://doi.org/10.1016/j.biortech.2013.07.083

Trenberth, K.E., Dai, A., van der Schrier, G., Jones, P.D., Barichivich, J., Briffa, K.R., Sheffield, J., 2014. Global warming and changes in drought. Nat. Clim. Change 4, 17–22. https://doi.org/10.1038/nclimate2067

Tzoraki, O., Dokou, Z., Christodoulou, G., Gaganis, P., Karatzas, G., 2018. Assessing the efficiency of a coastal Managed Aquifer Recharge (MAR) system in Cyprus. Sci. Total Environ. 626, 875–886. https://doi.org/10.1016/j.scitotenv.2018.01.160

US EPA, 2012. Estimation Programs Interface Suite™ for Microsoft® Windows V. ,. United States Environmental Protection Agency, Washington, DC, USA.

USEPA, 2012. Guidelines for Water Reuse 2012 (No. EPA/600/R-12/ 618), US Environmental Protection Agency and US Agency for International Development. Washington, DC, USA.

Vallejos, A., Sola, F., Pulido-Bosch, A., 2015. Processes Influencing Groundwater Level and the Freshwater-Saltwater Interface in a Coastal Aquifer. Water Resour. Manag. 29, 679–697. https://doi.org/10.1007/s11269-014-0621-3

Van Houtte, E., Verbauwhede, J., 2012. Sustainable groundwater management using reclaimed water: the Torreele/St-André case in Flanders, Belgium. J. Water Supply Res. Technol.-Aqua 61, 473–483. https://doi.org/10.2166/aqua.2012.057b

Van Houtte, K.M., Verbauwhede, S., 2020. Case Study 25: Water recycling with managed aquifer recharge in sand dunes of St-André (Koksijde) as one of the multiple safety barriers for drinking water to Veurne area, Belgium, in: MANAGING AQUIFER RECHARGE A Showcase for Resilience and Sustainability. Yan Zheng, Andrew Ross, Karen Villholth and Peter Dillon (eds), Paris, UNESCO., pp. 300–303.

van Vliet, M.T.H., Jones, E.R., Flörke, M., Franssen, W.H.P., Hanasaki, N., Wada, Y., Yearsley, J.R., 2021. Global water scarcity including surface water quality and expansions of clean water technologies. Environ. Res. Lett. 16, 024020. https://doi.org/10.1088/1748-9326/abbfc3

van Weert, F., 2009. Global Overview of Saline Groundwater Occurrence and Genesis 107.

Vandenbohede, A., Van Houtte, E., Lebbe, L., 2009. Sustainable groundwater extraction in coastal areas: a Belgian example. Environ. Geol. 57, 735–747. https://doi.org/10.1007/s00254-008-1351-8

Vandenbohede, A., Van Houtte, E., Lebbe, L., 2008. Groundwater flow in the vicinity of two artificial recharge ponds in the Belgian coastal dunes. Hydrogeol. J. 16, 1669–1681. https://doi.org/10.1007/s10040-008-0326-x

VanderPlas, J.T., 2018. Understanding the Lomb–Scargle Periodogram. Astrophys. J. Suppl. Ser. 236, 16. https://doi.org/10.3847/1538-4365/aab766

Varenne Agricole, 2022. Conclusions du Varenne agricole de l'eau et de l'adaptation au changement climatique.

Vernhet, Y., 2003. Carte géologique harmonisée du département de la Manche (No. BRGMIRP-52715-FR).

Vittecoq, B., Lachassagne, P., Lanini, S., Maréchal, J.C., 2010. Évaluation des ressources en eau de la Martinique : calcul spatialisé de la pluie efficace et validation à l'échelle du bassin versant. Rev. Sci. Eau 23, 361–373. https://doi.org/10.7202/045098ar

Voluntary Groundwater Watch List (No. V. 3.1), 2019. , COMMON IMPLEMENTATION STRATEGY FOR THE WATER FRAMEWORK DIRECTIVE AND THE FLOODS DIRECTIVE.

Voss, K.A., Famiglietti, J.S., Lo, M., de Linage, C., Rodell, M., Swenson, S.C., 2013. Groundwater depletion in the Middle East from GRACE with implications for transboundary water management in the Tigris-Euphrates-Western Iran region: GROUNDWATER DEPLETION IN THE MIDDLE EAST FROM GRACE. Water Resour. Res. 49, 904–914. https://doi.org/10.1002/wrcr.20078

Wada, Y., van Beek, L.P.H., van Kempen, C.M., Reckman, J.W.T.M., Vasak, S., Bierkens, M.F.P., 2010. Global depletion of groundwater resources: GLOBAL GROUNDWATER DEPLETION. Geophys. Res. Lett. 37, n/a-n/a. https://doi.org/10.1029/2010GL044571

Wang, Z., Walker, G.W., Muir, D.C.G., Nagatani-Yoshida, K., 2020. Toward a Global Understanding of Chemical Pollution: A First Comprehensive Analysis of National and Regional Chemical Inventories. Environ. Sci. Technol. 54, 2575–2584. https://doi.org/10.1021/acs.est.9b06379

Water JPI, 2022. EVIBAN. Evidence based assessment of NWRM for sustainable water management.

Werner, A.D., Bakker, M., Post, V.E.A., Vandenbohede, A., Lu, C., Ataie-Ashtiani, B., Simmons, C.T., Barry, D.A., 2013. Seawater intrusion processes, investigation and management: Recent advances and future challenges. Adv. Water Resour. 51, 3–26. https://doi.org/10.1016/j.advwatres.2012.03.004

Wilkinson, J.L., Boxall, A.B.A., Kolpin, D.W., Leung, K.M.Y., Lai, R.W.S., Galbán-Malagón, C., Adell, A.D., Mondon, J., Metian, M., Marchant, R.A., Bouzas-Monroy, A., Cuni-Sanchez, A., Coors, A., Carriquiriborde, P., Rojo, M., Gordon, C., Cara, M., Moermond, M., Luarte, T., Petrosyan, V., Perikhanyan, Y., Mahon, C.S., McGurk, C.J., Hofmann, T., Kormoker, T., Iniguez, V., Guzman-Otazo, J., Tavares, J.L., Gildasio De Figueiredo, F., Razzolini, M.T.P., Dougnon, V., Gbaguidi, G., Traoré, O., Blais, J.M., Kimpe, L.E., Wong, M., Wong, D., Ntchantcho, R., Pizarro, J., Ying, G.-G., Chen, C.-E., Páez, M., Martínez-Lara, J., Otamonga, J.-P., Poté, J., Ifo, S.A., Wilson, P., Echeverría-Sáenz, S., Udikovic-Kolic, N., Milakovic, M., Fatta-Kassinos, D., Ioannou-Ttofa, L., Belušová, V., Vymazal, J., Cárdenas-Bustamante, M., Kassa, B.A., Garric, J., Chaumot, A., Gibba, P., Kunchulia, I., Seidensticker, S., Lyberatos, G., Halldórsson, H.P., Melling, M., Shashidhar, T., Lamba, M., Nastiti, A., Supriatin, A., Pourang, N., Abedini, A., Abdullah, O., Gharbia, S.S., Pilla, F., Chefetz, B., Topaz, T., Yao, K.M., Aubakirova, B., Beisenova, R., Olaka, L., Mulu, J.K., Chatanga, P., Ntuli, V., Blama, N.T., Sherif, S., Aris, A.Z., Looi, L.J., Niang, M., Traore, S.T., Oldenkamp, R., Ogunbanwo, O., Ashfaq, M., Iqbal, M., Abdeen, Z., O'Dea, A., Morales-Saldaña, J.M., Custodio, M., de la Cruz, H., Navarrete, I., Carvalho, F., Gogra, A.B., Koroma, B.M., Cerkvenik-Flajs, V., Gombač, M., Thwala, M., Choi, K., Kang, H., Ladu, J.L.C., Rico, A., Amerasinghe, P., Sobek, A., Horlitz, G., Zenker, A.K., King, A.C., Jiang, J.-J., Kariuki, R., Tumbo, M., Tezel, U., Onay, T.T., Lejju, J.B., Vystavna, Y., Vergeles, Y., Heinzen, H., Pérez-Parada, A., Sims, D.B., Figy, M., Good, D., Teta, C., 2022. Pharmaceutical pollution of the world's rivers. Proc. Natl. Acad. Sci. 119, e2113947119. https://doi.org/10.1073/pnas.2113947119

Wuilleumier, A., Seguin, J.J., 2008. Réalimentation artificielle des aquifères en France 120.

WWAP, 2018. The United Nations World Water Development Report 2018 : Nature-based solutions for water. UNESCO Paris.

Yamamoto, H., Nakamura, Yudai, Moriguchi, S., Nakamura, Yuki, Honda, Y., Tamura, I., Hirata, Y., Hayashi, A., Sekizawa, J., 2009. Persistence and partitioning of eight selected pharmaceuticals in the aquatic environment: Laboratory photolysis, biodegradation, and sorption experiments. Water Res. 43, 351–362. https://doi.org/10.1016/j.watres.2008.10.039

Yuan, J., Van Dyke, M.I., Huck, P.M., 2016. Water reuse through managed aquifer recharge (MAR): assessment of regulations/guidelines and case studies. Water Qual. Res. J. 51, 357–376. https://doi.org/10.2166/wqrjc.2016.022

Zechmeister, M., Kürster, M., 2009. The generalised Lomb-Scargle periodogram. A new formalism for the floating-mean and Keplerian periodograms. Astron. Astrophys. 496, 577–584. https://doi.org/10.1051/0004-6361:200811296

Zhang, H., Xu, Y., Kanyerere, T., 2020. A review of the managed aquifer recharge: Historical development, current situation and perspectives. Phys. Chem. Earth Parts ABC 118–119, 102887. https://doi.org/10.1016/j.pce.2020.102887

Zheng, Y., Ross, A., Villholth, K.G., Dillon, P., 2020. MANAGING AQUIFER RECHARGE. A showcase for Resilience and Sustainability. Paris, UNESCO.

Zheng, Y., Vanderzalm, J., Hartog, N., Escalante, E.F., Stefan, C., 2022. The 21st century water quality challenges for managed aquifer recharge: towards a risk-based regulatory approach. Hydrogeol. J. https://doi.org/10.1007/s10040-022-02543-z